การพัฒนาโปรแกรมเพื่อทำนายค่าความดันลด ในระบบท่อสำหรับการไหลแบบสองวัฏภาค (ของเหลว - ก๊าซ)

นางวริศรา ปดิฐพร

วิทยานิพนธ์เป็นส่วนหนึ่งของการศึกษาตามหลักสูตรปริญญาวิศวกรรมศาสตรมหาบัณฑิต
สาขาวิศวกรรมเคมี ภาควิชาวิศวกรรมเคมี
คณะวิศวกรรมศาสตร์ จุฬาลงกรณ์มหาวิทยาลัย
ปีการศึกษา 2544

ISBN 974-03-1234-9

PROGRAM DEVELOPMENT FOR PREDICTING PRESSURE LOSS IN A TWO-PHASE PIPING SYSTEM (LIQUID-GAS)

Mrs. Varisara Paditporn

A Thesis Submitted in Partial Fulfillment of the Requirements
for the Degree of Master of Engineering in Chemical Engineering
Departmental of Chemical Engineering
Faculty of Engineering
Chulalongkorn University
Academic Year 2001

ISBN 974-03-1234-9

Thesis Title	Program Development for Predicting Pressure Loss in A Two-Phase Piping System(liquid-gas)
By	Mrs. Varisara Paditporn
Field of Study	Chemical Engineering
Thesis Advisor	Somprasong Srichai, Ph.D.
Thesis Co-advisor	Khun Noraphol Sookho

Accepted by the Faculty of Engineering, Chulalongkorn University in Partial Fulfillment of the Requirements for the Master 's Degree

.....Dean of Faculty of Engineering

(Professor Somsak Panyakeow, D.Eng.)

THESIS COMMITTEE

..... Chairman

(Professor Piyasan Praserthdam, Dr.Ing.)

..... Thesis Advisor

(Somprasong Srichai, Ph.D.)

..... Thesis Co-advisor

(Mr. Noraphol Sookho, Technologist)

..... Member

(Associate Professor Tawatchai Charinpanitkul, Dr.Eng.)

วริศรา ปดิฐพร : การพัฒนาโปรแกรมเพื่อทำนายค่าความดันลดในระบบท่อสำหรับการไหลแบบสองวัฏภาค (ของเหลว-ก๊าซ) (PROGRAM DEVELOPMENT FOR PREDICTING PRESSURE LOSS IN TWO-PHASE FLOW IN A PIPING SYSTEM (LIQUID-GAS)) อ.ที่ปรึกษา : ดร.สมประสงค์ ศรีชัย, อ.ที่ปรึกษาร่วม : นาย นรพล สุขโข, 106 หน้า ISBN 974-03-1234-9.

งานวิจัยฉบับนี้มีวัตถุประสงค์เพื่อพัฒนาโปรแกรมคอมพิวเตอร์สำหรับทำนายรูปแบบการไหลและคำนวณค่าความดันลดในท่อของของไหลแบบสองวัฏภาค (ของเหลว-ก๊าซ) ที่สภาวะอุณหภูมิคงที่ ซึ่งสามารถทำนายรูปแบบการไหลแบบสองวัฏภาคในท่อได้ทั้งแนวราบและแนวดิ่ง (ทิศขึ้นและทิศลง) การพัฒนาโปรแกรมได้ใช้โมเดลที่นำเสนอโดย Taitel Y. และ Duckler (1976) Taitel, Bomea และ Duckler (1980) และ Barnea, Shoham และ Taitel (1981) สำหรับทำนายรูปแบบการไหลในท่อทิศแนวราบ ทิศพุ่งขึ้น และทิศดิ่งลง ตามลำดับ สำหรับการคำนวณหาค่าความดันลดในระบบการไหลแบบสองวัฏภาคได้ใช้โมเดลที่นำเสนอโดย Taitel Y. และ Duckler (1980), Duckler และ Hubbard (1976), Duckler, Wick และ Cleveland (1964) , Fernandes, Semiat และ Duckler (1983) CS. Martin (1998).

โปรแกรมได้นำมาทดสอบเทียบกับผลจากการทดลองของนักวิจัยอื่นๆที่ทำการทดลองในท่อขนาด 0.75 - 3 นิ้ว ของน้ำและอากาศภายใต้สภาวะความดัน 1บรรยากาศ ถึง 5 บาร์เกจสามารถทำนายรูปแบบการไหลได้ในทิศทางแนวราบและแนวดิ่งได้ใกล้เคียงกับผลการทดลอง ยกเว้นบริเวณใกล้เคียงกับช่วงของการเปลี่ยนรูปแบบของการไหล ผลการคำนวณค่าความดันลดของรูปการไหล stratified flow จากโปรแกรมให้ค่าคลาดเคลื่อนมากกว่า 50%ที่ความดัน 1 บรรยากาศ ถึง 5 บาร์เกจ, ในท่อขนาด 0.75 ถึง 3 นิ้ว ความเร็วสัมพัทธ์ของก๊าซ 0.28 -0.56 ฟุต/วินาที, ความเร็วสัมพัทธ์ของน้ำ 5 - 22 ฟุต/วินาที และ slug flow จากโปรแกรมให้ค่าคลาดเคลื่อนอยู่ในช่วง ± 30 % ที่การทดลองที่ความดัน 1 บรรยากาศ ถึง 6 บาร์เกจ ในท่อขนาด 3 นิ้ว ความเร็วสัมพัทธ์ของก๊าซ 17 - 25 ฟุต/วินาที, ความเร็วสัมพัทธ์ของน้ำ 1 - 5 ฟุต/วินาที

ภาควิชา วิศวกรรมเคมี ลายมือชื่อนิสิต .....

ภาควิชา วิศวกรรมเคมี ลายมือชื่ออาจารย์ที่ปรึกษา .....

ปีการศึกษา 2544 ลายมือชื่ออาจารย์ที่ปรึกษาร่วม .....

4171488521 : MAJOR CHEMICAL ENGINEERING.

KEYWARD: TWO PHASE FLOW / FLOW PATTERN / PRESSURE LOSS / VOID FRACTION

VARISARA PADITPORN : PROGRAM DEVELOPMENT FOR PREDICTING PRESSURE LOSS IN A TWO-PHASE PIPING SYSTEM (LIQUID-GAS). THESIS ADVISOR : SOMPRASONG SRICHAI, Ph.D., THESIS CO ADVISOR: Mr. NORAPHOL SOOKHO, TECHNOLOGIST, THAI LUBE BASE PCL., 106 pp. ISBN 974-03-1234-9.

The objective of this research is to develop a computer program for predicting flow pattern and pressure loss in two-phase flow systems (gas-liquid) in isothermal cases of horizontal, vertical upward and vertical downward piping system. Visual Basic version 6.0 language was used for development of the two-phase program. Two-phase program was developed by using two-phase flow pattern models proposed by Taitel Y. and Duckler (1976), Taitel, Bornea and Duckler (1980), and Barnea, Shoham and Taitel (1981) for horizontal, vertical upward and vertical downward flow respectively. Two-phase pressure loss calculations were based on the studies of Taitel and Duckler (1980), Duckle and Hubbard (1975), Duckler, Wick and Cleveland (1964), Fernandes, Semiat and Duckler (1983) and Martin (1988).

Program results were tested against experimental data from other researchers for air and water in 0.75 - 3 inch under atmospheric pressure to 5 barG. The results of flow pattern prediction were consistent with the experimental data except some flow conditions close to the transition between flow patterns. Calculated pressure losses are over predicted by more than 50% for stratified flow under 1 BarA to 5 BarG, in 0.75 - 3 inch pipe, gas superficial velocity 0.28 - 0.56 ft/s, liquid superficial velocity 5 - 33 ft/s. Calculated pressure losses for slug flow are within ± 30% of the experimental value at 1 barA to 15 barG, in 3 inch pipe, air superficial velocity 17 - 25 ft/s, water superficial velocity 1 - 5 ft/s.

Department Chemical Engineering Student 's .....

Field of study Chemical Engineering Advisor 's .....

Academic year 2001 Co-Advisor 's .....

ACKNOWLEDGEMENT

The author would like to express her deepest gratitude to Dr. Somprasong Srichai, her adviser, for his continuous guidance, invaluable discussions, helpful suggestions and encouragement. She is also grateful to Professor Dr. Piyasan Praserthdam, Associate Professor Dr. Tawatchai Charinpanitkul, Mr. Noraphol Sookho as chairman and members of the thesis committee, for very helpful comments.

This research has been supported via Faculty of Engineering, Chulalongkorn University, CTCI (Thailand) Co., Ltd and Foster Wheeler International Corporation (Thailand Branch). The author would like to express her deep appreciation herein.

Finally, the author would like to give her sincere thanks to her parents, her boss , her collogues and friends for their encouragement throughout this study.

CONTENTS

CONTENTS (CONT.)

PAGE

Chapter

LIST OF TABLE

LIST OF TABLE (CONTINUE)

LIST OF FIGURE

LIST OF FIGURE (CONTINUE)

LIST OF FIGURE (CONTINUE)

FIGURE PAGE

NOMENCLATURE

LETERS	DESCRIPTIONS	DIMENSIONS
ε	void fraction	-
A	pipe cross sectional area	$inch^2$
Co	distribution parameter	-
dP	pressure drop	psi
$\frac{dP}{dL}$	unit pressure loss	psi/ft
D	pipe inside diameter	inch
α	angle of inclination	degree
e	characteristic height of roughness	ft
f	Moody friction factor	-
F	Modified Froude Number	-
$\frac{f_{TP}}{fo}$	ratio of two phase to single phase friction factor	-
g	acceleration of gravity	ft/s^2
g_c	gravitational factor	$lb_m ft/(lb_f\ s^2)$
H_L	Drift flux liquid hold up	
$\frac{h_L}{D}$	liquid height dimensionless	-
K	Bankoff flow parameter	-
Kd	Drift flux coefficient	-
λ	liquid volume fraction	-
L	sectional pipe length	ft
N_{FR}	Froude Number	-
NPS	norminal pipe size	inch
M	momentum	$lb_m/(ft^2\ s^2)$
P	pressure	psi
Q	volumetric flow rate	ft^3/s
R	ideal gas constant	$ft^3 lb_f/(in^2 lb\ mol\ ^oR)$
R_L	liquid hold up	-
Re	Reynolds number	-

NOMENCLATURE (CONT.)

LETERS	DESCRIPTIONS	DIMENSIONS
S	wetted perimeter	inch
T	temperature	^{o}F
u	velocity	ft/s
u_0	bubble rise velocity	ft/s
X	Lockhart-Matinelli parameter	-
x	gas quality	-
Y	slope parameter	-

Greek letter

μ	viscosity	cP
Pi	constant	-
ρ	density	lb_m/ft^3
σ	sigma surface tension	
τ	shear stress	$lb/(ft\ s^2)$
δ	liquid film thickness	inch
α	angle of inclination	degree

Subscript

a	acceleration effect
f	frictional effect
g	gravitation effect
G	gas
i	gas – liquid interface
L	liquid
$_{L}^{S}$	liquid superficial velocity
$_{G}^{S}$	gas superficial velocity
M	mean
W	pipe wall
TP	two-phase
S	slug
~	dimensionless

CHAPTER I

INTRODUCTION

A wide range of industrial systems, such as thermosiphon reboilers, chemical reactors, heat exchangers, refrigeration, distillation, natural gas pipe line transfer involve gas–liquid two-phase flow. Design of this type s of these system requires an understanding of the phenomena of two-phase flow for correctly predicting flow pattern, and pressure loss. An understanding of two-phase flow is essential for the reliable and cost-effective design of equipment and pipelines in the system.

Two-Phase flow is the simultaneous flow of two states of matter and can be a gas-solid, gas-liquid , or liquid-solid system. This study will however investigate two-phase flow for gas-liquid system, the phenomena of which is more complex than a single phase flow. Flow patterns shall be categorized by the flow condition, pipe orientation (horizontal, vertical upward and vertical downward direction) for determination of flow patterns and pressure loss.

Undesirable flow pattern such as slug flow in pipeline systems that are not adequate designed for this type of flow can result in additional force and pressure losses which can cause unstable pressure control leading to mechanical failure of the piping system, its support structure and related equipment. It is important to predict the flow pattern and pressure loss for two-phase flow system correctly and accurately in order to include this information in the design of pipe layout to meet both process requirement and mechanical design requirement.

There are a great number of researchers who have studied techniques for analyzing two-phase flow and proposed equations to predict pressure loss in empirical or physical mechanism basis. The proposed equation have been tested against the experimental data in the specific test condition and it is found that no one method of determining flow pattern and pressure loss calculation is good for all situations but a combination of each technique is required based on the conditions of the flow.

To facilitate in designing pipeline system involving two-phase gas-liquid flow, a software program is developed in this study for reducing the long calculation time. This program is used for predicting flow pattern and its associated pressure drop after giving, phase flow rate, physical properties and pipe orientation.

1.1 Objective

To develop a computer program for predicting flow pattern and calculating pressure loss from the predicted flow pattern in a two-phase gas liquid piping system.

1.2 Scope of work

Two-phase gas and liquid flow is limited in a concurrent flow for commercial pipe sizes. Gases and liquids are considered as Newtonian fluids flowing in an isothermal and steady state system with no phase change.

1 Flow pattern transitions are classified and studied by physical mechanism in horizontal & inclined, vertical upward and vertical downward direction as shown in Figure 1.2-1.

2 Pressure loss is calculated by use of the model based on the type of flow pattern that is calculated from parameters mentioned in item 1 above.

3 Total pressure loss in a piping system is calculated from the summation of individual pressure losses in each pipe route direction along the pipe length..

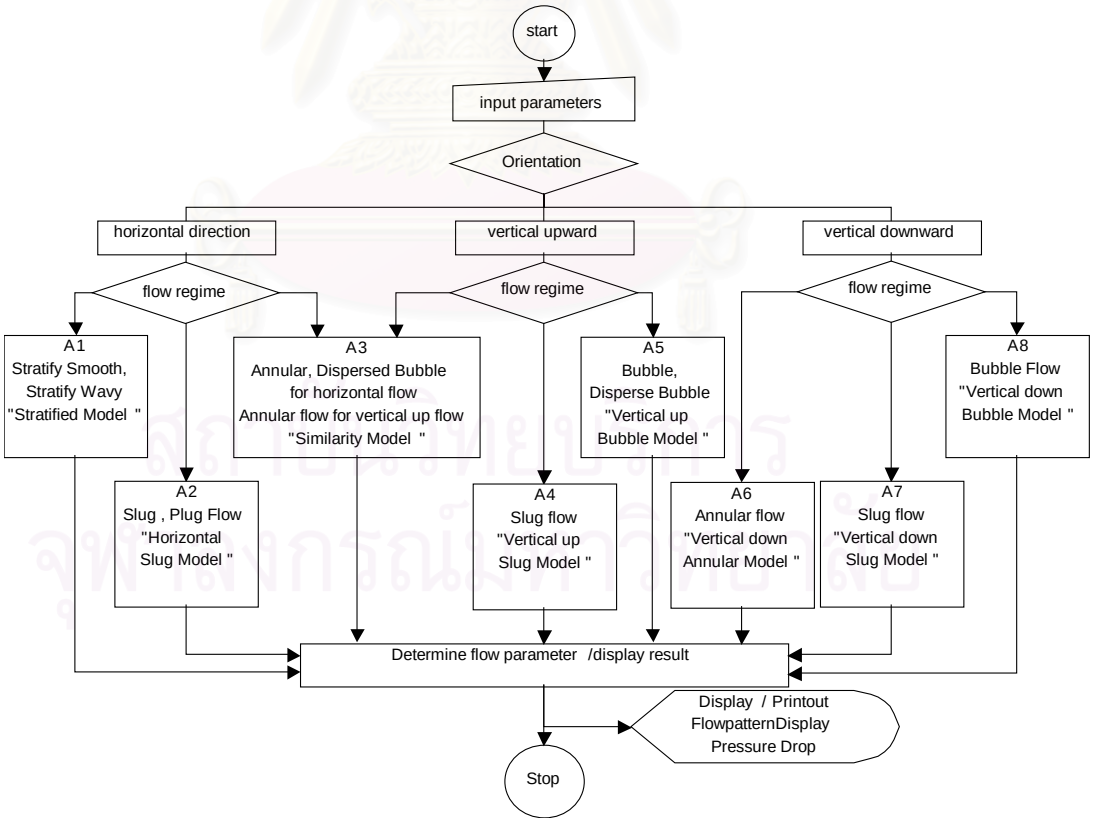

Figure 1.2-1 Main structure of developed program

CHAPTER II

LITERATURE REVIEW

One of the most important aspects of the study of two-phase flow in pipes is the understanding of flow pattern characteristics and pressure loss calculations. Many researchers have proposed flow pattern maps or flow regimes based on their experimental data. Some flow pattern maps are developed from empirical methods whilst others are developed on physical studies as shown in the flow pattern section. After predicting the flow pattern, liquid hold up is used to calculate pressure loss in two-phase gas-liquid systems in each of the flow models, The liquid hold up is the ratio of liquid cross sectional to the total pipe cross section area. Literature relating to this study appears in the following section.

2.1 Classification of Flow pattern

Two-Phase flow patterns can be classified into three broad categories namely, dispersed flow, separated flow, and intermittent flow as illustrated in Figure 2.1-1.

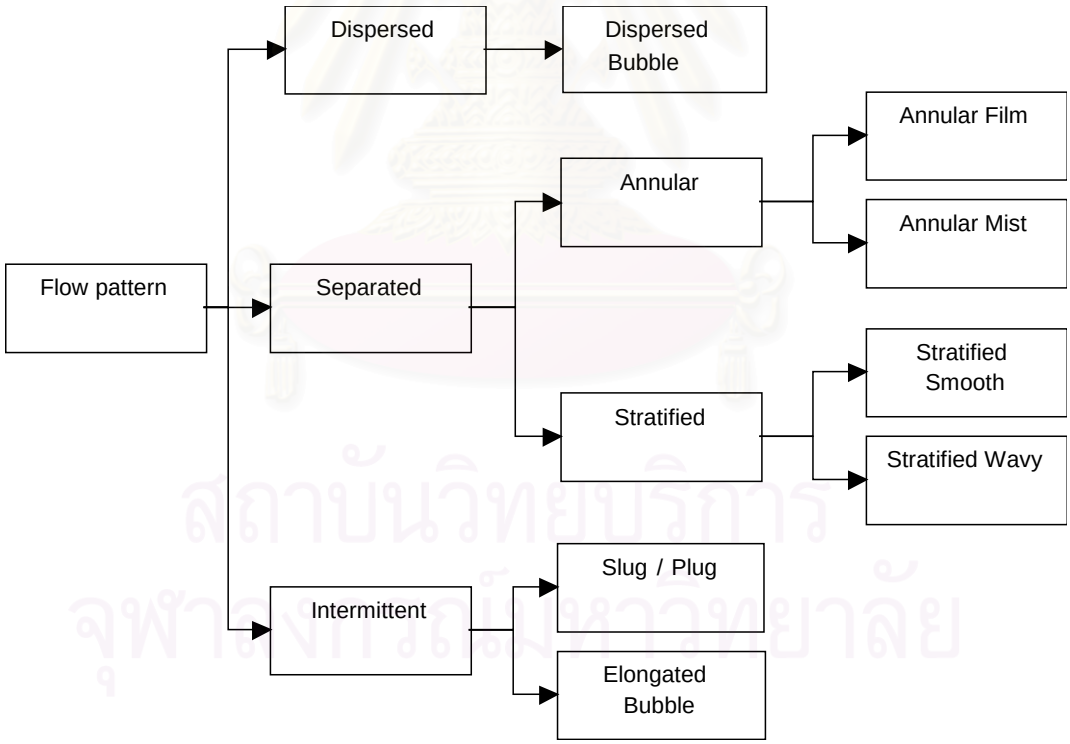

Figure 2.1-1 Flow pattern classification (Dr. Somprasong,1994)

Spedding and Ngyen (1979) proposed flow pattern maps from their experimental data in horizontal and vertical upward to vertical downward flows. Their experiment used air and water in a 4.55 cm diameter pipe. Air flow rates up to 500 kg/hr and water flow rates up to 5000 kg/hr were accommodated in the test rig. They found that some flow patterns such

as stratified flow appeared only in horizontal flow direction and not in vertical upward or downward flow. There were 13 distinguishable flow patterns as shown in Figure 2.1-2. These flow patterns can be combined in 4 main types.

(a) Stratified flow, designed type X, were those in which both gas and liquid phase was continuous without liquid droplet or bubble formation occurring. These include stratified, stratified plus ripple, stratified plus roll wave, annular flow. The condition for separated flow can be found from the small amount of gas and liquid flow in the pipe, stratified flow was occurred. As the gas flow rate was increased for a definite low liquid flow rate, the liquid surface was observed to pass successively from stratified flow to ripple waves and then roll waves. The condition of annular can be found from the slug when increasing gas flow rate until it is high enough that the liquid slug will be blown to be annular flow.

(b) Bubble and slug flow, designed type B, were those in which the gas phase was discontinuous while the liquid phase was continuous. The condition for bubble flow can be found at a very high liquid. Slug flow was observed when the amount of liquid was moderate and almost filled the pipe. Increasing the gas phase let to the formation of slug flow.

(c) Droplet flow, designed type C, were those in which the liquid phase was discontinuous and gas phase was continuous. The condition for droplet flow was observed when the degree of liquid was low until moderate and gas flow rate was high enough to dispersed small amount of liquid surface until the flow was completely droplet. Droplet flow can be developed from stratified flow and annular flow when increasing gas flow rate.

(d) Mixed flow, designed type M, were those in which both gas and liquid phase was discontinuous and thus includes all other flow patterns.

The data from Spedding et. al. indicated that for vertical upward flow, bubble and slug flow were found regardless of the magnitude of the liquid flow rate. In vertical downward flow, annular flow was found relatively easily and bubble flow was difficult to achieve.

The data from their experimental work was used to develop a flow pattern map using the volumetric flow rate ratio QL/QG and the Froude number $V_T / \sqrt{gD}$ for the X axis and Y axis respectively. Their proposed flow regime are shown in Figure 2.1-3, 2.1-4, 2.1-5 for horizontal, vertical upward and vertical downward flows respectively. The transition between the flow regimes of type B, X, M, and D were shown in solid lines and the further subdivisions of these main flow regime types are indicated by the dotted lines.

The proposed flow pattern maps were compared against other previous works and it was found that it was unlikely that a universal map could correctly predict flow regimes for two-phase flow situations. Spedding et.al. did not consider the effect of pipe diameter on the

type of flow regime which could be expected to have a significant effect on the accuracy of these maps.

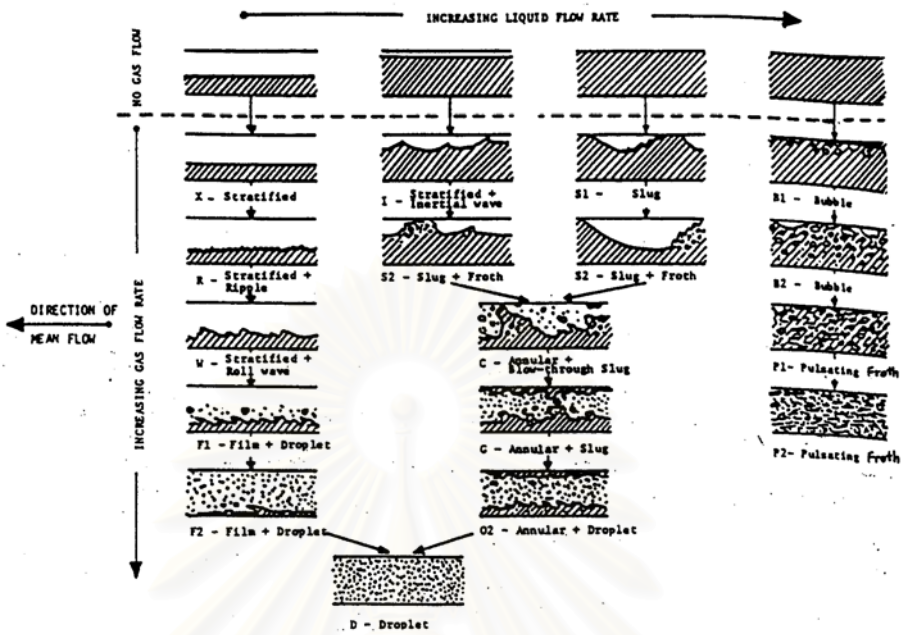

Figure 2.1-2 Schematic diagram of the flow pattern sequence observed for horizontal flow (Spedding et.al. 1979)

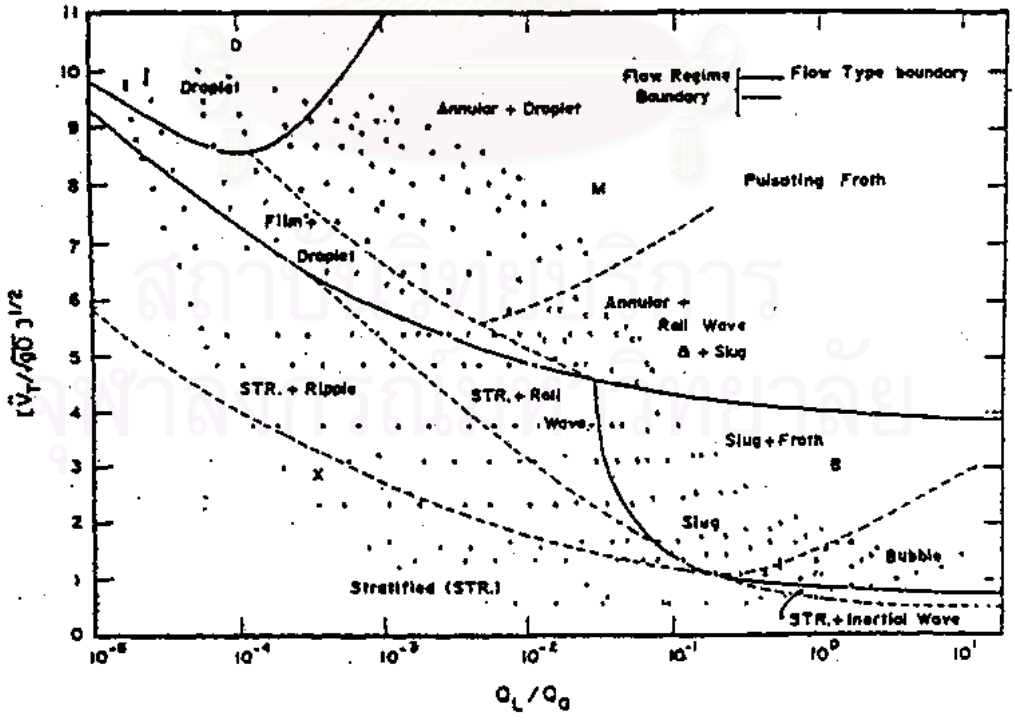

Figure 2.1-3 Flow pattern map for horizontal flow (Spedding et.al. 1979)

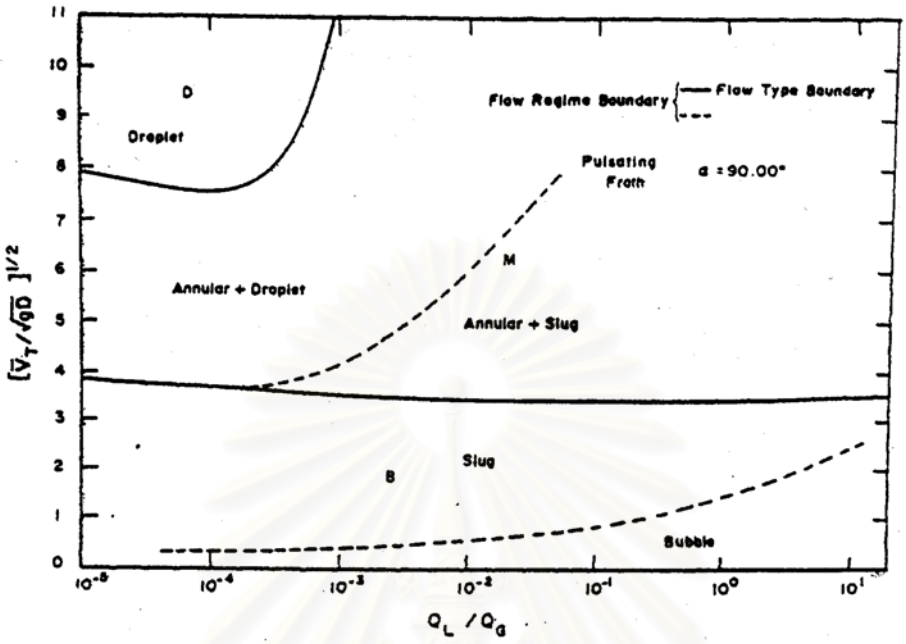

Figure 2.1-4 Flow pattern map for vertical upward flow (Spedding et.al. 1979)

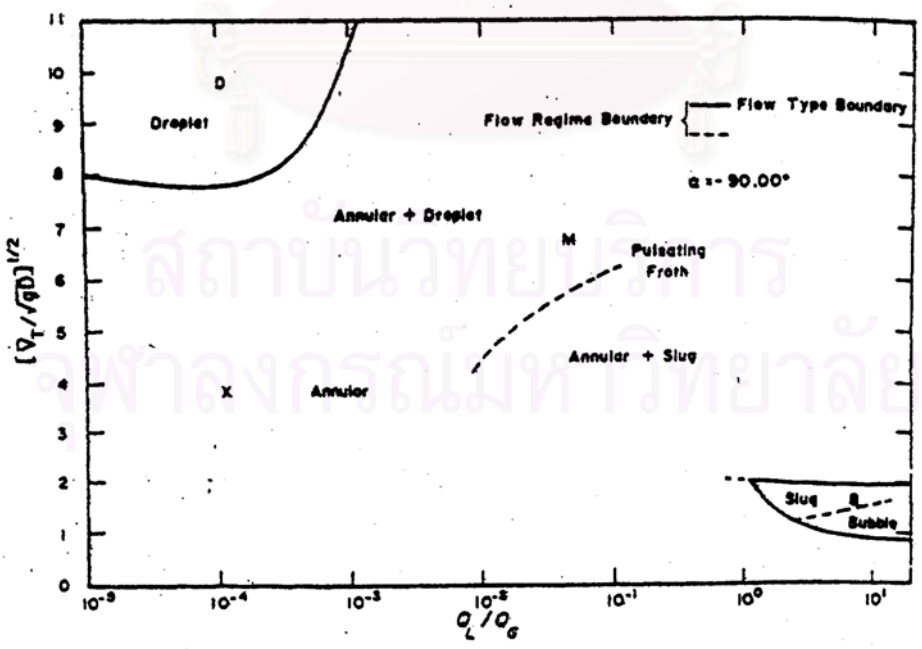

Figure 2.1-5 Flow pattern map for vertical downward flow (Spedding et.al. 1979)

Baker(1954) proposed an empirical map for horizontal flow based on air–water data. The correlation was plotted in terms of $\dot{m}_G/\lambda$ versus $\lambda\varphi/\dot{m}_G$ as shown in Figure 2.1-6 which is in terms of fluid properties. $\dot{m}_G$ and $\dot{m}_L$ were are defined as the gas and liquid mass velocities in lb/(hr- ft2). λ and φ are fluid property correction factors and are defined in below equations respectively.

$$\lambda = \left[\left(\frac{\rho_G}{0.075}\right)\left(\frac{\rho_L}{62.3}\right)\right]^{0.5} \tag{2-1}$$

$$\varphi = \frac{73.0}{\sigma}\left[\left(\frac{\mu_L}{1.0}\right)\left(\frac{62.3}{\rho_L}\right)^2\right]^{1/3} \tag{2-2}$$

where ρ_L and ρ_G are liquid and gas densities in lb/ft^3, μ_L is the liquid viscosity in centipoises and σ is the surface tension in dyne/cm. Flow patterns such as bubble, plug, stratified, wavy, slug, annular for oil and gas were observed in a 4 to 10 inch inside diameter range. Pressure loss was calculated using modified Fanning equation and it was found that the pressure drops for large pipe (8 inch and larger) were 40-60 % less than those predicted by Lockhart-Martinelli correlation (1949).

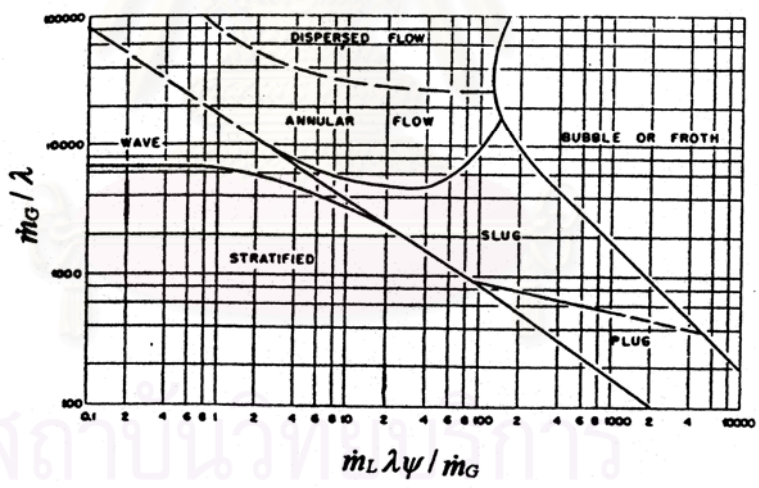

Figure 2.1-6 Flow patterns for horizontal two-phase flow (Baker et.al. 1958)

J.A., Manhane, G.A Gregory, K. Aziz(1974) introduced the use of superficial velocities coordinates in the flow pattern map. This has been widely accepted and has been used by most of researchers to date. Their flow pattern maps used a large data bank of data for fluids varying physical properties. The transition boundaries on the map were plotted bases on correlations developed from over 1000 data points from as air-water system. In order to apply the air–water flow pattern map to other liquids, physical property corrections were applied.

To correct the physical properties, the transition lines, which were a function of the gas and liquid velocities, would be multiplied by the correction factor give in Table 2.1-1 in which the parameter X was used to multiply to the value of u_G and parameter Y was used to multiply to the value of u_L.

$$X = \left(\frac{\rho_G}{0.0808}\right)^{0.2}\left(\frac{\rho_L}{62.4}\times\frac{72.4}{\sigma}\right)^{0.25}\left(\frac{\mu_G}{0.018}\right)^{0.2} \quad (2\text{-}3)$$

$$Y = \left(\frac{\mu_L}{1.0}\right)^{0.2}\left(\frac{\rho_L}{62.4}\times\frac{72.4}{\sigma}\right)^{0.25} \quad (2\text{-}4)$$

where ρ_L and ρ_G are liquid and gas densities in lb/ft^3, μ_L is the liquid viscosity in centipoises and σ is the surface tension in dyne/cm.

Table 2.2-1 Coordinates for transition boundaries of Mandhane et. al. (1974) flow pattern map

Transition boundary	UG (ft/s)	UL (ft/s)	Physical properties correction – multiply equation of transition boundary by
Stratified to elongated bubble	0.1 0.5	0.5 0.5	1.0/Y
Wave to Slug	7.5 40	0.3 0.3	Y
Elongated bubble and slug to dispersed bubble	0.1 230	14.0 14.0	Y
Stratified and elongated bubble to wave and slug	3.5 14.0 10.5 2.5	0.01 0.1 0.2 1.15	X
Wave and slug to Annular-mist	70 60 38 40 50 100	0.01 0.1 0.3 0.55 1.0 2.5	X
Dispersed bubble to Annular-mist	230 269	14.0 30	X

Flow pattern maps for two-phase flow in pipes of small hydraulic diameter were studied by J.W. Colwman, S. Girimella (1999). Round and rectangular tubes in the size of 1.3 mm to 5.5 mm inside diameter in the horizontal direction were used. Flow patterns for co-current flow of air–water mixtures were determined by video analysis to develop flow pattern maps and transitions. Gas and liquid superficial velocities were in the range of 0.1 to 100 m/s, and 0.01 to 10 m/s, respectively. Bubble, dispersed bubble, elongated bubble, slug, stratified wavy, annular flows were observed. The interaction of gravity, inertial shear and surface tension force and tube diameter were found to effect to flow pattern transition.

2.2 Pressure Loss

Lockhart-Martinelli (1949) proposed a correlation to predict pressure loss and liquid hold up of two-phase flow. Their experiment was performed with air and liquids including benzene, kerosene, water and various oils in pipes varying in diameter from 14.9 mm to 25.8 mm. They proposed a graphical correlation by assuming that the static pressure in both phases was equal, and the volume occupied by liquid plus the volume occupied by the gas at any instant must equal to total volume of the pipe. The parameter X, the dimensionless pressure drop, Φ_G and Φ_L was introduced as follows

$$\Phi_G{}^2 = \frac{(dp/dz)_{TP}}{(dp/dz)_G} \tag{2-5}$$

$$\Phi_L{}^2 = \frac{(dp/dz)_{TP}}{(dp/dz)_L} \tag{2-6}$$

$$X^2 = \frac{(dp/dz)_L}{(dp/dz)_G} \tag{2-7}$$

where $(dp/dz)_{TP}$ is the total two-phase pressure gradient.

Four sets of curves were given depending on whether the single phase in the pipe were laminar or turbulent (namely turbulent-turbulent, turbulent-laminar, laminar- turbulent, laminar- laminar flows where the first would given the state of the liquid flow alone and the second would the gas flow alone on pipe). However Lockhart and Martinelli 's correlation did not take into account the flow pattern, except that slug flow was excluded, and had limited accuracy. The multiplier Φ_G and Φ_L were fitted by Chisholm (1967) using the following equations:

$$\Phi_G{}^2 = 1 + CX + X^2 \tag{2-8}$$

$$\Phi_L{}^2 = 1 + \frac{C}{X} + \frac{1}{X^2} \tag{2-9}$$

Where C is a dimensionless parameter dependent on the nature (turbulent or laminar) of the gas and liquid phases. For the most common situation when both phases were turbulent, C had a value of 20. The above equations were found to fit the original correlation extremely well.

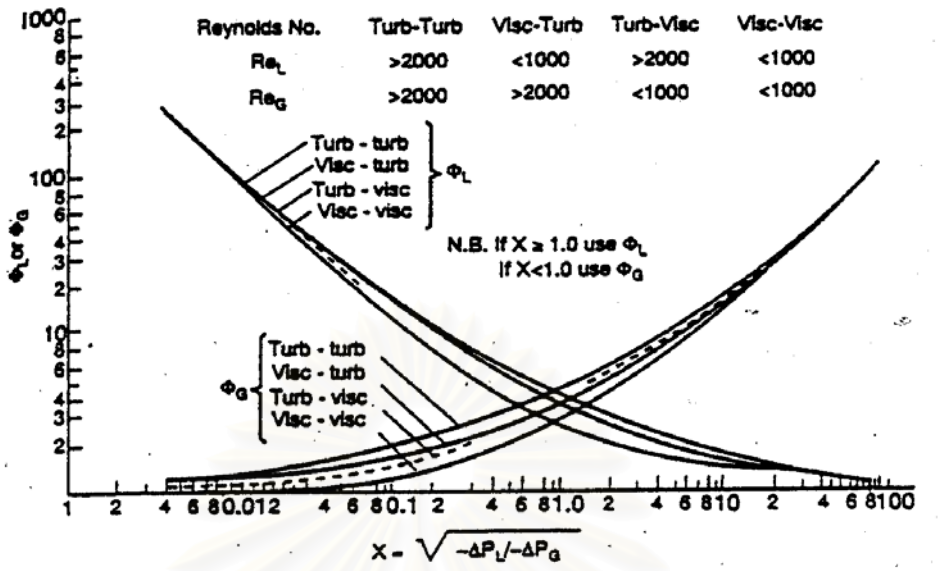

Figure 2.2-1 Correlation of Lockhart and Martinelli (1949) in which the pressure drop multiplier (Φ) and the hold up (ε) were related to X.

Hoogendoorn (1959) carried out experiments on air-water, air–oil system in a variety of pipe diameters (24, 50, 91,and 140 mm). The Lockhart and Martinelli 's correlation was applied for the pressure drop prediction and it was claimed that the correlation was accurate only for slug and froth flow at the atmospheric pressure. The gas phase hold up, ε_G, was corrected empirically with the slip velocity between the phases in m/s.

$$\frac{\varepsilon_G}{1-\varepsilon_G} = A\left(\varepsilon_G u'\right)^{0.85} \tag{2-10}$$

$$u' = \frac{u_G}{\varepsilon_G} - \frac{u_L}{1-\varepsilon_G} \tag{2-11}$$

where A constant is equal to 0.60

GA. Hughmark, B.S. Pressburg (1961) proposed generalized correlation for hold up and pressure drop in isothermal two-phase concurrent upward flow in vertical tubes. Both pressure drop and liquid hold up correlations could be predicted without knowing the exact flow pattern. These correlations were tested with the experimental data in the range of pipe diameter 0.4 to 2.34 inch.

J. Orikiszewski (1967) reported a comparative result of pressure loss calculations in two-phase gas liquid in gas lift production wells (in vertical pipes) between calculated methods and the measured methods from 148 oil wells. He calculated pressure losses from threes groups to compare with measured data.

1. Poettman and Carpenter (1952) and Tek (1961). This method does not consider liquid hold up in density and flow pattern prediction. Friction losses are calculated from an empirically correlated friction factor.

2. Hughmark and Pressburge (1961). This method uses liquid hold up in density calculations. The friction losses are based on of gas and liquid densities. Flow pattern is not involved in pressure loss calculations.

3. Griffith and Walli (1961) and Dons and Ross (1963). Liquid hold up is calculated from the basis of slip velocity (the different between gas and liquid velocities). The distinction of flow patterns is considered in pressure loss calculations.

From the above methods, the results were compared by determining the deviations. It was found that the most accurate method is the method in the third group, Don-Ros and Griffith-Wallis method, for two-phase in gas lift operation well. He found that there is no method which was accurate over the entire range of conditions used. Griffith-Wallis method was reliable in the low flow rate range of slug flow. It was not accurate in the high range. The Don-Ros method exhibited the same behavior except that it was inaccurate for the high-viscosity oil in the low flow rate. The considered flow patterns are bubble, slug, annular-slug and annular-mist.

Jiede Yang, Cem Sarica, Xuanzheng Chen, Chen Brill (1996) proposed a mechanistic model based on a slug structure for downward inclined pipe from air-kerosene tested data in a 2 inch, 75 ft length pipe. They proposed a method to calculate the slug transitional velocity, slug length, slug frequency and liquid hold up. The calculated pressure gradient was compared with the result of Duckler and Hubbard (1975) and found that the results of pressure loss from Duckler and Hubbard were high. Their method was also tested against experimental data. They concluded that the mechanistic model gave a good estimation of the pressure gradient with an average of $\pm$ 15%.

C. Sarica, O. Shoham, J. Brill and Y. Taitel (1991) proposed a result of two different types of flow patterns for operating off shore wet gas using Simplified Transient Simulator Program. The gas and liquid produced from the field were separated at the platform and transported to Gas Plant on shore. When heavier hydrocarbons condensed by the sea water temperature, liquid phase in pipe line could accumulate in the offshore section at low input flow rates. Slug flow conditions occurred and frequent pigging process was required. For high input flow rates, stratified flow condition occurred, resulting in less liquid accumulation and liquid was transported in to the onshore. These different modes were related in leak detection analysis for pipeline system. Liquid hold up and pressure loss calculation from their simulator were based on the method proposed by Begg and Brill correlation (1983).

Malasri (2001) studied two-phase air water flow in the vertical upward in glass tube, 19 mm inside diameter, at atmospheric pressure outlet conditions. The superficial gas velocity was in the range of 0.003 to 0.7 m/s and superficial liquid velocity was in the range of 0 to 0.742 m/s. By increase in the superficial air velocity, maintaining constant superficial water velocity bubble to slug flow transition occurred in a range of transition values, not a single point value.

Winai et. al (1995) studied the flow pattern map of air-water co-current flow at ambient condition and the flow pattern maps for developing steady state and transients flow were determined. The experiment was performed in 54 mm and 29 mm inside diameter. Flow pattern types of the form, stratified flow, stratified wavy, plug and slug flow were observed. In the developing the steady state flow, air flow rate was increased in small increments while the water flow rate was hold constant at the selected value. Transient flow experiments performed under constant air and water flow rate, followed by a sudden increase in the air flow rate, which resulted in temporary wavy flow occurring in the beginning with the final flow pattern being stratified flow. In the same manner temporary slug flow occurred in the stratified wavy flow condition.

CHAPTER III

CALCULATION BASIS

3.1 Flow pattern classification

The flow observed in two-phase gas liquid flow has many different configurations with respect to the distribution of the gas and liquid interfaces. Classification of flow patterns has not yet been accurately standardized and in many cases the flow pattern definition depends largely on the individual interpretation of each study. The following section describes characteristics of flow patterns categorized the pipe orientation.

3.1.1 Horizontal & inclined flow direction

Flow patterns for two phase flow in horizontal & inclination direction can be classified in five patterns based on physical mechanisms proposed by Taitel and Duckler (1976) as shown in Figure 3.1.1-1 and the descriptions are as below:

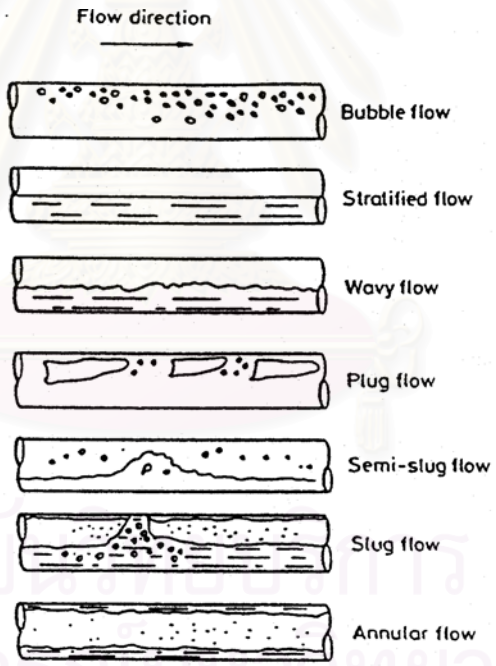

Figure 3.1.1-1 Flow patterns in horizontal direction (Taitel and Duckler 1976)

1) Stratified smooth (SS)

This pattern is found in a range of low gas velocities. Liquid flows along the bottom of the pipe, and the liquid surface is smooth. Sometime stratified smooth is called stratified flow.

2) Stratified wavy (SW)

The liquid flows as a stratified layer, but increased gas velocity causes its surface to develop waves. Sometime stratified wavy is called wavy flow.

3) Intermittent/slug and plug (I)

The liquid bridges the pipe cross section forming a slug or a plug. The liquid slug moves down the pipe at the gas velocity. Sometime intermittent is called slug or plug flow

4) annular with dispersed liquid (AD)

The liquid flows as an annular film on the pipe wall with the gas phase flowing as a central core. Some of the liquid is entrained as droplet in this gas core. The annular liquid film is thicker at the bottom than at the top of pipe, except at very low liquid rates, the liquid film is covered with the large waves.

5) dispersed bubble (DB)

At high liquid rates and low gas rates, the gas is dispersed as bubble in a continuous liquid phase. The concentration of these bubbles is higher above the pipe centerline than below.

3.1.2 Vertical upward direction

Flow patterns for two phase flow in vertical upward direction can be classified in four patterns from the study of Hewitt and Hall-Taylor (1970) as shown in figure 3.1.2-1 and the detail descriptions are as below:

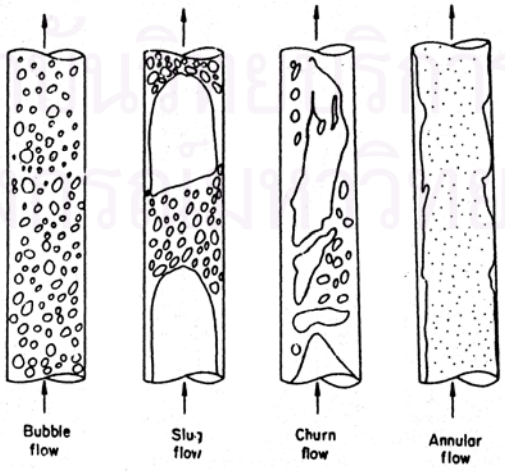

Figure 3.1.2-1 Flow patterns in vertical upward direction (Hewitt and Hall-Taylor 1970)

1) bubble flow

The gas phase is approximately uniformly distributed in the form of discrete bubbles in a continuous liquid phase.

2) slug flow

Most of the gas is located in a large bullet shaped bubble having a diameter almost equal to the pipe diameter. The gas bubbles move uniformly upward and are referred as “Taylor bubbles”. Taylor bubbles are separated by slugs of continuous liquid, bridging the pipe and contain small gas bubbles between the Taylor bubbles and the pipe wall. Liquid between pipe wall and the Taylor bubble flows downward in the form of a thin film.

3) churn flow

Churn flow is similar to slug flow but much more chaotic, frothy and disordered. The bullet shaped Taylor becomes narrow, and its shape is disordered. There is no clear structure and the flow is highly irregular. The Taylor bubble is destroyed by the high gas rate in the slug.

4) annular flow

Annular flow is characterized by the continuity of the gas phase in the core of pipe. Liquid phase moves upward partly as a wavy liquid film and partly in the form of liquid traveling as entrained droplet in the gas core.

3.1.3 Vertical downward direction

Flow patterns for two phase flow in downward direction can be classified in 3 (three) patterns based on experimental observed of Barnea, Shoham and Taitel (1982) as shown in figure 3.1.3-1 and the detail descriptions are as below:

1) annular flow

The most natural regime in vertical downward is annular flow. Similar to annular upward flow, it is characterized by the continuity of an axial gas core. Liquid phase move downward partly as liquid film and partly as in the forms of drops entrained in the gas core. Even at very low liquid rate without gas, the liquid moves as a symmetrical falling film.

2) intermittent flow

A high liquid flow rate transition from annular to slug flow will take place. The gas flows downward in the form of large bubbles that are separated by liquid slugs that bridge the pipe

and usually contain small gas bubbles. The major difference between downward slug and upward slug is that gas bubble shape of a downward slug is eccentric relative to the pipe axis.

3) dispersed bubble flow

Similar to upward flow, bubble flow is characterized by uniformed distributed bubbles in the continuous liquid phase.

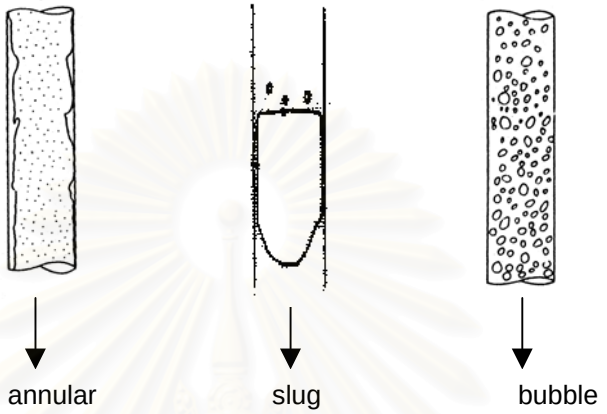

Figure 3.1.3-1 Flow patterns in vertical downward direction

3.2 Flow pattern map determination

Flow pattern maps are used for classification of flow patterns or flow regimes of two-phase gas liquid flow. Flow pattern map is based on physical concepts and the relationship between gas and liquid mass flow rate, fluid physical properties, pipe diameter, and angle of pipe inclination. Due to the difference of flow patterns found in the pipe orientation, the flow pattern map can be categorized in three main types (horizontal/ inclined, vertical upward and vertical downward direction map). Details of determination are as below.

3.2.1 Flow pattern map for horizontal and inclined flow direction

There are five basic flow patterns in analyzing flow patterns in horizontal flow: (SS) stratified smooth, (SW) stratified wavy, (I) intermittent–slug and plug, (AD) annular with dispersed liquid, and (DB) dispersed bubble. The process starts from the condition of stratified flow by obtaining the solution of the force balance equation. Combination of the pressure loss with fluid properties into dimensionless forms (X, Y, F, K) allows the classification of the flow pattern. The generalized flow pattern map is shown in Fig 3.2.1-1.

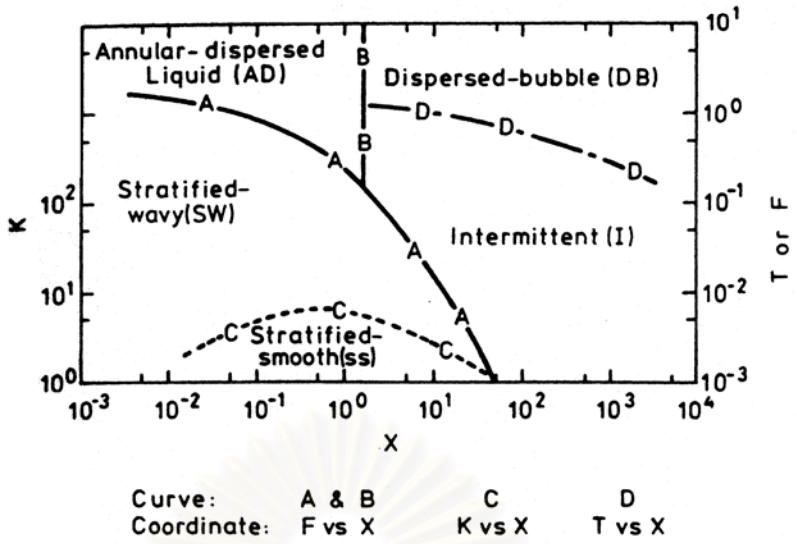

Fig 3.2.1-1 Flow pattern map for horizontal direction (Taitel and Duckler 1976)

$$X = \left[\frac{\left| \left(dP/dZ \right)_L^{\ S} \right|}{\left| \left(dP/dZ \right)_G^{\ S} \right|} \right]^{1/2} \tag{3-1}$$

$$Y = \frac{(\rho_L - \rho_G) g \sin(\deg)}{\left| \left(dP/dZ \right)_G^{\ S} \right|} \tag{3-2}$$

$$F = \frac{u_G^{\ S}}{\sqrt{Dg \cos\alpha}} \sqrt{\frac{\rho_G}{(\rho_L - \rho_G)}} \tag{3-3}$$

$$K = F \times (\mathrm{Re}_L^{\ S})^{1/2} \tag{3-4}$$

$$T = \left[\frac{(dP/dZ)_L^{\ S}}{(\rho_L - \rho_G) g \cos\alpha} \right]^{1/2} \tag{3-5}$$

where

X is the parameter introduced by Lockhart and Martinelli (1949) which is the ratio of liquid phase pressure drop and gas phase pressure drop along the pipe.

Y is a relative force acting on the liquid due to the gravity force and pressure drop of gas phase along the pipe

F is a dimensionless parameter modified with the density ratio named Froude Number.

K, T are dimensionless numbers used for determining horizontal flow transition

Flow patterns are separated by transition solid lines (A, B, C, D) on the map. The graph coordinates in the horizontal and vertical axis (K, X, T, F) and transition lines (A, B, C, D D) are summarized in Table 3.2.1-1.

Table 3.2.1-1 Flow pattern transition defined by dimensionless groups.

Transition	Dimensionless Group
stratified to intermittent (A)	F, X, A
stratified to annular dispersed liquid (A)	F, X, A
stratified smooth to stratified wavy(C)	K, X, C
intermittent to dispersed bubble (D)	T, X, D
intermittent to annular dispersed liquid (B)	F, X, B

1) Transition between stratified and non-stratified (Transition A)

At low flow rate, stratified flow is observed however as the flow increase to the range in which intermittent flow occurs the flow pattern changes to intermittent flow. As the liquid rate is increased while the gas rate is low, the liquid level rises and waves are formed and grow rapidly to block the gas flow and cause intermittent flow. Under conditions of high gas rates and low liquid rate, there is insufficient liquid flow and the liquid in the wave is swept up and round the pipe to form annular flow.

Consider the gas flow over a solid wave in the flat plate in Figure 3.2.1-2, liquid height h'_L, and the gas gap dimension h'_G. The equilibrium dimensions are h_L and h_G. Pressure at the equilibrium and above the wave are P and P'. If the motion of the wave is neglected, the condition for wave growth can be shown as

$$P - P' > (h_G - h'_G)(\rho_L - \rho_G)g \tag{3-6}$$

The pressure difference is determined by

$$P - P' = \frac{1}{2} \times \rho_G (u'^{\,2}_G - u^{\,2}_G) \tag{3-7}$$

The criterion for instability when C_1 is equal to 1 and the instability becomes

$$u_G > C_1 \times \left(\frac{g(\rho_L - \rho_G)h_G}{\rho_G} \right)^{0.5} \tag{3-8}$$

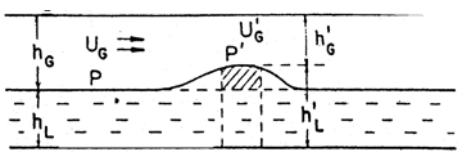

Figure 3.2.1-2 Instability for wave generation

This simple analysis can be easily extended to the round pipe and inclined pipe with the Taylor series. It is suggested that the below equation describes the conditions from stratified (S) to intermittent (I) and to annular dispersed liquid (A) flow.

$$u_G > C_2\left[\frac{(\rho_L-\rho_G)g\cos(\alpha)A_G}{\rho_G(dA_L/dh_L)}\right]^{1/2} \quad (3\text{-}9)$$

when parameter C_2 and (dA_L/dh_L) are determined by

$$C_2 = 1-\frac{h_L}{D} = 1-\tilde{h}_L \quad (3\text{-}10)$$

$$dA_L/dh_L = \sqrt{1-(2\tilde{h}_L-1)^2} \quad (3\text{-}11)$$

Transition between stratified and non-stratified flow can be written in dimensionless form as below equation. Note that all the terms in the square brackets are functions of $\tilde{h}_L$.

$$F^2\left[\frac{1}{C_2^{\,2}}\times\frac{\tilde{u}_G(d\tilde{A}_L/d\tilde{h}_L)}{\tilde{A}_G}\right]\geq 1 \quad (3\text{-}12)$$

where parameter $\tilde{u}_G$ and $\tilde{A}_G$ are determined by

$$\tilde{u}_G = \frac{\tilde{A}}{\tilde{A}_G} = \frac{\pi/4}{\tilde{A}_G} \quad (3\text{-}13)$$

$$\tilde{A}_G = 0.25\left[\cos^{-1}\left(2\tilde{h}_L-1\right)-\left(2\tilde{h}_L-1\right)\sqrt{1-\left(2\tilde{h}_L-1\right)^2}\right] \quad (3\text{-}14)$$

2) Transition between intermittent and annular dispersed liquid (transition B)

Equation (3-12) gives the relationship under which the flow pattern can be classed to be either stratified or non stratified. If it is observed that the flow is non stratified, the flow pattern can be then separated into intermittent or annular dispersed flow along the transition B. A stable slug can form when the supply of liquid in the film is large enough to maintained a slug flow. If the liquid level is not enough, the wave is swept by the high gas rate around the pipe wall as described by Butterworth (1972), and annular or annular mist will take place. It is suggested that intermittent flow will develop when liquid height in the pipe exceeds half the pipe diameter, as indicated below and if liquid level is less than half of the pipe, annular or annular dispersed liquid flow will result.

$$\frac{h_L}{D} = 0.5 \quad (3\text{-}15)$$

3) Transition between intermittent and dispersed bubble (transition D)

At high liquid rates and low gas rates, the equilibrium liquid level approaches the top of the pipe. With such a fast running liquid stream, the gas tends to mix with the liquid. It is suggested that the transition to dispersed bubble flow takes place when the liquid turbulent

fluctuations are strong enough to overcome the buoyancy forces tending to keep bubble at the top of pipe.

Levich (1962) estimated the turbulent force (surface force) related to the friction velocity term as follow.

$$F_T = \frac{1}{2}\rho_L {u_L}^2 \left(\frac{f_L}{2}\right) S_i \tag{3-16}$$

The force of buoyancy (body force) per unit length of the gas region is as below:

$$F_B = g(\cos\alpha)(\rho_L - \rho_G)A_G \tag{3-17}$$

When the effect of turbulent force (F_T) overcomes the buoyancy force (F_B), dispersed bubble flow occurs as indicated in below equation.

$$u_L \geq \left[\frac{4A_G g\cos\alpha}{S_i f_L}(1-\frac{\rho_G}{\rho_L})\right]^{1/2} \tag{3-18}$$

Transition between Intermittent and dispersed bubble flow can be written in dimensionless form as below:

$$T^2 \geq \left[\frac{8\tilde{A}_G}{\tilde{S}_i {\tilde{u}^2}_L (\tilde{u}_L \tilde{D}_L)^{-n}}\right] \tag{3-19}$$

Where n is the constant number, n is equal to 1.0 and 0.2 for laminar and turbulent flow respectively.

4) Transition between stratified smooth and stratified wavy

The waves, above the stratified smooth surface, are caused by the gas flow under conditions where the velocity of gas is sufficient to cause waves to form but slower than that needed for annular flow. It is generally accepted that waves will be initiated when the pressure force and shear force on the wave overcome the viscous dissipation in the waves.

The idea of Jefreys (1925,1926) on the wave generation has been used and some parameters have been simplified as shown in below equation.

$$u_G \geq \left[\frac{4\mu_L(\rho_L - \rho_G)g\cos\alpha}{0.01\rho_G u_L}\right]^{1/2} \tag{3-20}$$

Transition between Stratified Smooth and Stratified Wavy can be written in dimensionless terms as

$$K \geq \frac{2}{\tilde{u}_G\sqrt{\tilde{u}_L \times 0.01}} \tag{3-21}$$

3.2.2 Flow pattern map for vertical upward direction

The flow pattern map in vertical upward direction that was proposed by Taitel, Bornea and Dukler (1980) indicates four basic flow patterns (bubble, slug, churn, annular) for two-phase gas liquid flow in vertical upward direction. This classification is based on the study of Hewitt and Hall-Taylor (1970). The map is based on physical mechanisms as shown in Figure 3.2.2-1.

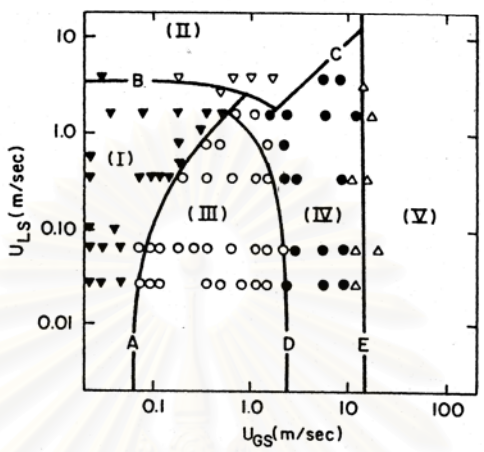

Figure 3.2.2-1 Flow pattern Map for Vertical upward direction, air-water at 25 ^{0}C, 0.1 MPa, 5.0cm pipe diameter (Taitel et. al 1980)
(I)-bubble, (II)-finely dispersed bubble, (III)-slug, (IV)-churn, (V)–annular.

1) Transition between bubble and slug (transition A)

When gas is introduced at low flow rates into a large diameter vertical column of liquid (flowing at low liquid rate), the gas phase is distributed into discrete bubbles moving in zigzag motion with the occasional appearance of larger bubbles. If the gas flow rate is increased, at these low liquid rates, the bubble density increases and a point is reached where the dispersed bubbles become so closely packed that many collisions occur. Slug flow requires a process of agglomeration or coalescence of these bubbles into a large vapor space, this results in the transition to slug flow as shown in Figure 3.2.2-2.

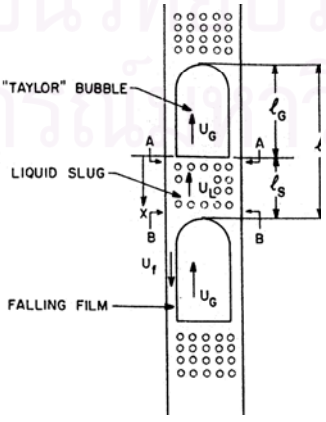

Figure 3.2.2-2 Slug flow geometry (Taitel 1980)

However when the liquid rate increases, the turbulent fluctuations can cause breakup of the large bubbles formed as a results of agglomeration. If this break up is strong enough to prevent re-coalescence, then the dispersed bubbles can be maintained.

Experiments suggests that the bubble void fraction (ε), at which slug flow occurs, is approximately 0.25 to 0.3 (Graffith and Synder 1964). A semi-theoretical approach to this problem was given by Radovicich and Moissis (1962), by considering a cubic lattice of the bubbles, and it was shown that this occurs at void fraction of approximately 0.3. If considering the spherical bubbles in the cubic lattice, the void fraction of gas can be, at most, 0.52.

Thus if liquid flow rates are low enough such that the bubble break up due to turbulent flow is small, the criteria for transition from bubble to slug flow is that the void fraction is between 0.25 and 0.52. To determine the bubble to slug transition, the equations below shall be combined.

If the gas bubbles rise at a velocity u_G, this velocity is related to the superficial gas ${u_G}^S$ by

$$u_G = \frac{Q_G}{A\varepsilon} = \frac{{u_G}^S}{\varepsilon} \tag{3-22}$$

where ε is the void fraction. Likewise, the average liquid velocity is given by the term of the liquid superficial velocity as

$$u_L = \frac{Q_L}{A(1-\varepsilon)} = \frac{{u_L}^S}{(1-\varepsilon)} \tag{3-23}$$

Designating u_0 as the rise velocity of the gas bubbles relative to the average liquid velocity, equation (3-22) and (3-23) yield

$${u_L}^S = {u_G}^S \frac{1-\varepsilon}{\varepsilon} - (1-\varepsilon)u_0 \tag{3-24}$$

The rise velocity u_0 has been proposed by Harmathy (1960) to be quite insensitive to bubble size and given by the relation of phase density (ρ) and surface tension (σ)

$$u_0 = 1.53 \times \left[\frac{g(\rho_L - \rho_G)\sigma}{{\rho_L}^2} \right]^{1/4} \tag{3-25}$$

By combining the above relations equation (3-22, 3-23, 3-24, and 3-25) and substituting the rise velocity of gas bubbles and the physical properties of the fluids, the transition from bubble to slug flow can be represented at a void fraction (ε) equal to 0.25 as shown in equation (3-26)

$${u_L}^S = 3.0{u_G}^S - 1.15 \times \left[\frac{g(\rho_L - \rho_G)\sigma}{{\rho_L}^2} \right]^{1/4} \tag{3-26}$$

2) Transition between bubble to dispersed bubble (transition B)

At higher liquid flow rates, turbulent forces act to break and disperse the gas phase into small bubbles even for void fractions higher than 0.25. The theory of breakup of immiscible fluid phases by turbulent forces was given by Hinze(1955). He determined that the magnitude of the dispersion results from a balance between surface tension force and turbulent fluctuations. His study of the relationship of surface tension and energy dissipation lead to the maximum stable diameter in the dispersed phase $d_{\max}$.

If the bubble size produced by the breakup process is large enough to permit deformation, then the void fraction approaches 0.25 and the large Taylor bubbles of slug flow are formed by the process of coalescence. If at high liquid rate, the turbulent breakup process can prevent agglomeration then the bubble size is small enough to remain a spherical bubble. The bubble size at which this occurs is given by Brodkey (1967) as a function of surface tension and buoyancy force, d_{crit}.

For $d_{\max} > d_{crit}$, the bubble rise velocity is almost independent of bubble size and the bubble rise velocity is given by equation (3-26), But once the turbulent fluctuations are strong enough to cause the bubbles to break into a smaller critical size, coalescence is suppressed and dispersed bubble flow must exist even for void fractions is over 0.25.

The dimensionless expression relating surface tension force, turbulent force, the critical size of rigid spherical bubble shape properties and pipe size at which turbulent induces dispersion take place is as below.

$$u_L{}^S + u_G{}^S = 4.0\left\{\frac{D^{0.429}\left(\sigma/\rho_L\right)^{0.089}}{\left(\mu_L/\rho_L\right)^{0.072}}\left[\frac{g\left(\rho_L-\rho_G\right)}{\rho_L}\right]^{0.466}\right\} \qquad (3\text{-}27)$$

3) Transition between slug and dispersed bubble(transition C)

However, regardless of how much turbulent force is available to disperse the mixture, bubble flow cannot exist at void fractions above 0.52. Thus the transition B delimiting dispersed bubble flow must terminate at transition which relates $u_L{}^S, u_G{}^S$ for void fractions equal to 0.52 in below equation.

$$u_L{}^S = 0.92u_G{}^S - 0.48\times 1.53\left[\frac{g\left(\rho_L-\rho_G\right)\sigma}{\rho_L{}^2}\right]^{1/4} \qquad (3\text{-}28)$$

4) Transition to annular (transition E)

At high gas flow rates the two-phase flow becomes annular. The liquid film flows adjacent to the wall and the gas flows in the center carrying entrained liquid droplets. The

liquid moves upwards due to the interfacial shear and form drag on the liquid surface and on the droplets. The effect of these forces, annular flow cannot exist, unless the gas velocity in the core is not sufficient to lift the entrained liquid droplet.

The minimum gas velocity required to suspend a drop is dependent on the gravity force and drag force acting on the liquid drop as shown below:

$$\frac{1}{2}Cd(\pi d^2/4)\rho_G u_G{}^2 = (\pi d^3/6)g(\rho_L - \rho_G) \qquad (3\text{-}29)$$

The droplet size (d) is determined by the balance between the impact force of the gas that tends to shatter the droplet and surface tension force that holds the droplet together. Hinze (1955) showed that the maximum stable droplet size related to surface tension , gas density and gas velocity is as shown below:

$$d = \frac{K\sigma}{\rho_G u_G{}^2} \qquad (3\text{-}30)$$

As suggested by Turner et. al (1969) value of K = 30 and C_d = 0.44 were selected. A characteristic of annular flow is that the film thickness is quite low even for relatively high liquid flow rates. As a result the true gas velocity (u_G) can be replaced by the superficial gas velocity rate ($u_G{}^S$) and the final transition boundary is given by

$$\frac{u_G{}^S \rho_G{}^{1/2}}{(\sigma g(\rho_L - \rho_G))^{1/4}} = 3.1 \qquad (3\text{-}31)$$

This simple criteria shows that the transition to annular pattern is independent of liquid flow rate and pipe diameter.

3.2.3 Flow pattern map for vertical downward direction

Flow pattern maps in the vertical downward direction have been proposed by Barnea, Shoham and Taitel (1981) and are based on physical mechanisms. Only three regimes were observed: annular flow, slug flow, and dispersed bubble flow.

The most natural flow regime in the vertical flow is the annular flow which takes the form of falling film at low gas rate and typical annular flow for high gas rate. When the liquid at low flow rate is introduced into a vertical downward pipe, without gas, it moves as a symmetrical falling film. When gas is introduced concurrently with the liquid, the gas flows through the liquid annulus, while the liquid flow along the pipe wall. The process to determine the flow regime begins with a check to determine if the flow is in the annular flow regime. If it is found that it is not annular flow, then the flow regime is either intermittent flow or dispersed bubble flow. Check is then performed to determine if the flow is intermittent or dispersed bubble flow.

From the force balance on the equilibrium annular flow in the gas phase and liquid phase, a solution of the force balance yields the film thickness as a function of superficial liquid and gas velocities, the physical properties of the fluid, and the pipe diameter. The film thickness shall be used to determine the flow pattern in vertical downward direction as shown in Figure 3.2.3-1a and Figure 3.2.3-1b.

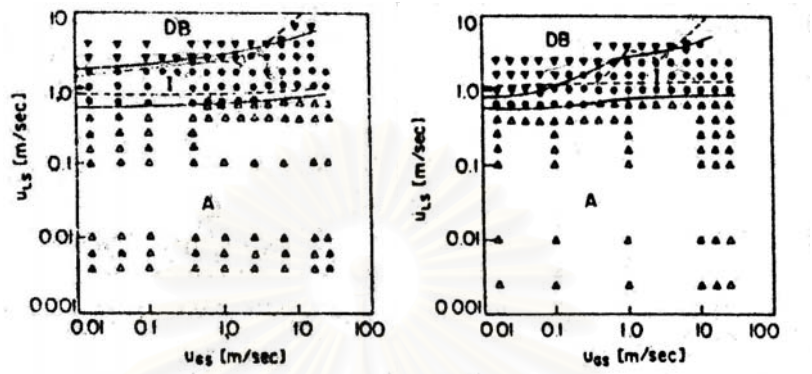

Figure 3.2.3-1a **Figure 3.2.3-1b**

Figure 3.2.3-1 Flow pattern map for vertical downward flow,2.5 cm pipe (a) and 5.0 cm(b)
——Experiment, - - - - - - Theory;
A= annular, I = intermittent, DB= dispersed bubble.

1) Transition between annular and slug

The criteria for transition from annular to slug flow occurs when the supply of liquid in the film is large enough to provide the liquid volume needed to maintain such a slug. When the liquid hold up in the slug flow is twice the liquid hold in annular flow then transition to slug flow occurs. From the study of Taitel et. al (1980) liquid hold up in the slug is equal to 0.7, Thus transition to slug flow will take place at

$$\frac{A_L}{0.7A} = 0.5 \qquad \text{or} \qquad \frac{A_L}{A} = 0.35 \tag{3-32}$$

2) Transition between slug and dispersed bubble

The transition from slug to dispersed bubble flow takes place when sufficient turbulent force is available to overcome interfacial tension to dispersed gas into small bubbles, thus the basis of Taitel et.al.(1980) , for the case of vertical upward flow, is applicable here and may give the transition line as below:

$$u_L^{\,S} + u_G^{\,S} = 4.0\left\{\frac{D^{0.429}\left(\sigma/\rho_L\right)^{0.089}}{\left(\mu_L/\rho_L\right)^{0.072}}\left[\frac{g\left(\rho_L-\rho_G\right)}{\rho_L}\right]^{0.466}\right\} \tag{3-33}$$

3.3 Pressure loss

In single phase flow, Bernoulli theorem expresses the application of the law of conservation of energy to the flow of fluids in a pipe. The total energy (total head H) at any particular point, above some reference plane, is equal to the sum of the elevation head (Z), the pressure head ($\frac{P}{\rho}$), and the velocity head ($\frac{u^2}{2g}$) as follows:

$$Z + \frac{P}{\rho} + \frac{u^2}{2g} = H \tag{3-34}$$

In two-phase flow, the type of flow pattern is major factor to define the cause of pressure loss. In general, there are four types of pressure drop in two phase gas-liquid flow: friction, acceleration, elevation, and minor loss. Pressure loss can be calculated from the unit pressure loss multiplied by pipe length. And the total pressure loss (P_T) is the summation of individual loss as below.

$$P_T = P_f + P_a + P_g + P_{fit} \tag{3-35}$$

3.3.1 Frictional Pressure Loss (ΔP_f)

Friction loss is a result of unit pressure loss multiplied by pipe length.

$$P_f = \Delta P_f \times \Delta Z \tag{3-36}$$

3.3.2 Acceleration Pressure loss (ΔP_a)

Acceleration loss is determined by the distribution of gas and liquid over the pipe cross sectional area. In a near homogeneous flow, the velocity is quite uniform, and mixture velocity change can be used to find the acceleration pressure loss

$$\Delta P_a = \frac{1}{g_C A_P}\left[(Momentum \cdot rate)_{downstream} - (Momentum \cdot rate)_{upstream}\right] \tag{3-37}$$

$$P_a = \Delta P_a \times \Delta Z \tag{3-38}$$

3.3.3 Elevation Pressure Loss (ΔP_g)

The density of gas and liquid in the inclination occupies a fraction ε and (1-ε) of the total volume, the elevation head can be calculated as follows

$$\Delta P_g = \rho_L g(1-\varepsilon) + \rho_G g(\varepsilon) \tag{3-39}$$

Elevation loss is calculated from the pressure loss per unit length (ΔP_g) multiplied by pipe length (ΔZ) in the individual flow pattern

$$P_g = \Delta P_g \times \Delta Z \tag{3-40}$$

3.3.4 Minor loss from valves or fittings (ΔP_{fit})

The pressure drop due to fittings ΔP_{fit} for a particular segment can be calculated from the same concept of minor loss in single-phase flow. This loss is independent of orientation or flow pattern. Many experimental studies shown that the pressure loss due to valves and fitting is proportional to a constant power of velocity, fluid density and resistance coefficient (K) as shown in below equation.

$$\Delta P_{fit} = (f\frac{L}{D}) \times \frac{\rho u^2}{2} = (K) \times \frac{\rho u^2}{2} \quad (3\text{-}41)$$

The K value for sudden enlargements ($Kenl$) and Sudden Contractions ($Kcon$) are calculated from inside diameter on inlet side (d_1) and outlet side (d_2) proposed by C.C. Heald in Cameron Hydraulic Data (1988)

$$Kenl = \left(1 - \frac{d_1^2}{d_2^2}\right)^2 \quad (3\text{-}42)$$

$$Kcon = \left(1 - \frac{d_1^2}{d_2^2}\right) \quad (3\text{-}43)$$

The K value for pipe fittings in terms of equivalent length (L) feet of valves, friction factor (f) for $90^0, 45^0$ elbow, etc are shown in Table 3.4.1-1 and the total fitting loss (P_{fit}) depends on the number of fittings (N) in the system

$$P_{fit} = \Delta P_{fit} \times N \quad (3\text{-}44)$$

Table 3.3.4-1 Representative equivalent length in pipe diameter (L/D) of various valves and fittings (Data from The Crane, 1988).

Description of Product				Equivalent Length In Pipe Diameters (L/D)
Globe Valves	Stem Perpendicular to Run	With no obstruction in flat, bevel, or plug type seat	Fully open	340
		With wing or pin guided disc	Fully open	450
	Y-Pattern	(No obstruction in flat, bevel, or plug type seat)		
		– With stem 60 degrees from run of pipe line	Fully open	175
		– With stem 45 degrees from run of pipe line	Fully open	145
Angle Valves		With no obstruction in flat, bevel, or plug type seat	Fully open	145
		With wing or pin guided disc	Fully open	200
Gate Valves	Wedge, Disc, Double Disc, or Plug Disc		Fully open	13
			Three-quarters open	35
			One-half open	160
			One-quarter open	900
	Pulp Stock		Fully open	17
			Three-quarters open	50
			One-half open	260
			One-quarter open	1200
	Conduit Pipe Line		Fully open	3**
Check Valves	Conventional Swing		0.5†...Fully open	135
	Clearway Swing		0.5†...Fully open	50
	Globe Lift or Stop; Stem Perpendicular to Run or Y-Pattern		2.0†...Fully open	Same as Globe
	Angle Lift or Stop		2.0†...Fully open	Same as Angle
	In-Line Ball		2.5 vertical and 0.25 horizontal†...Fully open	150
Foot Valves with Strainer		With poppet lift-type disc	0.3†...Fully open	420
		With leather-hinged disc	0.4†...Fully open	75
Butterfly Valves (8-inch and larger)			Fully open	40
Cocks	Straight-Through	Rectangular plug port area equal to 100% of pipe area	Fully open	18
	Three-Way	Rectangular plug port area equal to 80% of pipe area (fully open)	Flow straight through	44
			Flow through branch	140
Fittings	90 Degree Standard Elbow			30
	45 Degree Standard Elbow			16
	90 Degree Long Radius Elbow			20
	90 Degree Street Elbow			50
	45 Degree Street Elbow			26
	Square Corner Elbow			57
	Standard Tee	With flow through run		20
		With flow through branch		60
	Close Pattern Return Bend			50

**Exact equivalent length is equal to the length between flange faces or welding ends.

†Minimum calculated pressure drop (psi) across valve to provide sufficient flow to lift disc fully.

3.4 Pressure loss in stratified flow

Pressure loss in stratified smooth and stratified wavy flow can be calculated from the force balance equation of gas phase and liquid phase. The equilibrium stratified flow is shown in Fig 3.4-1. It is assumed that the gas and liquid are flowing separately as stratified pattern. From the uniform steady state flow, hydraulic gradient is negligible. The value of pressure gradient in gas phase and liquid is equal. Unit pressure loss can be calculated by substitution of flow parameters in below equations.

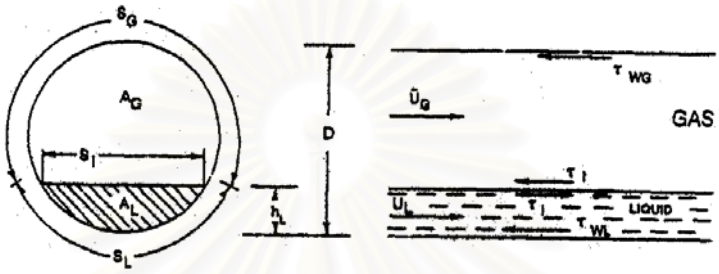

Figure 3.4-1 Equilibrium Stratified flow

$$-A_L(dP/dZ)_L - \tau_{WL}S_L + \tau_i S_i + \rho_L A_L g\sin(\alpha) = 0 \quad (3\text{-}45)$$

$$-A_G(dP/dZ)_G - \tau_{WG}S_G - \tau_i S_i + \rho_G A_G g\sin(\alpha) = 0 \quad (3\text{-}46)$$

where

$(dP/dZ)_L$, $(dP/dZ)_G$ = pressure gradients (pressure loss per unit length) in the liquid and gas phases.

A_G, A_L = cross sectional areas for flow for the gas and liquid phases.

τ_{WG}, τ_{WL}, τ_i = wall shear stress for the pipe perimeter contacting the gas and liquid, and the interfacial shear stress respectively.

S_G, S_L, S_i = pipe perimeters in contact with gas and liquid and interface perimeter respectively.

ρ_G, ρ_L = density of gas and liquid phase

g = acceleration of gravity

α = angle of inclination of pipe from horizontal , positive for downward and negative in upward direction, radian unit.

For a uniform steady state stratified flow and a minor value of hydraulic gradient in a horizontal pipe, the value of $(dP/dZ)_G$ is assumed to be equal to $(dP/dZ)_L$. The force balance equation for the liquid phase and gas phase can be combined into a single equation as below.

$$\tau_{WG}\frac{S_G}{A_G}-\tau_{WL}\frac{S_L}{A_L}+\tau_i S_i\left(\frac{1}{A_L}+\frac{1}{A_G}\right)+(\rho_L-\rho_G)g\sin\alpha=0 \qquad (3\text{-}47)$$

To solve the above equation and calculate the pressure loss in the two-phase system, the two-phase variables and the physical properties shall be substituted in equation (3-47). Shear stress at the liquid wall surface, gas wall surface and gas/liquid interface can be calculated from these empirical equations

$$\tau_{WL}=f_L\frac{\rho_L u_L^{\,2}}{2} \qquad (3\text{-}48)$$

$$\tau_{WG}=f_G\frac{\rho_G u_G^{\,2}}{2} \qquad (3\text{-}49)$$

$$\tau_i=f_i\frac{\rho_G(u_G-u_i)^2}{2} \qquad (3\text{-}50)$$

The friction factor f for laminar flow ($\mathrm{Re}<2300$) and turbulent flow($\mathrm{Re}\geq 2300$) can be determined from equation (3-51) and (3-52). Miller (1980) suggested that a single iteration produced a result within 1 percent if the initial estimate was calculated from the modified Colebrook ‘s equation as equation (3-52). Friction factors for fully developed flow in circular pipes from the Moody chart are also shown in Appendix B.

$$f=\frac{\mathrm{Re}}{64} \qquad (3\text{-}51)$$

$$f=0.25\left(\frac{e/D}{3.7}+\frac{5.74}{\mathrm{Re}^{\,0.9}}\right)^{-2} \qquad (3\text{-}52)$$

$$f_i\approx f_G \qquad (3\text{-}53)$$

where

$\mathrm{Re}=$ Reynolds Number

e = pipe roughness (see details in Appendix B)

D = inside diameter of pipe

The Reynolds number of liquid and gas phase is calculated by using the actual velocity and hydraulic diameter of each phase, not the superficial velocity and pipe diameter.

$$\mathrm{Re}=\frac{\rho\, uD}{\mu} \qquad (3\text{-}54)$$

Hydraulic diameters are suggested by Agrawal et. al (1973)

$$D_L = \frac{4A_L}{S_L} \tag{3-55}$$

$$D_G = \frac{4A_G}{S_G + S_i} \tag{3-56}$$

Superficial velocities and gas, liquid velocity are calculated as below.

$$u_G{}^S = \frac{Q_G}{A} \tag{3-57}$$

$$u_L{}^S = \frac{Q_L}{A} \tag{3-58}$$

$$u_G = \frac{Q_G}{A(\varepsilon)} = \frac{u_G{}^S}{\varepsilon} \tag{3-59}$$

$$u_L = \frac{Q_L}{A(1-\varepsilon)} = \frac{u_L{}^S}{(1-\varepsilon)} \tag{3-60}$$

Void fraction (ε) is the ratio of pipe cross sectional area occupied by gas phase per total pipe cross sectional area.

$$\varepsilon = \frac{A_G}{A} \tag{3-61}$$

The parameter A_G, A_L, S_G, S_L, S_i, and others are geometric function of the dimensionless liquid height, $\frac{h_L}{D}$, and can be evaluated as follows:

$$\tilde{h}_L = \frac{h_L}{D} \tag{3-62}$$

$$\tilde{S}_G = \cos^{-1}\left(2\tilde{h}_L - 1\right) \tag{3-63}$$

$$\tilde{S}_L = \pi - \cos^{-1}\left(2\tilde{h}_L - 1\right) \tag{3-64}$$

$$\tilde{S}_i = \sqrt{1-\left(2\tilde{h}_L - 1\right)^2} \tag{3-65}$$

$$S_G = \tilde{S}_G \times D \tag{3-66}$$

$$S_L = \tilde{S}_L \times D \tag{3-67}$$

$$S_i = \tilde{S}_i \times D \tag{3-68}$$

$$\tilde{A}_G = 0.25\left[\cos^{-1}\left(2\tilde{h}_L - 1\right) - \left(2\tilde{h}_L - 1\right)\sqrt{1-\left(2\tilde{h}_L - 1\right)^2}\right] \tag{3-69}$$

$$\tilde{A}_L = 0.25\left[\pi - \cos^{-1}\left(2\tilde{h}_L - 1\right) + \left(2\tilde{h}_L - 1\right)\sqrt{1-\left(2\tilde{h}_L - 1\right)^2}\right] \tag{3-70}$$

$$\tilde{A} = \frac{\pi}{4} \tag{3-71}$$

$$A_G = \tilde{A}_G \times D^2 \tag{3-72}$$

$$A_L = \tilde{A}_L \times D^2 \tag{3-73}$$

$$\tilde{u}_G = \frac{\tilde{A}}{\tilde{A}_G} \tag{3-74}$$

$$\tilde{u}_L = \frac{\tilde{A}}{\tilde{A}_L} \tag{3-75}$$

$$\frac{d\tilde{A}_L}{d\tilde{h}_L} = \sqrt{1-\left(2\tilde{h}_L - 1\right)^2} \tag{3-76}$$

Pressure drop for one phase alone in a pipe is calculated from below equations. These calculation results are then used to evaluate flow pattern and pressure loss in stratified flow using the equation (3-45) or (3-46).

$$\left|\left(dP/dZ\right)_L{}^S\right| = 4 f_{WL}\left[\frac{\rho_L\left(u_L{}^S\right)^2}{2D}\right] \tag{3-77}$$

$$\left|\left(dP/dZ\right)_G{}^S\right| = 4 f_{WG}\left[\frac{\rho_G\left(u_G{}^S\right)^2}{2D}\right] \tag{3-78}$$

3.5 Pressure loss in horizontal slug flow

A horizontal slug model was proposed by Duckler and Hubbard in 1975. This study was carried out in a 1.5 inch pipe, 65 ft long in the horizontal plane. It is tested against the proposed model with good agreement. A sketch of an idealized slug in a fully establish flow is shown in Figure 3.5-1.

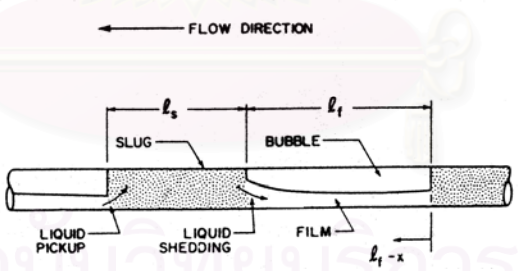

Figure 3.5-1 A sketch of idealized slug flow

The mechanism of slug formation is shown in Figure 3.5-2.

1) Liquid and gas flow concurrently in a pipe. At the gas and liquid velocities under which slug flow takes place, the liquid layer decelerates as it moves along the pipe. So liquid level increases, such that a wave develops on the liquid surface. The liquid height increases to the point where it bridges the pipe and momentarily blocks the gas flow rate. (See Figure 3.5-2A, 3.5-2B, 3.5-2C)

2) When the liquid bridging occurs, the liquid appears to be accelerated to the gas velocity. In this manner the accelerated liquid acts as a scoop, picking up the slow moving liquid in the film ahead of it and accelerating it to slug velocity. The fast moving liquid build its volume and eventually becomes a liquid slug (See Figure 3.5-2D)

3) As the slug is formed, liquid is shed from the back of the slug and forms a liquid film of length (l_f) below the gas zone. This liquid film decelerates rapidly from the slug velocity to a much lower velocity, due to the effect of wall and interfacial shear.

4) The liquid slug gains liquid film which has been shed from the preceding slug, and thus the slug picks up liquid at the same rate that it is shed, making it stable. The slug unit length is constant ($l_f + l_S$)

5) The slug mixing zone occurs at the slug nose of length ($l_S + l_f$). In this zone, the liquid film ahead of the slug is overrun by the fast moving slug. The liquid is accelerated to the slug velocity via violent mixing and entrains with it gas bubbles.

If the gas rate and slug velocity increase, the degree of aeration of the slug increases. If liquid slugs begin to bypass the gas, the slug cannot maintain a competent bridge to block the gas. This is the point at which the annular flow pattern begins.

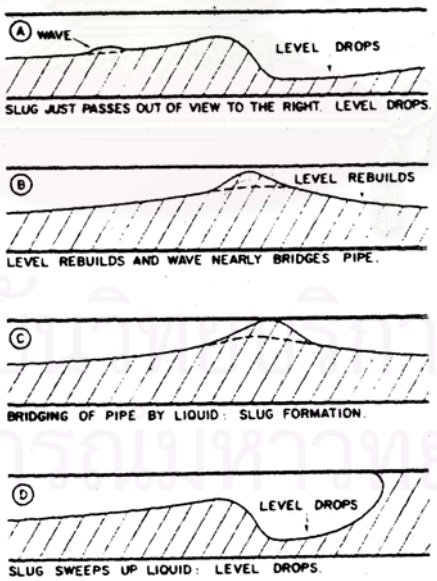

Figure 3.5-2 Process of slug formation

3.5.1 Pressure loss from frictional effect (ΔP_f)

In a liquid slug, pressure drop due to wall friction occurs behind the mixing eddy. The similarity Model (case I) developed by Taitel et. al (1964) is used to determine the pressure loss through friction. The two-phase is assumed to be homogeneous mixed phase.

$$\Delta P_f = \frac{2 f_S \left[\rho_L R_S + \rho_G (1 - R_S)\right] u_S{}^2 (l_S - l_m)}{2 g_C D \times l} \tag{3-79}$$

3.5.2 Pressure loss from acceleration effect (ΔP_a)

In a stable liquid slug, there is a difference between the liquid film velocity and slug velocity. The pressure force to accelerate this liquid film to slug velocity cause a pressure loss in the system:

$$\Delta P_a = \frac{x}{A g_c} (u_S - u_t) \tag{3-80}$$

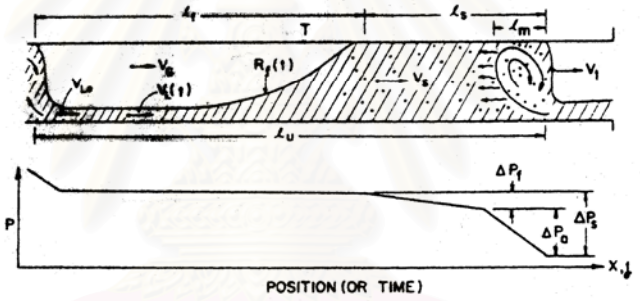

Figure 3.5.2-1 Pressure loss in Horizontal slug model

The above flow parameters can be calculated by the following equations. Liquid hold up (R_S) is calculated from an experimental correlation given by Gregory, Nicholson, and Aziz (1978) as a function of the average slug velocity (u_S) in units of feet per second.

$$R_S = \frac{1}{1 + (u_S / 28.405)^{1.39}} \tag{3-81}$$

$$u_S = u_L{}^S + u_G{}^S \tag{3-82}$$

Based on the experimental data from the study of Duckler et. al (1985) in small diameter pipes, the liquid slug length (l_S) can be evaluated as below

$$l_S = 30D \tag{3-83}$$

Translational velocity at the slug nose (u_t) is the sum of the slug velocity and rate of build up at the front due to film pick up

Translational Velocity at The slug nose	=	Mean fluid velocity in the slug	+	Apparent velocity gain by adding fluid in the slug nose
U_t		U_S		$\frac{x}{\rho_L A R_S}$

$$u_t = \left(u_S + \frac{x}{\rho_L A R_S} \right) u_S = (1 + C) u_S \tag{3-84}$$

The relation between Re_S and C can be approximated from experiment by observing the log linear relationship over the range 30,000< Re_S <400,000. The constant C can be calculated from the relation of Re_S as below.

$$C = \frac{x}{\rho_L A R_S u_S} = 0.021 \ln(\mathrm{Re}_S) + 0.022 \tag{3-85}$$

Where Re_S is the two phase Reynolds Number from similarity model proposed by Duckler et al (1964).

$$\mathrm{Re}_S = D u_S \frac{\rho_L R_S + \rho_G (1 - R_S)}{\mu_L R_S + \mu_G (1 - R_S)} \tag{3-86}$$

Slug frequency:

$$\nu_S = \frac{u_t}{l_U} = 0.0226 \frac{\left[1.29 \left(u_G{}^S + u_L{}^S \right) + 0.35 \sqrt{gD} \right] (1 - \beta)}{20 D} \tag{3-87}$$

Length of liquid film:

$$l_f = l - l_S \tag{3-88}$$

Fraction of pipe flow area occupied by film (R_f) can be calculated from:

$$l_S = \frac{u_S}{\nu_S (R_S - R_f)} \left[\frac{W_L}{\rho_L A u_S} - R_f + C (R_S - R_f) \right] \tag{3-89}$$

The length of the mixing eddy appears to depend on the relative velocity between slug and film velocity head from observation.

$$l_m = 0.3 \cdot Velocity \cdot Head = \frac{0.3 (u_S - u_t)^2}{2 g_c} \left(\frac{\rho_L}{s_L} \right) \tag{3-90}$$

where s_L is the specific weight of the liquid.

3.6 Pressure loss in annular and bubble flow (Similarity model)

The similarity model was proposed by Duckler, Wicks and. Cleveland (1964). The experimental data from many sources are grouped and selected by flow condition. Many data were rejected due to error. 2,620 data points were selected to evaluate the most widely used correlations for two–phase pressure drop and liquid hold up for annular and dispersed bubble flow. This model is a so called “black box” method which is flow pattern independent.

Liquid hold up (R_L) used in pressure drop calculation and two-phase flow parameters calculation is based on the Hughmark correlation.

In this model the parameters for two phase flow corresponding to the Euler number (Note that the Euler no. is twice the friction factor) and Reynolds numbers for a single phase flow will be developed. If two flow systems in single phase flow are dynamically similar, it can be shown that the Reynolds no. and the Euler no. for the two phase system must be equal. If the dynamic similarity is to exist, the two phase density (ρ_{TP}), two phase viscosity(μ_{TP}), liquid volume fraction (λ_L) are defined by,

$$\rho_{TP} = \rho_L \frac{{\lambda_L}^2}{R_L} + \rho_G \frac{(1-\lambda_L)^2}{(1-R_L)} C1 \qquad (3\text{-}91)$$

$$\mu_{TP} = \mu_L \lambda_L + \mu_G (1-\lambda_L) C2 \qquad (3\text{-}92)$$

$$\lambda_L = \frac{Q_L}{Q_L + Q_G} = \frac{{u_L}^S}{{u_L}^S + {u_G}^S} \qquad (3\text{-}93)$$

Case I This case is used for friction pressure loss calculation in horizontal slug flow which is a homogeneous mixed with negligible slip. Under this conditions, $C1 = C2 = 1$, $\lambda_L = R_L$, $(1-\lambda_L) = R_G$. The mixture properties are defined by

$$\rho_{TP} = \rho_L \lambda_L + \rho_G (1-\lambda_L) \qquad (3\text{-}94)$$

$$\mu_{TP} = \mu_L \lambda_L + \mu_G (1-\lambda_L) \qquad (3\text{-}95)$$

Case II This case is used for friction pressure loss calculation in slug flow (in vertical upward, vertical down flow), bubble flow (in horizontal, vertical upward and vertical down flow) and annular flow for (in horizontal, vertical upward flow) when slip take place. The constant $C1$ and $C2$ is assumed to be 1, the mixture properties are defined by

$$\rho_{TP} = \rho_L \frac{{\lambda_L}^2}{R_L} + \rho_G \frac{(1-\lambda_L)^2}{(1-R_L)} \qquad (3\text{-}96)$$

$$\mu_{TP} = \mu_L \lambda_L + \mu_G (1-\lambda_L) \qquad (3\text{-}97)$$

3.6.1 Hughmark Liquid hold up (R_L)

Liquid hold up can be calculated from the Hughmark correlation, which is a modification of the one originally proposed by Bankoff (1960), as shown in Figure 3.6.1-1.

$$(1-R_L)=\frac{K}{(1/x-1)[(\rho_G/\rho_L)+1]} \tag{3-98}$$

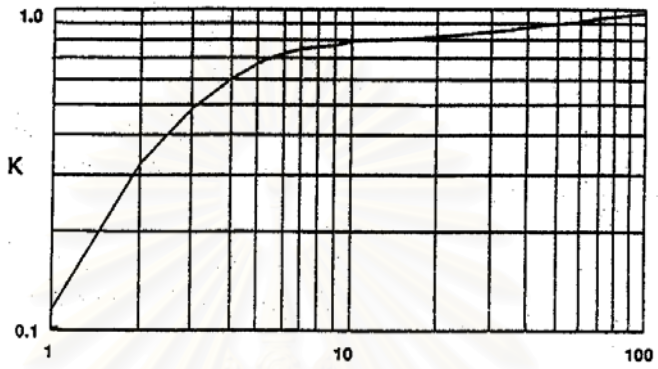

$$Z=\frac{\mathrm{Re}^{1/6}\,N_{FR}{}^{0.125}}{\lambda^{0.25}}$$

Figure 3.6.1-1 Hughmark 's liquid hold up Correlation

where the Bankoff parameter (K), Z parameter, liquid volume fraction (λ), Froude Number (N_{FR}), and Reynolds number (Re) are calculated as below:

$$Z=\frac{(\mathrm{Re})^{0.167}\cdot(N_{FR})^{0.125}}{\lambda^{0.25}} \tag{3-99}$$

$$N_{FR}=\frac{u_{TP}{}^2}{gD} \tag{3-100}$$

$$\mathrm{Re}_{TP}=\frac{DG_{TP}}{R_L\mu_L+(1-R_L)\mu_G} \tag{3-101}$$

Liquid volume fraction, two-phase velocity, two-phase mass velocity, and quality are calculated as below:

$$u_{TP}=u_L{}^S+u_G{}^S \tag{3-102}$$

$$G_{TP}=\frac{(\rho_L Q_L+\rho_G Q_G)}{A} \tag{3-103}$$

$$x=\frac{Q_G\rho_G}{(Q_G\rho_G+Q_L\rho_L)} \tag{3-104}$$

3.6.2 Pressure Loss

Frictional Pressure Loss and Gravitation Pressure Loss are calculated by the equation derived by the dynamic similarity in two corresponding points. Flow parameter formula from experimental data and liquid hold up are used to calculate pressure loss as below.

$$\Delta P_f = \frac{f_{TP}\rho_{TP}\left(u_L{}^S + u_G{}^S\right)^2}{2g_C D} \quad (3\text{-}105)$$

$$\Delta P_g = \frac{g}{g_c}\left[\rho_L R_L + \rho_G\left(1-R_L\right)\right] \quad (3\text{-}106)$$

Two-phase friction factor is calculated from the normalized curve $\frac{f_{TP}}{f_0}$ in Figure 3.6.2-3 or below equations.

$$\alpha(\lambda) = 1.0 - \{\frac{\ln\lambda}{1.281 - 0..478(-\ln\lambda) + 0.444(-\ln\lambda)^2 - 0.094(-\ln\lambda)^3 + 0.00843(-\ln\lambda)^4}\} \quad (3\text{-}107)$$

$$f_0 = 0.00140 + \frac{0.125}{\mathrm{Re}_{TP}{}^{0.32}} \quad (3\text{-}108)$$

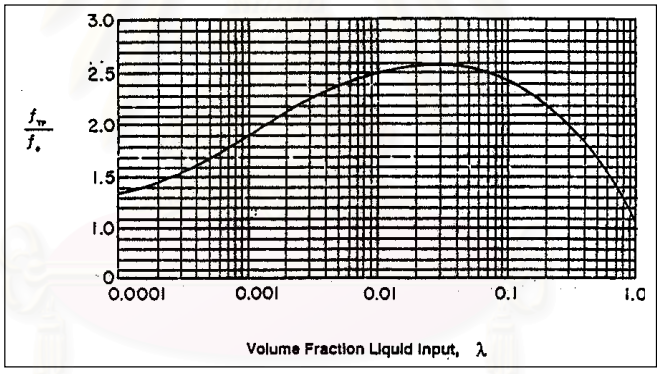

Figure 3.6.2-1 Normalized curve $\frac{fTP}{f_0}$

3.7 Pressure loss in vertical upward slug flow

A vertical upward Slug flow model was proposed by Fernandes, Semiat and Duckler (1983). Their physical model was developed from the equilibrium isothermal, concurrent gas-liquid in vertical upward pipes at low pressures in a steady state flow. The cause of pressure loss has three components, namely friction loss, acceleration loss, and elevation loss.

3.7.1 Pressure loss from frictional effect (ΔP_f)

In general the gas density and viscosity are much lower than liquid density and viscosity. The Taylor bubble is a region of negligible pressure loss. Frictional pressure loss

From the liquid slug can be calculated using the similarity case II with bubble distributed in the slug by Taitel et. al(1964). Void fraction in the liquid slug(α_{LS}) equals to 0.25.

$$\Delta P_f = \frac{2 f_{TP} \rho_{TP} u_{LLS}^{\ 2}}{D} l_{LS} = 40 f_{TP} \rho_{TP} u_{LLS}^{\ 2} \quad (3\text{-}109)$$

Liquid volume fraction (λ_L) is calculated from

$$\lambda_L = u_{LLS}(1-\alpha_{LS}) \big/ (u_L^{\ S} + u_G^{\ S}) \quad (3\text{-}110)$$

3.7.1 Pressure loss from acceleration effect (ΔP_a) Liquid film around the Taylor Bubble falls in a reversed direction with a liquid film velocity, (u_{LTB}). The liquid slug velocity (u_{LLS}) is in upward direction. The acceleration pressure gradient results from the force needed to accelerate the liquid in the film to liquid slug velocity

$$\Delta P_a = (\rho_L u_{LTB} / g_C)(1-\alpha_{TB}) \times (u_{LTB} + u_{LLS}) \quad (3\text{-}111)$$

3.7.2 Pressure loss from gravitational effect (ΔP_g) pressure loss is calculated from average void fraction over slug unit (α_{SU}).

$$\Delta P_g = (g/g_C)[\rho_L(1-\alpha_{SU}) + \rho_G(1-\alpha_{SU})] \quad (3\text{-}112)$$

A sketch of an idealized slug pattern is shown in Figure 3.7-1. The large Taylor Bubbles flow upward at a translation velocity (u_N), its nose shape is almost perfectly bubbled shaped and flat at the tail. The gas Taylor bubble length (l_{TB}) is constant in the axial direction when assumed to have constant volume. Small entrained are distributed almost uniformly over the liquid slug length, except at the tail of Taylor bubble. The small bubble quantity is high after the slug tail. The void fraction in the Taylor bubble, liquid slug, and after the Taylor bubble are defined as α_{TB}, α_{LS} α_H respectively. These small bubbles are distributed evenly over the slug length (l), except at the tail of Taylor bubble where the void fraction (α_H) is considerably higher than the void fraction in liquid slug (α_{LS}) because of the amount of entrained gas bubbles from the falling film to the back of the Taylor bubble. The abbreviation of Taylor bubble and liquid slug are as below.

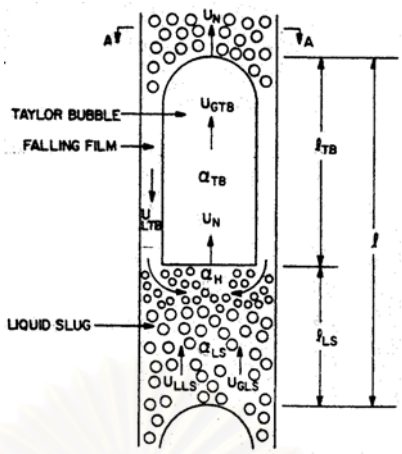

Figure 3.7.1-1 A slug unit for vertical upward slug model

l_{TB} = length of gas Taylor bubble

l_{LS} = length of liquid slug

l = length of slug unit

u_{GTB} = velocity of the gas in the Taylor bubble

u_{GTB} = velocity of the gas in the liquid slug

u_{LTB} = velocity of the liquid in the Taylor bubble

u_{LLS} = velocity of the liquid in the liquid slug

u_N = velocity of translation of Taylor bubble

The average void fraction over the slug unit (α_{SU}) is the ratio of the volume of gas in the slug unit (V_G) and volume of the slug unit itself (V_{SU}). It can be rearranged in the form of Taylor bubble void fraction α_{TB}, void fraction in the liquid slug (α_{LS}) and β ratio as below.

$$\alpha_{SU} = V_G / V_{SU} = (l_{TB} A_{GTB} + l_{LS} A_{GLS}) / [A \times (l_{TB} + l_{LS})] \quad (3\text{-}113)$$

$$\alpha_{SU} = \beta \alpha_{TB} + (1-\beta) \times \alpha_{LS} \quad (3\text{-}114)$$

$$\alpha_{TB} = \frac{A_{GTB}}{A} \quad (3\text{-}115)$$

$$\alpha_{LS} = \frac{A_{GLS}}{A} \quad (3\text{-}116)$$

$$\beta = \frac{l_{TB}}{l_{TB} + l_{LS}} \tag{3-117}$$

where A_{GTB} represents the cross sectional area of the cylindrical portion of Taylor bubble, A_{GLS} is the effective cross sectional area occupied by gas in the liquid slug.

Superficial gas and liquid velocities can be calculated from the over all mass balance of incompressible gas bubbles. Thus mass and volume balance are equivalent. Consider the flow of the slug unit through a fixed cross sectional plane. The time interval that the Taylor bubble takes to pass the cross section plane in Taylor bubble length (l_{TB}) and liquid slug length (l_{LS}) are Δt_{TB} and Δt_{LS} at translation velocity (u_N).

$$\Delta t_{TB} = l_{TB} / u_N \tag{3-118}$$

$$\Delta t_{LS} = l_{LS} / u_N \tag{3-119}$$

The volume of gas carried upward by the Taylor bubble and volume of gas carried by liquid slug are V_{GTB} and V_{GLS}.

$$V_{GT\,B} = u_{GTB}(A\alpha_{TB})\Delta t_{TB} = l_{TB}(A\alpha_{TB})(u_{GTB}/u_N) \tag{3.120}$$

$$V_{GLS} = u_{GLS}(A\alpha_{LS})\Delta t_{LS} = l_{LS}(A\alpha_{TB})(u_{GLS}/u_N) \tag{3.121}$$

During the time corresponding to the passage of one slug unit ($\Delta t = \Delta t_{TB} + \Delta t_{LS}$), the volume of gas entering the cross section area is equal to the summation of gas volume being carried by the liquid slug and Taylor bubble in a slug unit.

$$V_{GTB} = Q_G(\Delta t_{TB} + \Delta t_{LS}) = (u_G{}^S A)[(l_{TB} + l_{LS})/u_N] \tag{3.122}$$

Superficial gas velocity can be calculated by combined equations (3.121) and (3.122).

$$u_G{}^S = \beta\alpha_{TB}u_{GTB} + (1-\beta)\alpha_{LS}u_{GLS} \tag{3-123}$$

Liquid superficial velocity can be calculated in the same manner as the above method.

$$u_L{}^S = (1-\beta)\times(1-\alpha_{LS})u_{LLS} - \beta(1-\alpha_{TB})u_{LTB} \tag{3-124}$$

Translation velocity is related to other flow parameters by below equations. The Taylor bubble travels through the two-phase mixture of liquid slug at a transnational velocity, u_N, greater than that of either the gas or liquid phase. Thus, independent continuity relation can

be developed by considering the flow relative to the nose of the Taylor bubble. For liquid phase one obtains

$$(u_N - u_{GLS})\alpha_{LS} = (u_N - u_{GTB})\alpha_{TB} \quad (3\text{-}125)$$

The above equation states that in a coordinate system which translates upward , the rate of liquid flow approaching the nose from the slug is equal to that being drained in the film. The same concept, applied to the gas phase gives

$$(u_N - u_{LLS}) \times (1 - \alpha_{LS}) = (u_N + u_{LTB}) \times (1 - \alpha_{TB}) \quad (3\text{-}126)$$

The rise velocity of a Taylor Bubble is calculated using a slight modification of the equation by Collins, Davidson and Harrison (1978). A Taylor bubble moves steadily upwards with a rise velocity (u_N) in the stagnant liquid. For water which is not very viscous, an approximate analytical solution leads to a specific constant value for rise velocity of 0.35. The mean velocity of liquid just ahead of the Tailor Bubbly is approximate to $u_G{}^S + u_L{}^S$. Further, near the nose of Taylor bubble at the center of the tube, where the velocity is the highest, the liquid velocity is approximated to $1.29 \times (u_G{}^S + u_L{}^S)$.

$$u_N = 0.35\sqrt{gD} + 1.29 \times (u_G{}^S + u_L{}^S) \quad (3\text{-}127)$$

Bubble velocity in the liquid slug can be estimated by the rise velocity, and buoyancy forces acting on the bubbles. Liquid film velocity around the Taylor bubble can be calculated from the film thickness relation as

$$u_{GLS} = u_{LLS} + 1.53 \times \left[\frac{\sigma g(\rho_L - \rho_G)}{\rho_L{}^2}\right]^{1/4} \sqrt{1 - \alpha_{LS}} \quad (3\text{-}128)$$

$$u_{LTB} = 9.916 \times \left[gD\left(1 - \sqrt{\alpha_{TB}}\right)\right]^{1/2} \quad (3\text{-}129)$$

From the above assumption, one approach to solve the solution of flow parameters is to assume the void fraction in the liquid slug (α_{LS}) equals to 0.25. This void fraction value exists at the transition from bubble to slug flow which is proposed by Taitel et. al(1980). Stable liquid slug (l_S) from experimental work of Fernandes et. al shows that $l_S \approx 20D$ which agrees with the proposal of Taitel et. al(1980). Two-phase pressure loss in the slug flow can be calculated by these calculated flow parameter as the previously mentioned.

3.8 Pressure loss in vertical upward bubble flow

This model is based on the study of Dukler et. al. In this flow pattern, a continuous swarm of bubbles flows upward with the liquid stream. Buoyancy force cause bubbles to flow past the liquid phase so that bubbles velocity is higher than the liquid with the difference between gas and liquid velocity called rise velocity.

Pressure loss can be calculated from the two-phase friction factor (f_{TP}) as shown in Figure 3.6-3 and void fraction (ε) value from rise velocity

3.8.1 Pressure loss from frictional effect (ΔP_f)

Frictional pressure loss can be calculated using the similarity case II model proposed by Taitel et. al (1964) and other flow parameters.

$$\Delta P_f = \frac{f_{TP}\rho_{TP}(u_L^S + u_G^S)^2}{2g_c D} \quad (3\text{-}130)$$

3.8.2 Pressure loss from gravitation effect (ΔP_g)

$$\Delta P_g = \frac{g}{gc}\left[\varepsilon\rho_G + (1-\varepsilon)\rho_l\right] \quad (3\text{-}131)$$

3.8.3 Void fraction (ε)

Void fraction can be calculated from the definition of rise bubble velocity and superficial phase velocity (u_G^S, u_L^S)

$$u_0 = u_L - u_G \quad (3\text{-}132)$$

$$\frac{u_G^S}{\varepsilon} = \frac{u_L^S}{(1-\varepsilon)} + u_0 \quad (3\text{-}133)$$

$$\frac{u_G^S}{u_L^S} = \frac{\varepsilon}{(1-\varepsilon)} + \varepsilon\frac{1.53\left(\sigma g(\rho_L - \rho_G)\right)^{0.25}}{u_L^S \rho_L{}^{0.5}} \quad (3\text{-}134)$$

It should be noted that at low liquid flow rate, bubble flow will occur if the average void fraction does not exceed 0.25. But at high liquid rate, the turbulent forces tend to break up the larger Taylor bubble which is formed at void fraction above 0.25 and bubble flow can exist at void fractions as high as 0.5. So the calculated void fraction shall be in the range of 0.25 to 0.5.

3.9 Pressure loss in vertical down annular flow

Pressure loss in annular flow can be calculated in the same manner as the stratified model. Force balances on the gas and liquid are rearranged in the form of film thickness (δ) and the proposed correlation of others parameter for solving the unit pressure balance of annular flow. Details of calculations are as below.

The process of analyzing transition for vertical downward flow is started from annular flow determination. When gas is introduced concurrently with the liquid in a pipe, the gas flows along the pipe core while the liquid flows separately along the pipe wall as shown in Figure 3.9-1. The force exerted on the fully developed flow can be described by determining force balance per unit pipe length between liquid phase and gas phase:

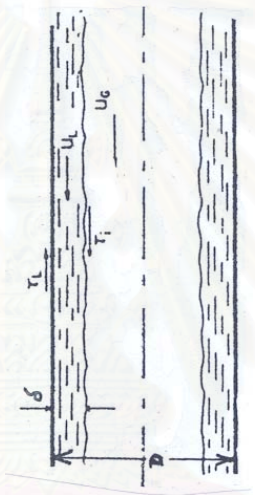

Figure 3.9-1 Equilibrium Annular flow

$$-A_L(dP/dZ)_L - \tau_{WL}S_L + \tau_i S_i + \rho_L A_L g = 0 \quad (3\text{-}135)$$

$$-A_G(dP/dZ)_G - \tau_i S_i + \rho_G A_G g = 0 \quad (3\text{-}136)$$

For a uniform steady state and in the absence of hydraulic gradient, the value of $(dP/dZ)_G$ is equal to $(dP/dZ)_L$. The pressure balance in the liquid and gas phases are combined as below:

$$\tau_i S_i\left(\frac{1}{A_L}+\frac{1}{A_G}\right)+(\rho_L-\rho_G)g-\tau_{WL}\frac{S_L}{A_L}=0 \quad (3\text{-}137)$$

A dimensionless liquid film thickness ($\tilde{\delta}$) is defined as the ratio of liquid film height per pipe diameter. This dimensionless parameter can be calculated at each flow condition and its physical properties by below equation.

$$\frac{\tau_i}{D\left(\tilde{\delta}-\tilde{\delta}^2\right)\left(1-2\tilde{\delta}\right)}+g\left(\rho_L-\rho_G\right)-\frac{\tau_L}{D\left(\tilde{\delta}-\tilde{\delta}^2\right)}=0 \quad (3\text{-}138)$$

Pressure loss in annular flow is calculated from the flow parameters and the liquid film thickness as indicated in these equations.

$$\tilde{\delta}=\frac{\delta}{D} \quad (3\text{-}139)$$

$$S_L=\pi D \quad (3\text{-}140)$$

$$S_i=2\pi\left(\frac{D}{2}-\delta\right)=\pi\left(D-2\delta\right) \quad (3\text{-}141)$$

$$A_L=\frac{\pi D^2}{4}-\pi\left(\frac{D}{2}-\delta^2\right)=\pi\left(D\delta-\delta^2\right) \quad (3\text{-}142)$$

$$A_G=\pi\left(\frac{D}{2}-\delta\right)^2 \quad (3\text{-}143)$$

$$D_L=\frac{4A_L}{S_L}=4D\left(\tilde{\delta}-\tilde{\delta}^2\right) \quad (3\text{-}144)$$

$$D_G=\frac{4A_G}{S_L}=D\left(1-2\tilde{\delta}^2\right) \quad (3\text{-}145)$$

$$u_G=\frac{Q_G}{A_G}=\frac{4u_G{}^S}{1-4\tilde{\delta}+4\tilde{\delta}^2} \quad (3\text{-}146)$$

$$u_L=\frac{Q_L}{A_L}=\frac{u_L{}^S}{4\left(\tilde{\delta}-\tilde{\delta}^2\right)} \quad (3\text{-}147)$$

Shear stress at the liquid wall and interface (τ_{WL}, τ_i) and friction factor are calculated from the correlation proposed in 3.4 Stratified model from equations (3-48) to (3-53) respectively.

3.10 Pressure loss in vertical downward slug flow

Pressure loss in vertical downward slug consists of friction loss and gravitational loss. Friction loss can be calculated using the similarity model by Taitel et. al(1964) and the gravitation pressure loss using liquid hold up calculated from drift flux which is proposed by C.S, Martin (1998).

3.10.1 Pressure loss from frictional effect (ΔP_f)

Frictional pressure loss can be calculated by the similarity model case I as below

$$\Delta P_f = \frac{f_{TP}\rho_{LS}u_m{}^2}{2gcD} \times \frac{l_S}{l_T} \quad (3\text{-}148)$$

where l_S is liquid slug length, l_T is total slug unit length, u_m is the mixture velocity.

These following flow parameters are calculated from the similarity model. Void fraction of liquid slug (ε) is assumed to be 0.25 by Dukler et. al.(1980). Thus the value of two-phase friction factor (f_{TP}) is evaluated at a liquid volume fraction value (λ) equal to 0.75.

3.10.2 Pressure loss from gravitation effect (ΔP_g)

$$\Delta P_g = \frac{g}{gc}\left[H_L\rho_L + (1-H_L)\rho_G\right] \quad (3\text{-}149)$$

3.10.3 Drift flux Liquid hold up (H_L)

Liquid hold up can be calculated from the gas superficial velocity ($u_G{}^S$) and the Taylor bubble velocity (u_b). For the vertical downward slug model, average constant value of the distribution parameters C_0 and Drift flux coefficient K value are 1 and -0.6 respectively.

$$H_L = 1 - \frac{u_G{}^S}{u_b} \quad (3\text{-}150)$$

$$u_b = c_0 u_m + K\frac{\left[gD(\rho_L - \rho_G)\right]^{0.5}}{\rho_L{}^{0.5}} \quad (3\text{-}151)$$

Because the void fraction of the liquid slug is around 0.25, H_L obtained from the above equation is limited to 0.75.

3.11 Pressure loss in vertical downward bubble flow

Pressure for vertical downward bubble flow can be calculated in the same manner as vertical downward slug flow. The similarity model is used for frictional pressure loss calculations and Drift flux model is used for gravitational loss and liquid hold up (H_L). Details of the calculations are as below.

3.11.1 Pressure loss from frictional effect (ΔP_f):

Frictional pressure loss can be calculated using the similarity model case II by Taitel et. al (1964) using the flow parameters as indicated:

$$\Delta P_f = \frac{f_{TP}\rho_{TP}U_m^{\ 2}}{2gcD} \tag{3-152}$$

3.11.2 Pressure loss from gravitation effect (ΔP_g)

Gravitation pressure loss is calculated using equation (3-149)

3.11.3 Drift flux Liquid hold up (H_L)

C.S Martin (1973) obtain the value of constant parameter C_0 = 0.9 and the value of K equal to zero from his experimental data. The liquid hold up for vertical downward flow is simply calculated as

$$H_L = 1 - \frac{u_G^{\ S}}{0.9u_m} \tag{3-153}$$

CHAPTER IV

PROGRAM DEVELOPMENT

4.1 Program basis

The basis of the two-phase flow program is developed from the physical mechanisms from experimental data of air and water in the pipe at low pressure and room temperature. The list of the original scope of experimental condition ranges used to develop the models is shown in Table 4.1-1, 4.1-2, 4.1-3 for horizontal, vertical upward and vertical downward direction respectively. The unit conversion table is shown in Table 4.1-4.

Table 4.1-1 Basis of horizontal flow pattern determination

Item	Description	English unit	Metric unit
1	Source of data reference	Manhane et. al. 1974	Manhane et. al. 1974
2	Fluid type	air - water	air - water
3	Pipe size, ID	1 inch	2.5 cm
4	Pipe length, L	-	-
5	Temperature	77 ^{0}F	25 ^{0}C
6	Pressure, P	14.7 PsiA	0.1 Mpa
7	Range of Velocity, U_L^S	0.03-26 ft/s	0.01 - 8 m/s
8	Range of Velocity, U_G^S	0.33-260 ft/s	0.1 - 80 m/s
9	Range of Volume flow rate, Q_L	0.07-50 (10^{-3}) ft^3/s	0.02-16 (10^{-3}) m^3/s
10	Range of Volume flow rate, Q_G	0.7-530 (10^{-3}) ft^3/s	0.2-160 (10^{-3}) m^3/s

Table 4.1-2 Basis of vertical upward flow pattern determination

Item	Description	English unit	Metric unit
1	Source of data reference	Taitel et. al. 1980	Taitel et. al. 1980
2	Fluid type	air-water	air-water
3	Pipe size, ID	1 - 2 inch	2.5 - 5.1 cm
4	Pipe length, L	28 ft	8.5m
5	Temperature	77 degF	25 degC
6	Pressure, P	14.7 PsiA	0.1 Mpa
7	Range of Velocity, U_L^S	0.1 - 10 ft/s	0.03 - 3 m/s
8	Range of Velocity, U_G^S	0.1 - 100 ft/s	0.03 - 30m/s
9	Range of Volume flow rate, Q_L	0.2 - 20 (10^{-3})ft^3/s	0.06 - 6 (10^{-3}) m^3/s
10	Range of Volume flow rate, Q_G	0.2 -200 (10^{-3})ft^3/s	0.06-60 (10^{-3}) m^3/s

Table 4.1-3 Basis of vertical downward flow pattern determination

Item	Description	Metric unit	English unit
1	Source of data reference	Barnea et. al. 1981	Barnea et. al. 1981
2	Fluid type	air-water	air-water
3	Pipe size, ID	2.5 - 5.1 cm	1 - 2 inch
4	Pipe length, L	10 m	33 ft
5	Temperature	25 ^{0}C	77 ^{0}F
6	Pressure, P	0.1 MPa	14.7 PsiA
7	Range of Velocity, U_L^S	0.02 - 20 m/s	0.07 - 65 ft/s
8	Range of Velocity, U_G^S	0.05 - 5 m/s	0.16 - 16 ft/s
9	Range of Volume flow rate, Q_L	0.04 - 40 (10^{-3}) m^3/s	0.1 - 130 (10^{-3}) ft^3/s
10	Range of Volume flow rate, Q_G	0.1-10 (10^{-3}) m^3/s	0.3 - 33 (10^{-3}) ft^3/s

Table 4.1-4 Unit of measurement

Abbreviation	Dimension	English unit	To convert to SI multiply by	
			Factor	SI Unit
A	Cross section area	$inch^2$	6.5416	cm^2
d	Pipe inside diameter	inch	2.54	cm
deg	Angle of inclination	degree	Pi/180	radian
g	Acceleration of gravity	32.174ft/s^2	-	9.81m/s^2
L	Length	ft	0.3048	m
mu	Viscosity	cP	1	(10^{-3})Ns/m^2
P	Pressure	psi	0.07031	kg/cm^2
Ps	Pressure loss	Psi/100 ft	0.23068	$kg/(cm^2$x100m)
Q	Flow rate	ft^3/s	35.3145	m^3/s
Rho	Density	lbm/ft^3	16.0184	kg/m^3
Surf_L	Surface tension	lbf/ft	14.5938	N/m
T	Temperature	deg F	(T-32)/1.8	deg C
V	Velocity	ft/s	0.3048	m/s

4.2 Program layout

The developed program is called " Two-Phase program". It is designed to reduce the time required to perform of manual calculations for flow pattern, pressure loss, and two-phase flow iterations of gas-liquid flow in pipeline systems. The program is developed in Visual Basic version 6.0 and is run under Microsoft Windows. Each run result is stored in the Notepad application which the user to print out the result for review and record keeping.

The program has two sections, namely the input section and the results section. Details of each section are as explained below. The program is ready for calculation once the data of the flow condition of the gas and liquid is entered in the input box and the pipe orientation is

selected. The result of calculation i.e., flow pattern, and pressure loss will be shown in the provided results box.

4.2.1 Input Section

Information of calculation data such as calculation number, revision, date, can be input to provide a history record of the calculation. A save button command supports the save and retrieve functions. This function helps the user when the input data is required repeatedly to calculate flow over many line sections in many cases. The benefit of this is in the terms of input time saving and the human error factor in the inputting process.

Process input data such as physical properties for the gas phase and liquid phase. and pipe size properties are as shown in Figure 4.3.1-1. All input boxes must be filled in to allow the calculation process to be completed. Input descriptions are listed as below:

1. Liquid volume flow rate and Gas volume flow rate (QL,QG)
2. Liquid density and gas density (rhoL, rhoG)
3. Liquid viscosity, gas viscosity (muL,muG)
4. Surface tension (sur_f)
5. NPS : norminal pipe size
6. Schedule : schedule of pipe
7. D(id) : inside diameter, The program provides values of inside diameter based on the input nominal pipe size and pipe schedule. The commercial pipe size are based on ANSI B31.3 Standard (See more detail in Appendix A). A specific value can be input by user as an option.
8. Inclination: angle of pipe orientation
9. Length: length of pipe

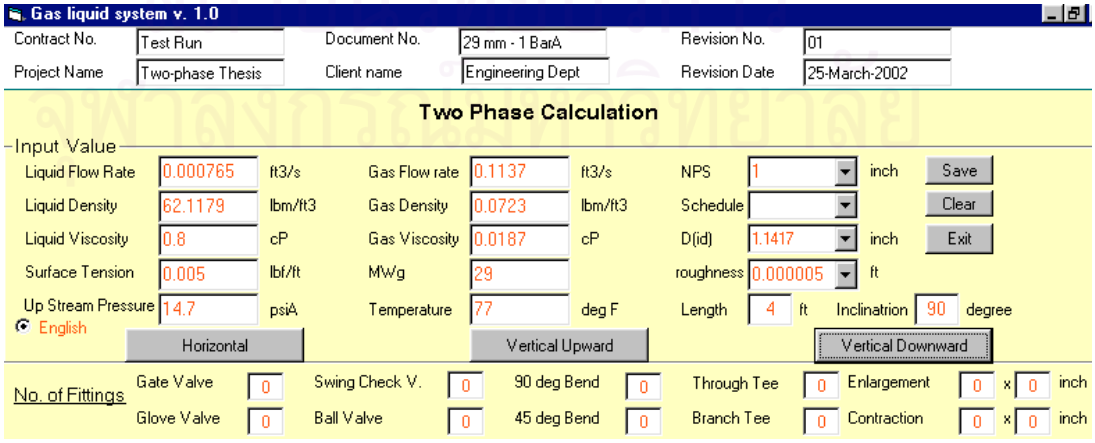

Figure 4.2.1-1 Program 's Input screen

4.2.2 Calculation result

Result of Two Phase flow pattern and pressure is shown in a provided list box separate into horizontal flow or vertical upward or vertical downward flow as below:

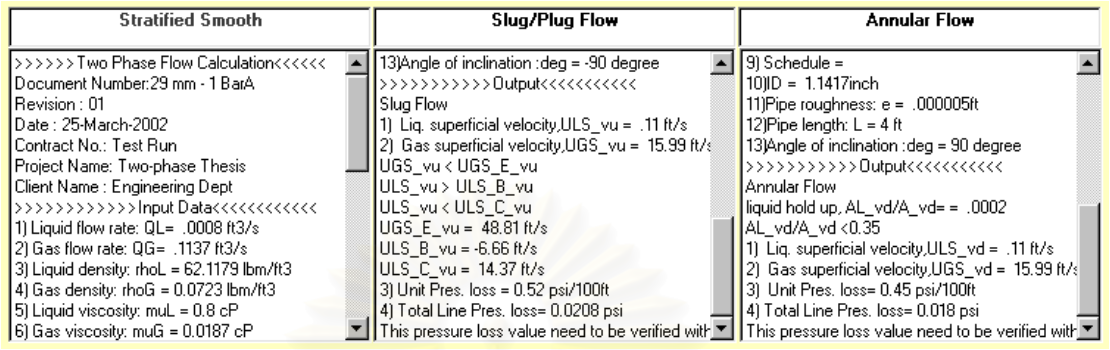

Figure 4.2.2-1 Results section screen

4.3 Calculation Procedure

The process of flow pattern determination starts when all the input data has been filled in completely and pipe orientation has been selected. The calculation procedures of horizontal direction, vertical upward and vertical downward are shown in Figure 4.3-1, 4.3-2, 4.3-3 respectively.

Once the program has completed the flow pattern determination, it continues to calculate pressure loss based on the proposed models of each flow pattern. A flow chart of the program procedure for stratified model, horizontal slug model, similarity model, vertical upward slug model, vertical upward bubble model, annular downward model, vertical down slug model, and vertical down bubble model are shown in Figure 4.3-4, 4.3-5, 4.3-6, 4.3-7, 4.3-8, 4.3-9, 4.3-10, 4.3-11 respectively.

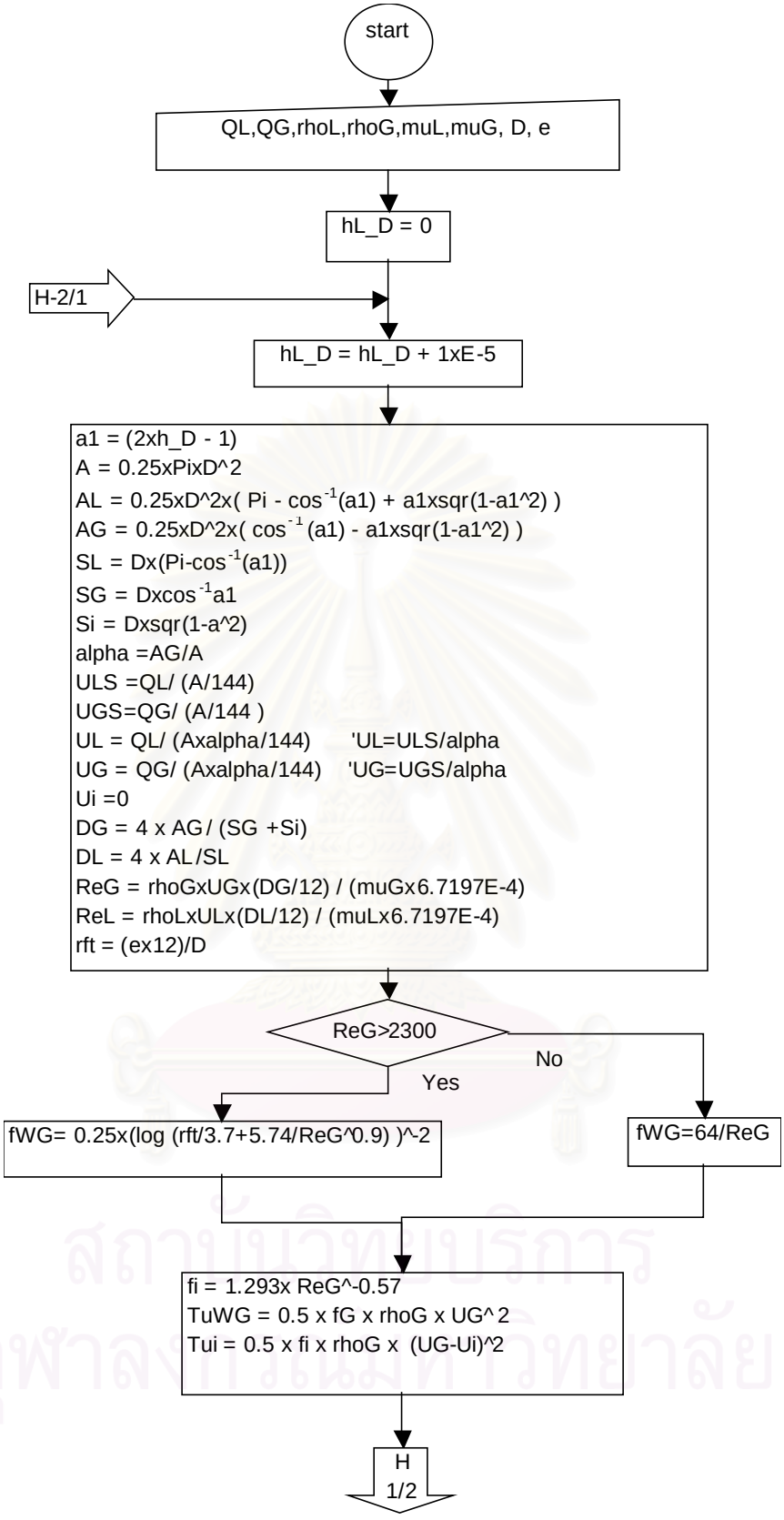

Figure 4.3-1 Flow chart for horizontal flow pattern

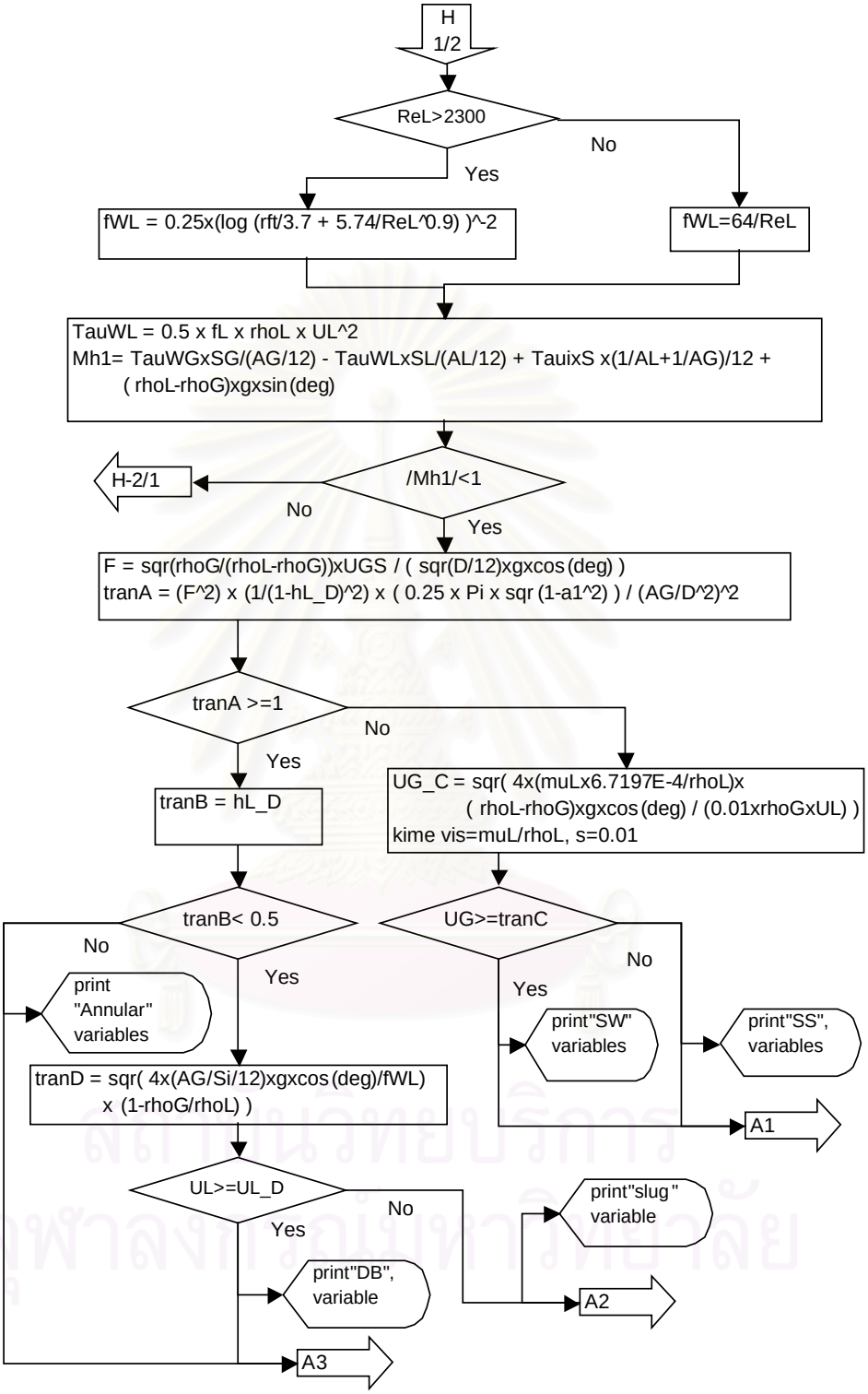

Figure 4.3-1(Cont.) Flow chart for horizontal flow pattern

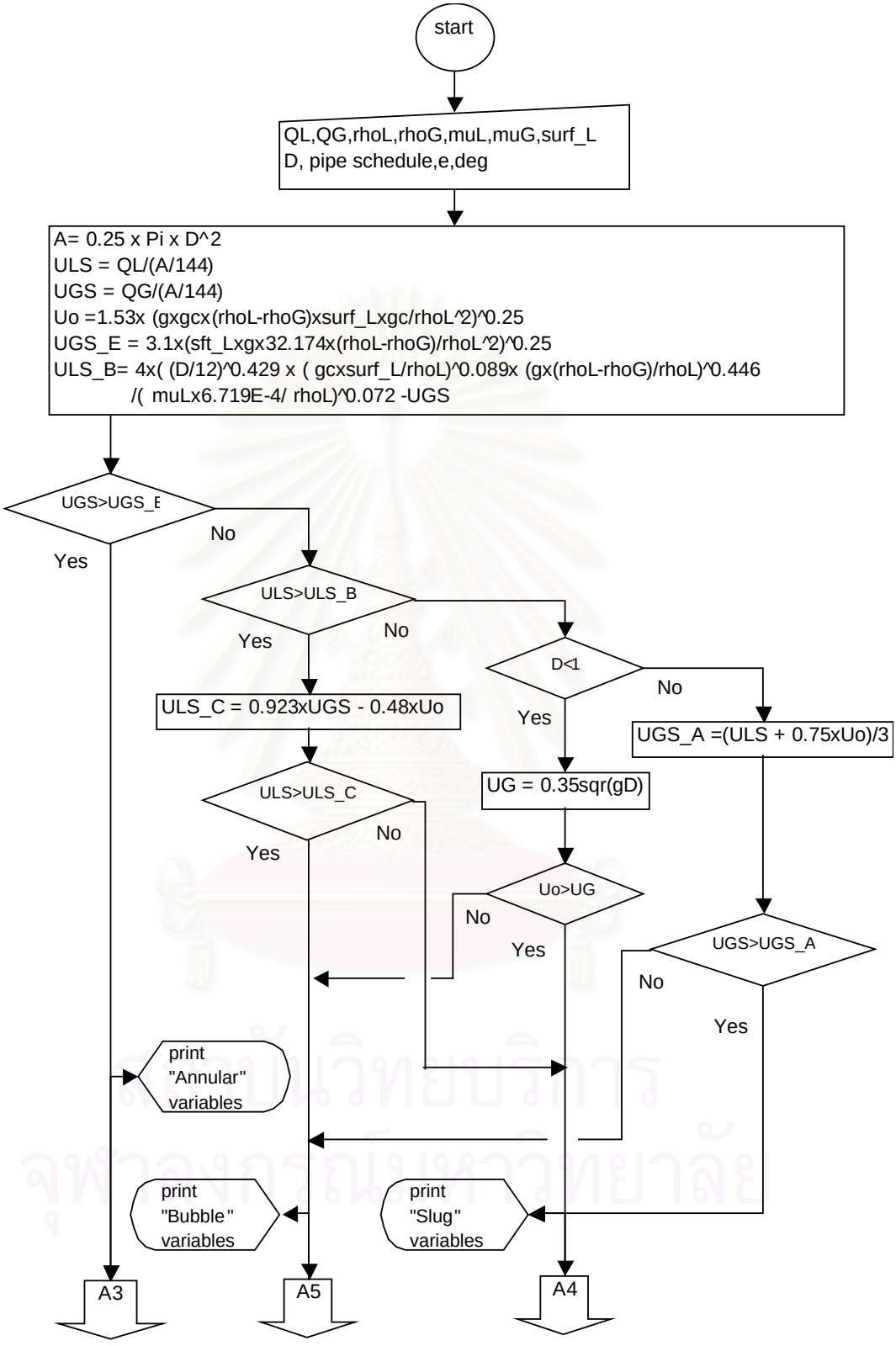

Figure 4.3-2 Flow chart for vertical upward flow pattern

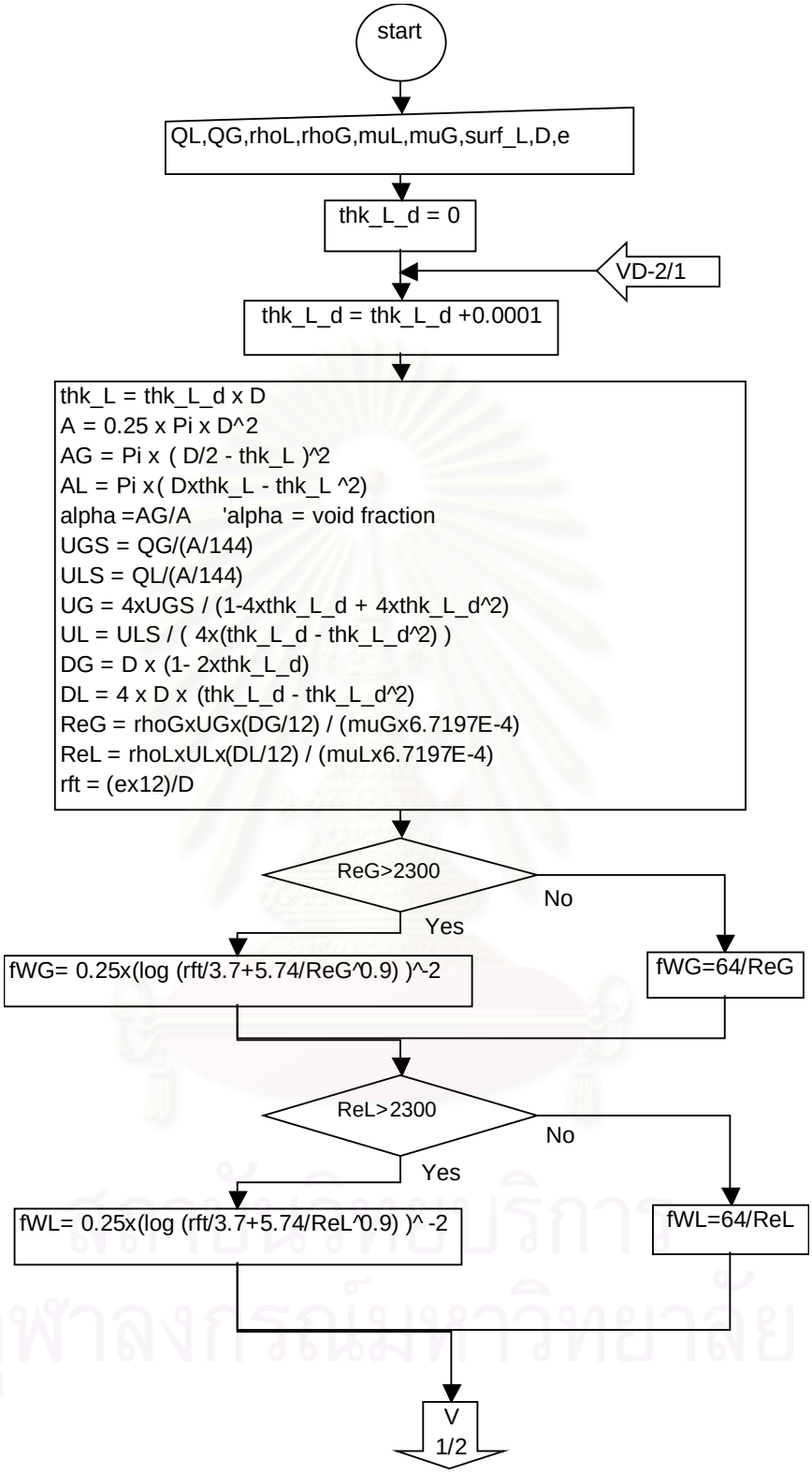

Figure 4.3-3 Flow chart for vertical downward flow pattern

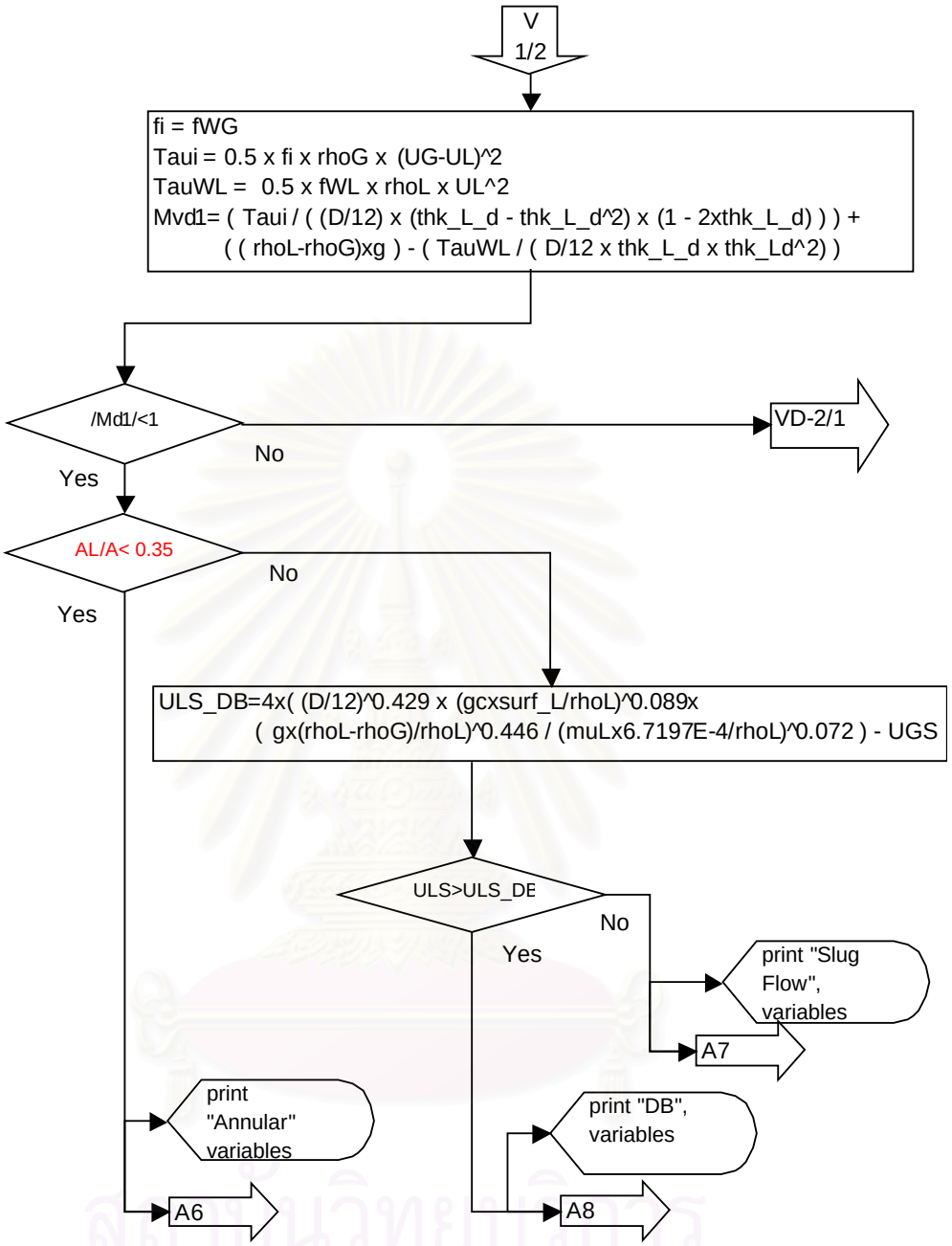

Figure 4.3-3 (Cont.) Flow chart for vertical downward flow Pattern

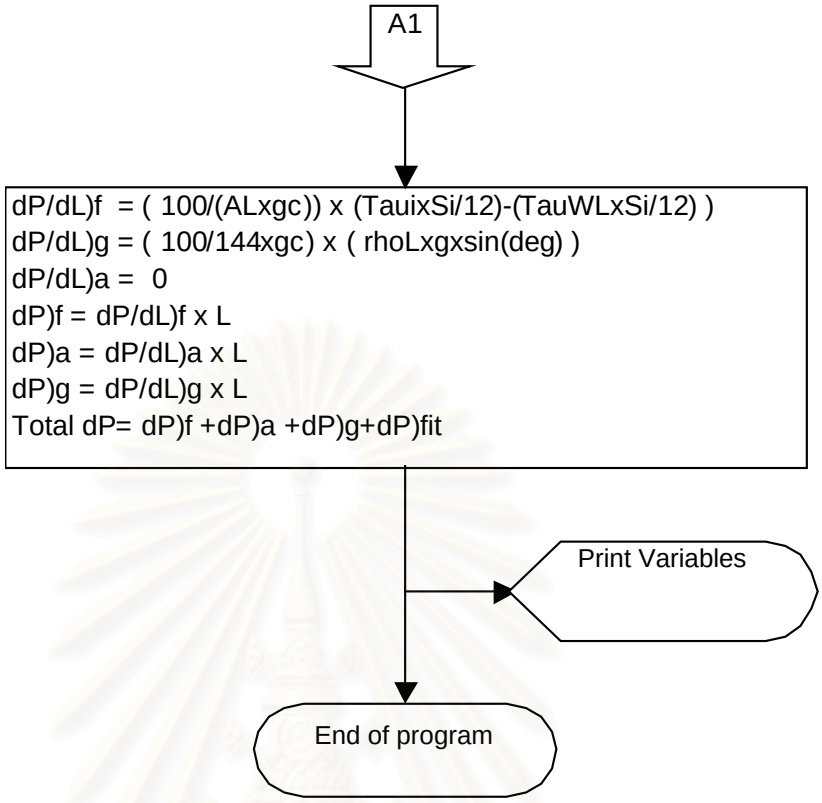

Figure 4.3-4 Flow chart for stratified model

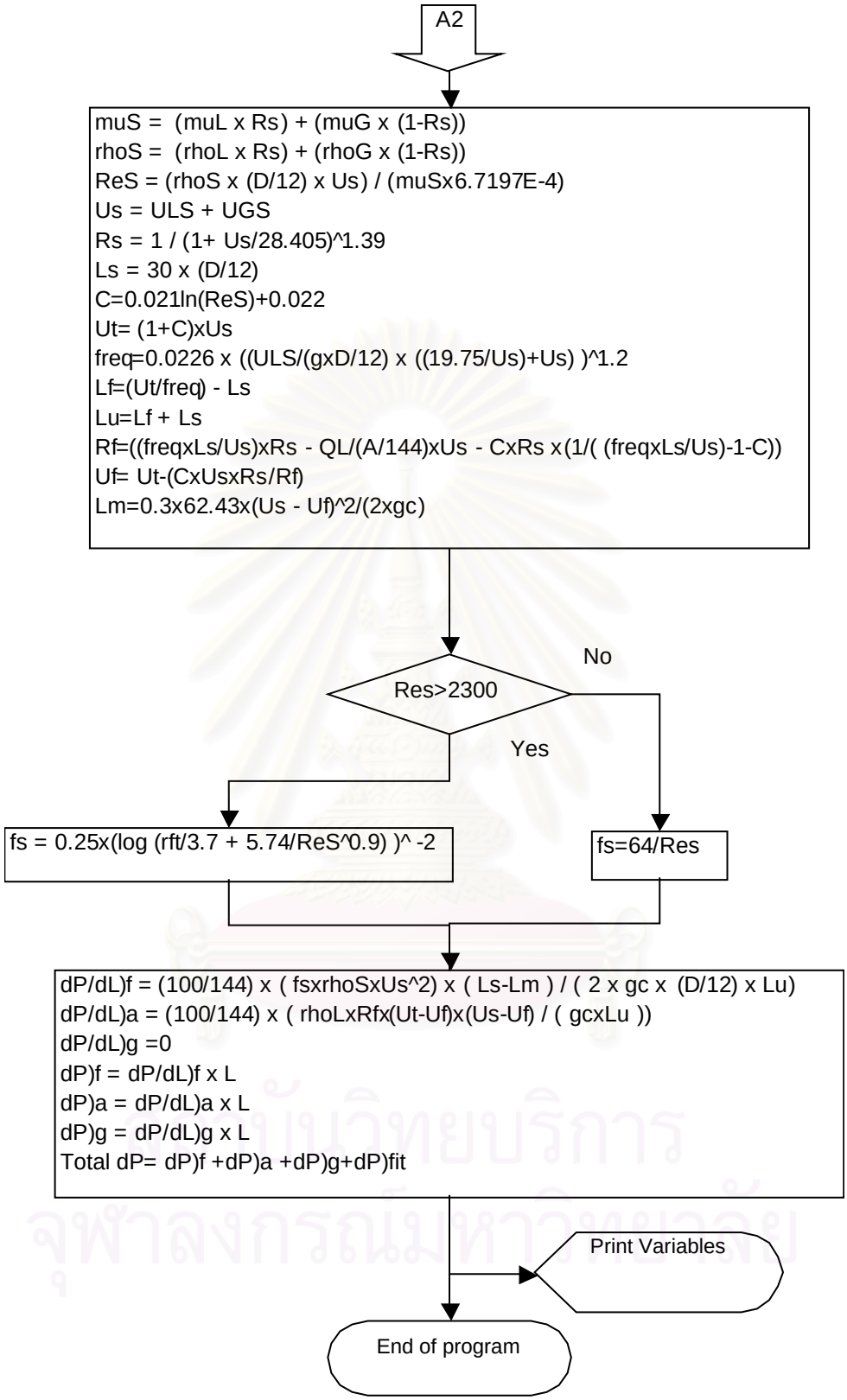

Figure 4.3-5 Flow chart for horizontal slug model

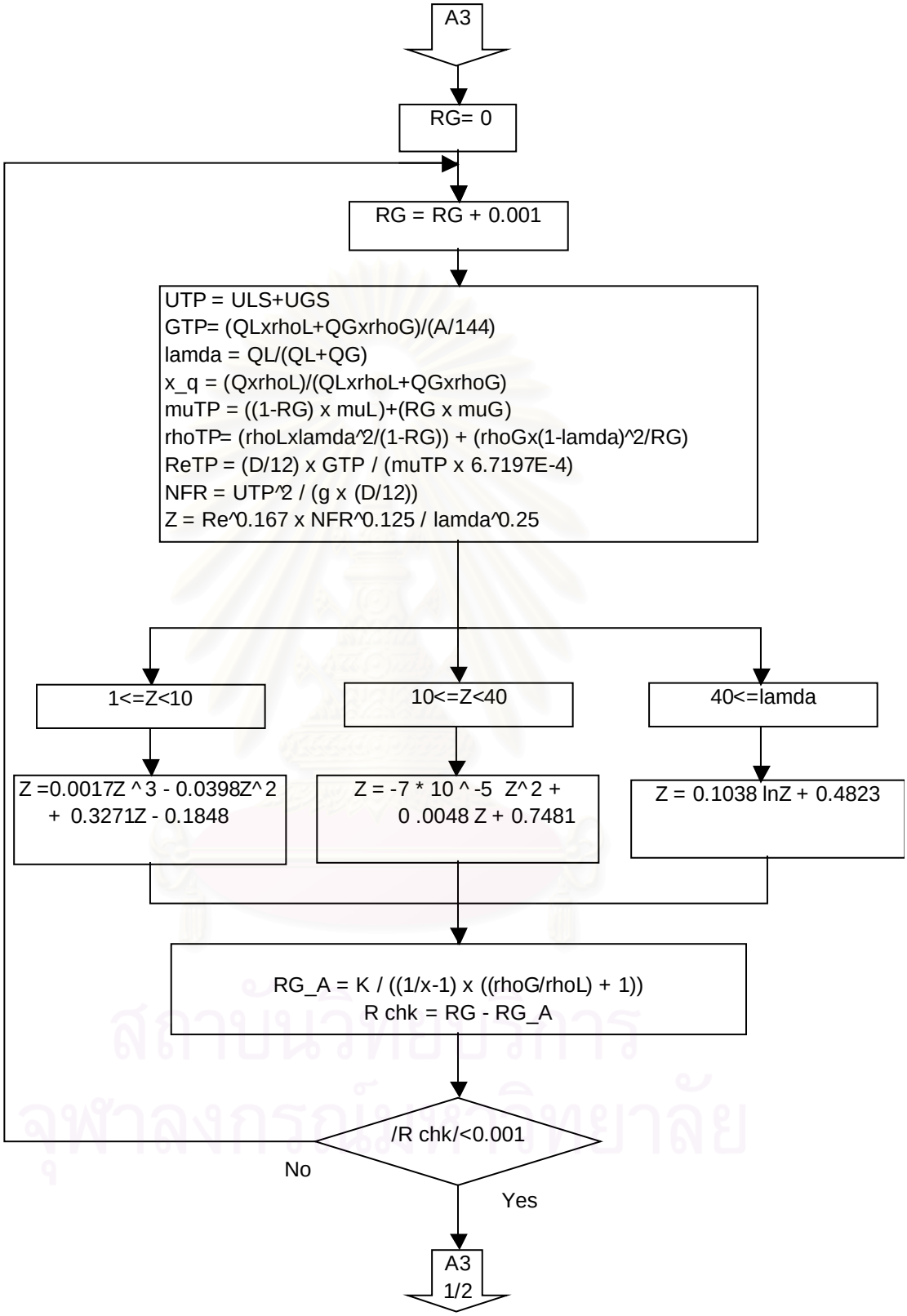

Figure 4.3-6 Flow chart for annular and bubble flow (similarity model)

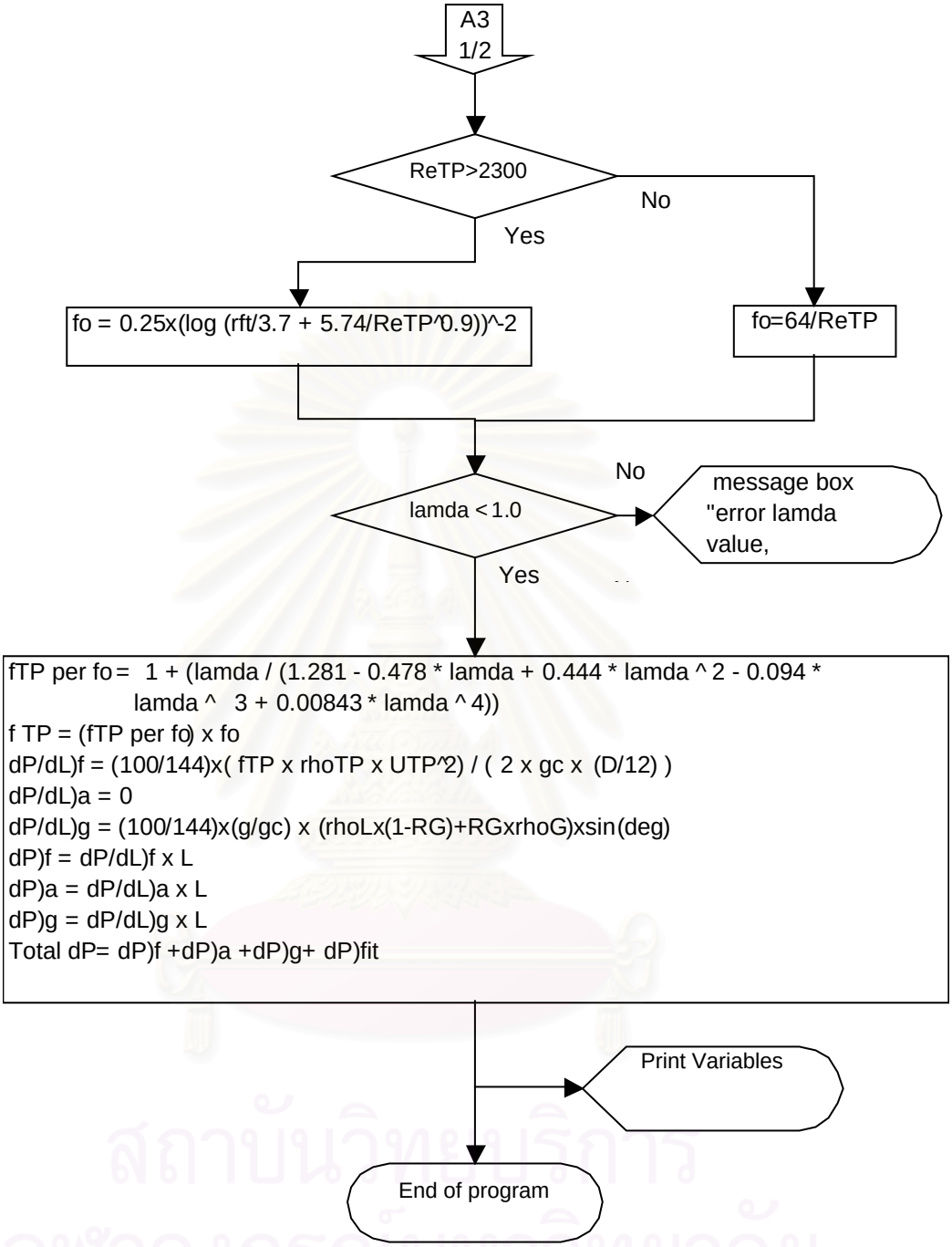

Figure 4.3-6 (Cont.) Flow chart for annular and bubble flow (similarity model)

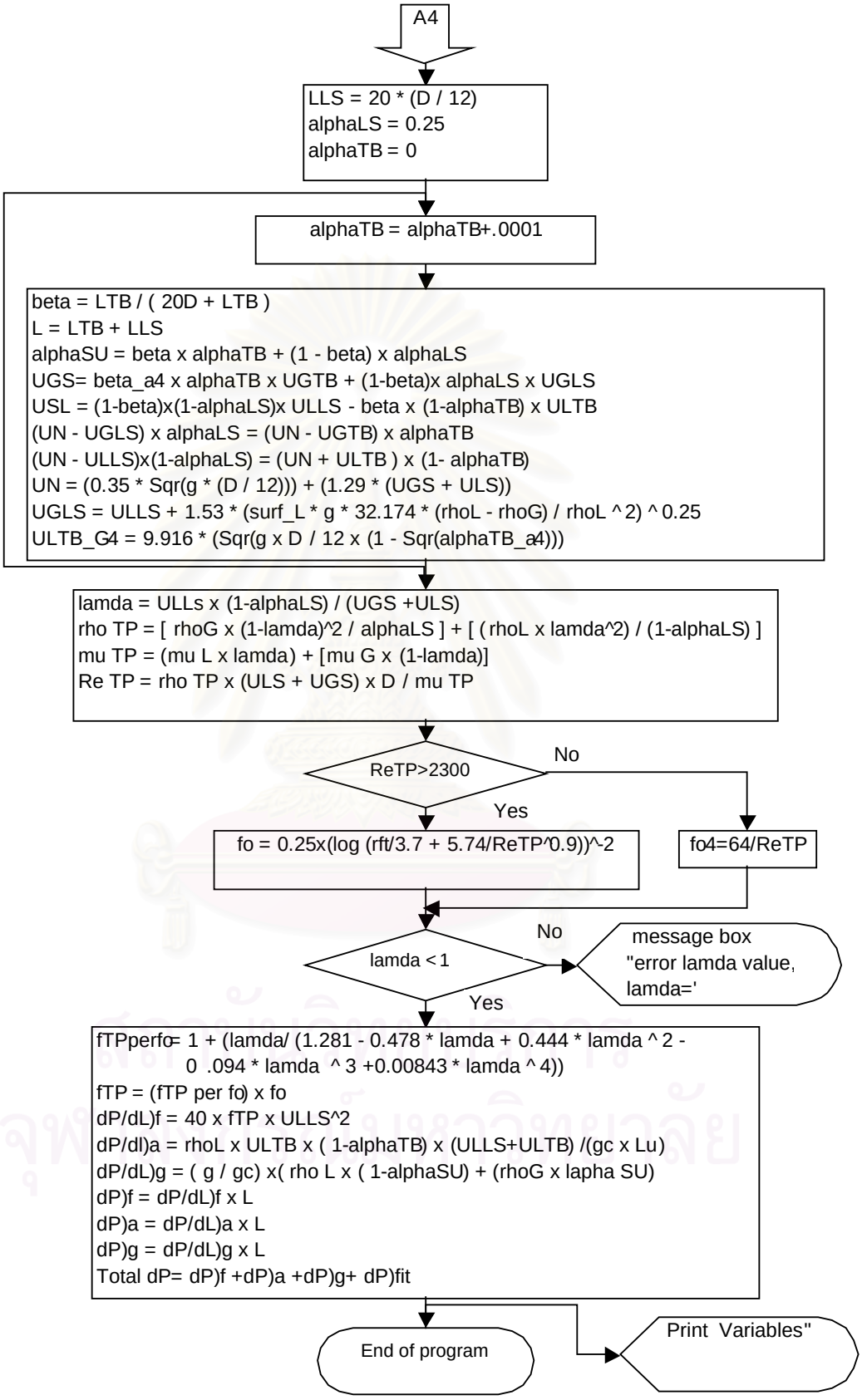

Figure 4.3-7 Flow chart for vertical upward slug model

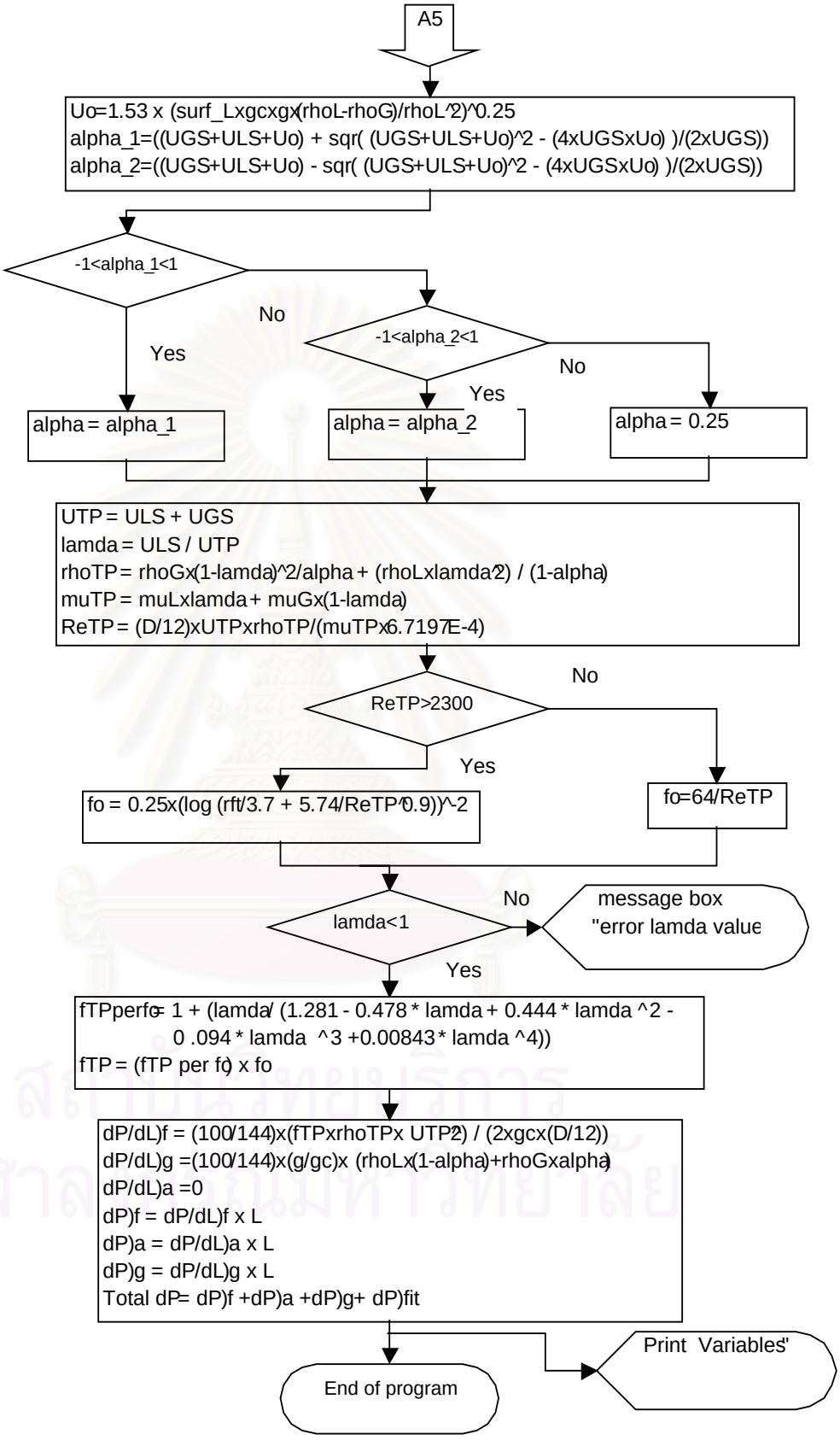

Figure 4.3-8 Flow chart for vertical upward bubble model

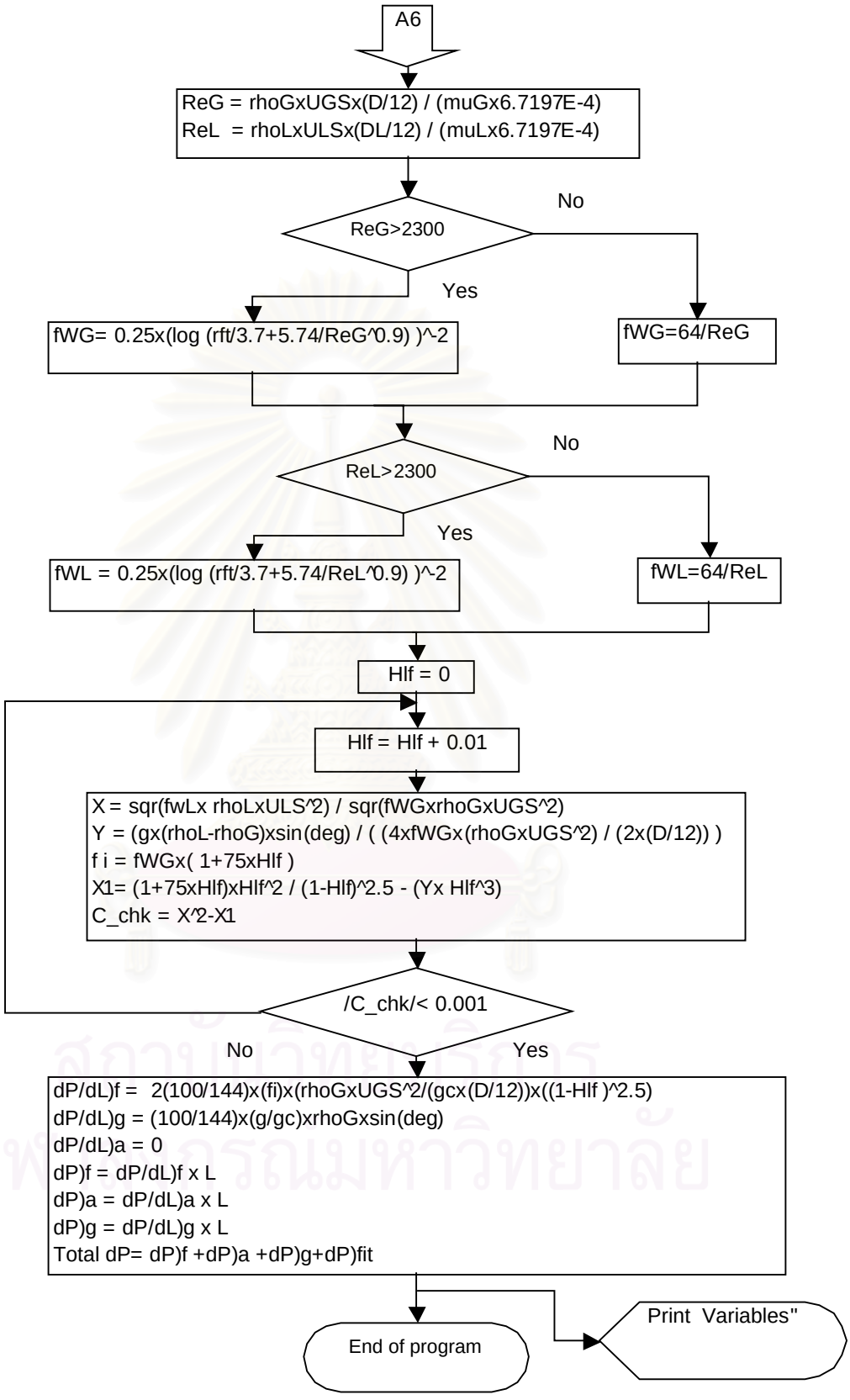

Figure 4.3-9 Flow chart for annular downward model

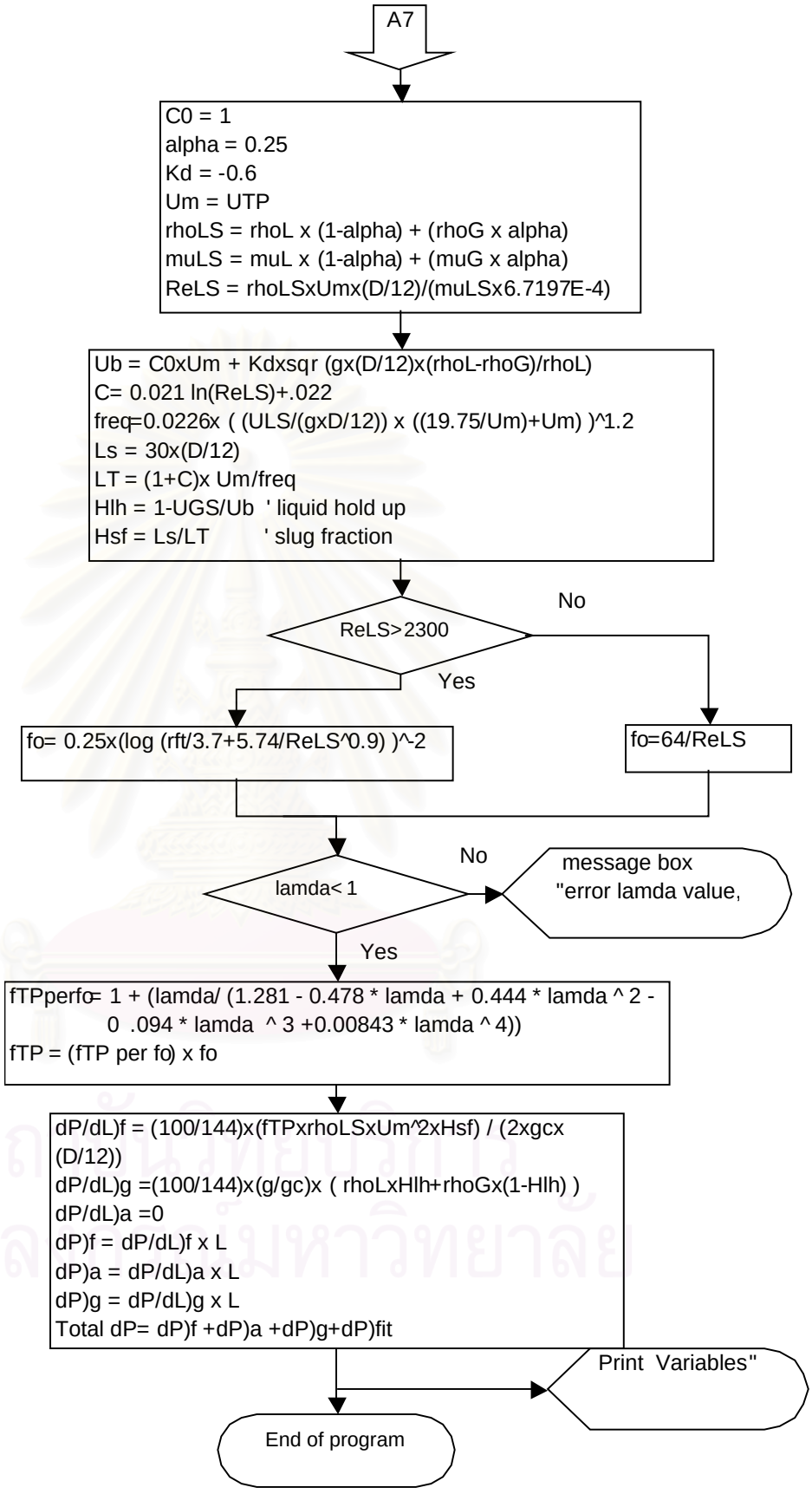

Figure 4.3-10 Flow chart for vertical down slug model

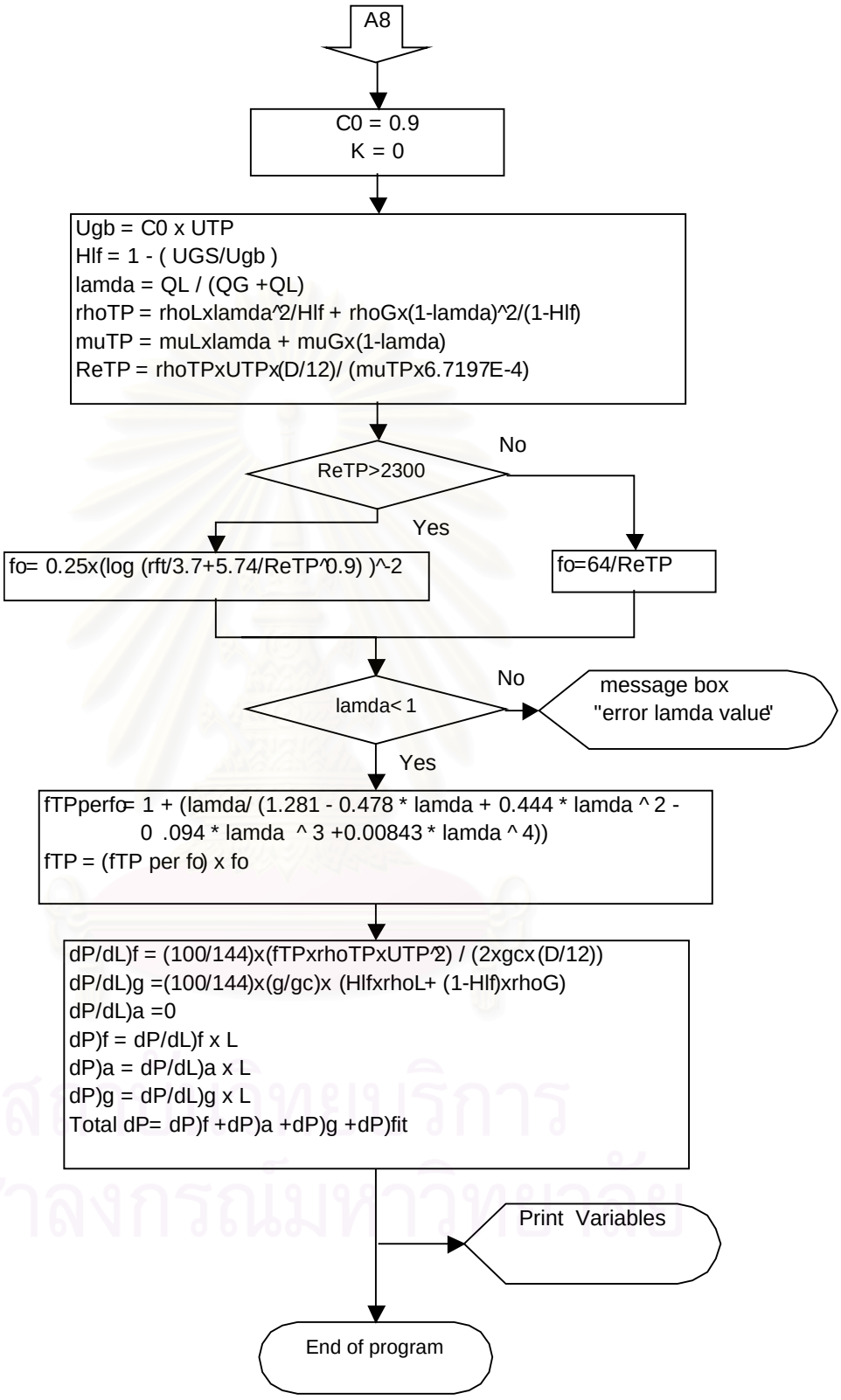

Figure 4.3-11 Flow chart for vertical down bubble model

CHAPTER V

PROGRAM RESULT AND DISCUSSION

The developed program has been tested against the experimental data generated by other researchers. The tested data comes from experiments per formed with an air-water system in pipe under low pressure conditions. The program accuracy is tested in the term of flow pattern prediction as well as pressure loss calculation with the raw experimental data in the below section.

5.1 Program Result

The flow pattern prediction and pressure loss calculation accuracy is tested separately in three pipe orientations, namely horizontal, vertical upward and vertical downward. The ranges of pipe diameter were between 1 inch to 3 inch.

5.1.1 Flow pattern prediction result in the horizontal direction

The flow pattern prediction was tested against experimental data in 29 mm, 54 mm glass pipe under atmospheric outlet condition and 77.92 mm carbon pipe at 5 barG pressure.

Table 5.1.1-1 Program result compared with air-water system at room temperature, 1 barA, ID = 29 mm in horizontal direction.

Superficial velocity		Flow pattern		Flow pattern result
ULS(ft/s)	UGS(ft/s)	Experiment	Predict	
0.11	8.08	Stratified	SW	correct
0.11	11.39	Stratified	SW	correct
0.11	13.88	Stratified	SW	correct
0.11	15.99	Stratified	SW	correct
0.11	17.85	Stratified	SW	correct
0.07	11.39	Stratified	SW	correct
0.07	15.99	Stratified	SW	correct
0.07	19.53	Stratified	SW	correct
0.07	22.52	Stratified	SW	correct
0.07	25.15	Stratified	SW	correct
0.07	27.52	Stratified	SW	correct
0.07	29.71	Stratified	SW	correct
0.07	31.72	Stratified	SW	correct
0.07	33.63	Stratified	SW	correct

Properties are ρ_L = 62.1179 lbm/ft3, μ_L =0.8 cP; ρ_G =0.0723 lbm/ft3, μ_G =0.02 cP , σ = 0.005 lbf/ft (Raw Data from Winai W. and Wattanapong K 1996)

Table 5.1.1-2 Program result compared with air-water system at 20 ^{o}C, 5 BarG, ID=77.92 mm in horizontal direction

Superficial velocity		Flow pattern		Flow pattern result
ULS(ft/s)	UGS(ft/s)	Experiment	Predict	
0.13	3.12	stratified	SS	correct
0.13	4.92	stratified	SS	correct
0.26	4.92	stratified	SS	correct
0.2	5.91	stratified	SS	correct
0.33	8.86	stratified	SS	correct
0.39	8.69	stratified	SS	correct
0.49	10.5	stratified	SW	correct
0.52	14.76	stratified	AN	incorrect
0.66	14.76	stratified	AN	incorrect
0.33	18.37	stratified	SW	correct
0.72	19.03	stratified	AN	incorrect
0.95	23.62	stratified	AN	incorrect
0.33	25.59	stratified	AN	incorrect
0.98	27.56	stratified	AN	incorrect
0.85	29.53	stratified	AN	incorrect
0.49	6.89	Slug	SS	incorrect
0.52	8.86	Slug	SS	incorrect
0.69	10.17	Slug	SW	incorrect
0.75	11.48	Slug	AN	incorrect
0.82	14.76	Slug	AN	incorrect
0.98	16.4	Slug	AN	incorrect
1.05	18.37	Slug	AN	incorrect
1.21	18.37	Slug	AN	incorrect
1.25	20.01	Slug	AN	incorrect
1.28	24.28	AN	AN	correct
0.95	22.97	AN	AN	correct
0.69	23.29	AN	AN	correct
0.59	26.25	AN	AN	correct
0.46	26.25	AN	AN	correct
0.33	26.57	AN	AN	correct

Properties are ρ_L = 62.32 lbm/ft3, μ_L =1.0 cP; ρ_G =0.46 lbm/ft3, μ_G =0.02 cP, σ = 0.005 lbf/ft (Raw data from Dr. Somprasong, 1994)

Table 5.1.1-3 Program result compared with air-water system at room temperature, 1 barA, ID=54 mm in horizontal direction

Superficial velocity		Flow pattern		Flow pattern result
ULS(ft/s)	UGS(ft/s)	Experiment	Predict	
0.24	4.73	Stratified	SW	correct
0.24	5.27	Stratified	SW	correct
0.24	5.73	Stratified	SW	correct
0.24	6.68	Stratified	SW	correct
0.24	7.06	Stratified	SW	correct
0.1	6.3	Stratified	SW	correct
0.1	7.06	Stratified	SW	correct
0.1	8.48	Stratified	SW	correct
0.1	11.17	Stratified	SW	correct
0.1	13.44	Stratified	SW	correct
0.1	15.76	Stratified	SW	correct
0.1	17.61	Stratified	SW	correct
0.1	20.63	Stratified	SW	correct

Properties are ρ_L = 62.1179 lbm/ft3, μ_L =0.8 cP, ρ_G =0.0723 lbm/ft3, μ_G =0.02 cP, σ = 0.005 lbf/ft (Raw data from Winai, et. al1996)

5.1.2 Flow pattern prediction result in vertical upward direction

The flow pattern prediction for vertical upward flow was tested against experimental data for flow condition in 50.74 mm, 25 mm and 19 mm pipe under atmospheric outlet conditions

Table 5.1.2-1 Program result compared with air-water system data at room temperature P= 1 BarA, ID= 50.74 mm in vertical upward direction

Superficial velocity		Flow pattern		Result
ULS(ft/s)	UGS(ft/s)	Experiment	Calculated	
0.07	0.10	Bubble	Bubble	Correct
0.07	0.16	Bubble	Bubble	Correct
0.33	0.16	Bubble	Bubble	Correct
0.95	0.16	Bubble	Bubble	Correct
1.94	0.16	Bubble	Bubble	Correct
1.94	0.33	Bubble	Bubble	Correct
2.26	0.66	Bubble	Bubble	Correct
3.22	0.23	Bubble	Bubble	Correct
3.22	0.59	Bubble	Bubble	Correct
6.56	0.26	Bubble	Bubble	Correct
6.56	0.49	Bubble	Bubble	Correct
9.84	0.98	Bubble	Bubble	Correct
9.84	1.64	Bubble	Bubble	Correct

Table 5.1.2-1 (Cont.) Program result compared with air-water system data at room temperature P= 1 BarA, ID= 50.74 mm in vertical upward direction

Superficial velocity		Flow pattern		Result
ULS(ft/s)	UGS(ft/s)	Experiment	Calculated	
0.33	1.31	Slug	Slug	Correct
0.33	2.30	Slug	Slug	Correct
0.33	3.28	Slug	Slug	Correct
0.33	3.44	Slug	Slug	Correct
0.66	2.30	Slug	Slug	Correct
0.66	2.95	Slug	Slug	Correct
0.66	6.23	Slug	Slug	Correct
0.98	2.62	Slug	Slug	Correct
0.98	3.28	Slug	Slug	Correct
0.98	6.56	Slug	Slug	Correct
1.31	4.92	Slug	Slug	Correct
1.31	6.23	Slug	Slug	Correct
1.51	3.94	Slug	Slug	Correct
1.51	6.56	Slug	Slug	Correct
1.97	19.69	Slug	Annular	Incorrect
2.95	22.97	Slug	Annular	Incorrect
2.95	26.25	Slug	Annular	Incorrect
2.95	29.53	Slug	Annular	Incorrect

Properties are ρ_L = 62.32 bm/ft3, μ_L =1.0 cP; ρ_G =0.46 lbm/ft3, μ_G =0.018 cP, σ = 0.005 lbf/ft (Raw data from R.C. Fernandes , R.Semiat and A.E. Duckler. (1983)

Table 5.1.2-2 Program result compared with air-water system data at room temperature, P= 1BarA, ID=19 mm in vertical upward direction

Superficial velocity		Flow pattern		Result
ULS(ft/s)	UGS(ft/s)	Experiment	Calculated	
0.04	0.02	Bubble	Slug	Incorrect
0.06	0.04	Bubble	Slug	Incorrect
0.08	0.04	Bubble	Slug	Incorrect
0.10	0.02	Bubble	Slug	Incorrect
0.12	0.02	Bubble	Slug	Incorrect
0.15	0.02	Bubble	Slug	Incorrect
0.17	0.04	Bubble	Slug	Incorrect
0.19	0.04	Bubble	Slug	Incorrect
0.21	0.04	Bubble	Slug	Incorrect
0.23	0.06	Bubble	Slug	Incorrect
0.25	0.04	Bubble	Slug	Incorrect
0.25	0.06	Bubble	Slug	Incorrect

Properties are ρ_L = 62.12 bm/ft3, μ_L =0.8 cP; ρ_G =0.0727 lbm/ft3, μ_G =0.018 cP cP, σ = 0.005 lbf/ft (Raw data from Malasri Janumporn, 2001)

Table 5.1.2-2 (Cont.) Program result compared with air-water system data at room temperature, P= 1BarA, ID=19 mm in vertical upward direction

Superficial velocity		Flow pattern		Result
ULS(ft/s)	UGS(ft/s)	Experiment	Calculated	
0.27	0.04	Bubble	Slug	Incorrect
0.27	0.06	Bubble	Slug	Incorrect
0.29	0.06	Bubble	Slug	Incorrect
0.31	0.06	Bubble	Slug	Incorrect
0.35	0.04	Bubble	Slug	Incorrect
0.35	0.06	Bubble	Slug	Incorrect
0.37	0.04	Bubble	Slug	Incorrect
0.40	0.04	Bubble	Slug	Incorrect
0.42	0.06	Bubble	Slug	Incorrect
0.47	0.06	Bubble	Slug	Incorrect
0.48	0.06	Bubble	Slug	Incorrect
0.50	0.08	Bubble	Slug	Incorrect
0.04	0.08	Slug	Slug	Correct
0.06	0.10	Slug	Slug	Correct
0.08	0.08	Slug	Slug	Correct
0.10	0.10	Slug	Slug	Correct
0.12	0.08	Slug	Slug	Correct
0.13	0.10	Slug	Slug	Correct
0.15	0.10	Slug	Slug	Correct
0.17	0.10	Slug	Slug	Correct
0.19	0.12	Slug	Slug	Correct
0.21	0.13	Slug	Slug	Correct
0.23	0.13	Slug	Slug	Correct
0.25	0.13	Slug	Slug	Correct
0.27	0.13	Slug	Slug	Correct
0.29	0.13	Slug	Slug	Correct
0.31	0.13	Slug	Slug	Correct
0.33	0.13	Slug	Slug	Correct
0.35	0.15	Slug	Slug	Correct
0.37	0.15	Slug	Slug	Correct
0.39	0.17	Slug	Slug	Correct
0.40	0.17	Slug	Slug	Correct
0.42	0.17	Slug	Slug	Correct
0.44	0.17	Slug	Slug	Correct
0.47	0.19	Slug	Slug	Correct
0.48	0.19	Slug	Slug	Correct
0.52	0.19	Slug	Slug	Correct

Properties are ρ_L = 62.12 bm/ft3, μ_L =0.8 cP; ρ_G =0.0727 lbm/ft3, μ_G =0.018 cP , σ = 0.005 lbf/ft (Raw data from Malasri Janumporn, 2001)

Table 5.1.2-3 Program result compared with air-water system data at room temperature, P= 1 BarA , ID=25 mm in vertical upward direction

Superficial velocity		Flow pattern		Result
ULS(ft/s)	UGS(ft/s)	Experiment	Calculated	
5.25	0.23	Bubble	Slug	Incorrect
5.25	0.43	Bubble	Slug	Incorrect
5.25	0.66	Bubble	Slug	Incorrect
5.25	0.92	Bubble	Slug	Incorrect
5.25	1.97	Bubble	Slug	Incorrect
9.51	0.23	Bubble	Bubble	Correct
9.51	0.43	Bubble	Bubble	Correct
9.51	0.66	Bubble	Bubble	Correct
9.51	0.92	Bubble	Bubble	Correct
9.51	1.97	Bubble	Bubble	Correct
9.51	2.30	Bubble	Bubble	Correct
9.51	4.27	Bubble	Bubble	Correct
9.51	6.56	Bubble	Bubble	Correct
0.01	0.23	Slug	Slug	Correct
0.01	0.43	Slug	Slug	Correct
0.01	0.66	Slug	Slug	Correct
0.01	0.92	Slug	Slug	Correct
0.01	1.97	Slug	Slug	Correct
0.01	2.30	Slug	Slug	Correct
0.01	4.27	Slug	Slug	Correct
0.01	6.56	Slug	Slug	Correct
0.01	9.84	Slug	Slug	Correct
0.01	19.69	Slug	Slug	Correct
0.09	0.23	Slug	Slug	Correct
0.09	0.43	Slug	Slug	Correct
0.09	0.66	Slug	Slug	Correct
0.09	0.92	Slug	Slug	Correct
0.09	1.97	Slug	Slug	Correct
0.09	2.30	Slug	Slug	Correct
0.09	4.27	Slug	Slug	Correct
0.09	6.56	Slug	Slug	Correct
0.09	9.84	Slug	Slug	Correct
0.09	19.69	Slug	Slug	Correct
0.13	0.92	Slug	Slug	Correct
0.13	1.97	Slug	Slug	Correct
0.13	2.30	Slug	Slug	Correct
0.13	4.27	Slug	Slug	Correct
0.23	0.92	Slug	Slug	Correct
0.23	1.97	Slug	Slug	Correct
0.23	2.30	Slug	Slug	Correct
0.23	4.27	Slug	Slug	Correct
0.30	0.23	Slug	Slug	Correct
0.30	0.92	Slug	Slug	Correct
0.30	1.97	Slug	Slug	Correct
0.30	2.30	Slug	Slug	Correct

Properties are ρ_L = 62.1179 lbm/ft3, μ_L =0.8 cP; ρ_G =0.0727 lbm/ft3, μ_G =0.018 cP , σ = 0.005 lbf/ft (Raw data from Taitel Bornea and Duckler, 1980)

Table 5.1.2-3(Cont.) Program result compared with air-water system data at room temperature, P= 1 BarA , ID=25 mm in vertical upward direction

Superficial velocity		Flow pattern		Result
ULS(ft/s)	UGS(ft/s)	Experiment	Calculated	
0.30	4.27	Slug	Slug	Correct
0.66	0.23	Slug	Slug	Correct
0.66	0.92	Slug	Slug	Correct
0.66	1.97	Slug	Slug	Correct
0.66	2.30	Slug	Slug	Correct
0.66	4.27	Slug	Slug	Correct
0.92	0.23	Slug	Slug	Correct
0.92	0.43	Slug	Slug	Correct
0.92	0.66	Slug	Slug	Correct
0.92	0.92	Slug	Slug	Correct
0.92	2.30	Slug	Slug	Correct
0.92	4.27	Slug	Slug	Correct
0.92	6.56	Slug	Slug	Correct
0.92	9.84	Slug	Slug	Correct
0.92	13.12	Slug	Slug	Correct
0.92	19.69	Slug	Slug	Correct
1.48	0.43	Slug	Slug	Correct
1.48	0.66	Slug	Slug	Correct
1.48	0.92	Slug	Slug	Correct
1.48	1.97	Slug	Slug	Correct
1.48	2.30	Slug	Slug	Correct
1.48	4.27	Slug	Slug	Correct
1.48	6.56	Slug	Slug	Correct
1.48	9.84	Slug	Slug	Correct
1.48	13.12	Slug	Slug	Correct
1.48	19.69	Slug	Slug	Correct
1.97	0.43	Slug	Slug	Correct
1.97	0.66	Slug	Slug	Correct
1.97	0.92	Slug	Slug	Correct
1.97	1.97	Slug	Slug	Correct
1.97	2.30	Slug	Slug	Correct
1.97	4.27	Slug	Slug	Correct
1.97	6.56	Slug	Slug	Correct
1.97	9.84	Slug	Slug	Correct
1.97	13.12	Slug	Slug	Correct
1.97	19.69	Slug	Slug	Correct
0.01	59.06	Annular	Annular	Correct
0.01	85.30	Annular	Annular	Correct
0.09	59.06	Annular	Annular	Correct
0.09	85.30	Annular	Annular	Correct
0.92	59.06	Annular	Annular	Correct
0.92	85.30	Annular	Annular	Correct
1.48	59.06	Annular	Annular	Correct
1.48	85.30	Annular	Annular	Correct

Properties are ρ_L = 62.1179 lbm/ft3, μ_L =0.8 cP; ρ_G =0.0727 lbm/ft3, μ_G =0.018 cP, σ = 0.005 lbf/ft (Raw data from Taitel Bornea and Duckler, 1980)

5.1.3 Flow pattern prediction result in vertical down direction

Flow patterns prediction for vertical downwards flow was tested against experimental data flow in 25 mm and 51 mm carbon steel pipe at atmospheric pressure.

Table 5.1.3-1 Program result compared with air-water system data at room temperature, P= 1 BarA, ID= 25mm in vertical downward direction

Superficial velocity		Flow pattern		Result
uLS(ft/s)	uGS(ft/s)	Experiment	Calculated	
3.28	1.31	Slug	Slug	Correct
4.92	1.31	Slug	Slug	Correct
8.20	1.31	Bubble	Slug	Incorrect
13.12	1.31	Bubble	Bubble	Correct
1.48	1.97	Annular	Annular	Correct
1.97	1.97	Annular	Annular	Correct
3.28	1.97	Slug	Slug	Correct
4.92	1.97	Slug	Slug	Correct
8.20	1.97	Bubble	Slug	Incorrect
13.12	1.97	Bubble	Bubble	Correct
0.03	3.28	Annular	Annular	Correct
0.33	3.28	Annular	Annular	Correct
0.49	3.28	Annular	Annular	Correct
0.98	3.28	Annular	Annular	Correct
1.48	3.28	Annular	Annular	Correct
1.97	3.28	Annular	Annular	Correct
3.28	3.28	Slug	Slug	Correct
4.92	3.28	Slug	Slug	Correct
8.20	3.28	Slug	Slug	Correct
13.12	3.28	Bubble	Bubble	Correct
1.97	6.56	Annular	Annular	Correct
3.28	6.56	Slug	Slug	Correct
4.92	6.56	Slug	Slug	Correct
8.20	6.56	Slug	Slug	Correct
13.12	6.56	Bubble	Bubble	Correct
1.97	19.69	Annular	Annular	Correct
3.28	19.69	Slug	Slug	Correct
4.92	19.69	Slug	Slug	Correct
8.20	19.69	Slug	Slug	Correct
0.33	32.81	Annular	Annular	Correct
0.49	32.81	Annular	Annular	Correct
0.98	32.81	Annular	Annular	Correct
1.48	32.81	Annular	Annular	Correct
1.97	32.81	Annular	Annular	Correct
3.28	32.81	Slug	Annular	Incorrect
4.92	32.81	Slug	Slug	Correct
8.20	32.81	Slug	Slug	Correct
13.12	32.81	Slug	Bubble	Incorrect

Properties are ρ_L = 62.12 lbm/ft3, μ_L =0.8 cP; ρ_G = 0.0727 lbm/ft3, μ_G =0.018 cP, σ = 0.005 lbf/ft (Raw data from Barnea, Shoham, Taitel, 1981)

Table 5.1.3-1(Cont.) Program result compared with air-water system data at room temperature, P= 1 BarA, ID= 25mm in vertical downward direction

Superficial velocity		Flow pattern		Result
uLS(ft/s)	uGS(ft/s)	Experiment	Calculated	
3.28	3.28	Slug	Slug	Correct
3.28	6.56	Slug	Slug	Correct
3.28	9.84	Slug	Slug	Correct
3.28	21.33	Slug	Slug	Correct
3.28	32.81	Slug	Slug	Correct
4.92	0.05	Bubble	Slug	Incorrect
4.92	0.13	Slug	Slug	Correct
4.92	0.33	Slug	Slug	Correct
4.92	1.31	Slug	Slug	Correct
4.92	1.64	Slug	Slug	Correct
4.92	3.28	Slug	Slug	Correct
4.92	6.56	Slug	Slug	Correct
4.92	9.84	Slug	Slug	Correct
4.92	21.33	Slug	Slug	Correct
4.92	32.81	Slug	Slug	Correct
9.84	0.05	Bubble	Bubble	Correct
9.84	0.13	Bubble	Bubble	Correct
9.84	0.33	Bubble	Bubble	Correct
9.84	1.31	Bubble	Bubble	Correct
9.84	1.64	Bubble	Bubble	Correct
9.84	3.28	Slug	Bubble	Incorrect
9.84	6.56	Slug	Bubble	Incorrect
9.84	9.84	Slug	Bubble	Incorrect
9.84	21.33	Slug	Bubble	Incorrect
9.84	32.81	Slug	Bubble	Incorrect
13.12	0.05	Bubble	Bubble	Correct
13.12	0.13	Bubble	Bubble	Correct
13.12	0.33	Bubble	Bubble	Correct
13.12	1.31	Bubble	Bubble	Correct
13.12	1.64	Bubble	Bubble	Correct
13.12	3.28	Bubble	Bubble	Correct
13.12	6.56	Bubble	Bubble	Correct
13.12	9.84	Bubble	Bubble	Correct
13.12	21.33	Slug	Bubble	Incorrect
13.12	32.81	Slug	Bubble	Incorrect

Properties are ρ_L = 62.12 lbm/ft3, μ_L =0.8 cP; ρ_G = 0.0727 lbm/ft3, μ_G =0.018 cP, σ = 0.005 lbf/ft (Raw data from Barnea, Shoham, Taitel, 1981)

Table 5.1.3-2 Program result compared with air-water system data at room temperature, ID=51mm in vertical downward direction

Superficial velocity		Flow pattern		Result
uLS(ft/s)	uGS(ft/s)	Experiment	Calculated	
0.03	0.05	Annular	Annular	Correct
0.33	0.05	Annular	Annular	Correct
0.49	0.05	Annular	Annular	Correct
0.98	0.05	Annular	Annular	Correct
1.48	0.05	Annular	Annular	Correct
1.97	0.05	Slug	Annular	Incorrect
3.28	0.05	Bubble	Slug	Incorrect
4.92	0.05	Bubble	Slug	Incorrect
8.20	0.05	Bubble	Slug	Incorrect
1.48	0.07	Annular	Annular	Correct
1.97	0.07	Annular	Annular	Correct
3.28	0.07	Bubble	Slug	Incorrect
4.92	0.07	Bubble	Slug	Incorrect
8.20	0.07	Bubble	Slug	Incorrect
1.48	0.13	Annular	Annular	Correct
1.97	0.13	Slug	Annular	Incorrect
3.28	0.13	Bubble	Annular	Incorrect
4.92	0.13	Bubble	Slug	Incorrect
8.20	0.13	Bubble	Slug	Incorrect
1.48	0.20	Annular	Slug	Incorrect
1.97	0.20	Slug	Annular	Incorrect
3.28	0.20	Bubble	Slug	Incorrect
4.92	0.20	Bubble	Slug	Incorrect
8.20	0.20	Bubble	Slug	Incorrect
0.03	0.33	Annular	Annular	Correct
0.33	0.33	Annular	Annular	Correct
0.49	0.33	Annular	Annular	Correct
0.98	0.33	Annular	Annular	Correct
1.48	0.33	Annular	Annular	Correct
1.97	0.33	Slug	Annular	Incorrect
3.28	0.33	Bubble	Slug	Incorrect
4.92	0.33	Bubble	Slug	Incorrect
8.20	0.33	Bubble	Slug	Incorrect
1.48	0.66	Annular	Annular	Correct
1.97	0.66	Slug	Annular	Incorrect
3.28	0.66	Slug	Slug	Correct
4.92	0.66	Slug	Slug	Correct
8.20	0.66	Bubble	Slug	Incorrect
1.48	1.31	Annular	Annular	Correct
1.97	1.31	Annular	Annular	Correct

Properties are ρ_L = 62.12 lbm/ft3, μ_L =0.8 cP; ρ_G =0.00727 lbm/ft3, μ_G =0.0187 cP (Raw data from Barnea, Shoham, Taitel, 1981)

Table 5.1.3-2 (Cont.) Program result compared with air-water system data at room temperature, ID=51mm in vertical downward direction

Superficial velocity		Flow pattern		Result
uLS(ft/s)	uGS(ft/s)	Experiment	Calculated	
0.03	0.05	Annular	Annular	Correct
0.03	0.13	Annular	Annular	Correct
0.03	0.33	Annular	Annular	Correct
0.03	1.31	Annular	Annular	Correct
0.03	3.28	Annular	Annular	Correct
0.03	6.56	Annular	Annular	Correct
0.03	21.33	Annular	Annular	Correct
0.33	0.05	Annular	Annular	Correct
0.33	0.13	Annular	Annular	Correct
0.33	0.33	Annular	Annular	Correct
0.33	1.31	Annular	Annular	Correct
0.33	3.28	Annular	Annular	Correct
0.33	6.56	Annular	Annular	Correct
0.33	21.33	Annular	Annular	Correct
0.98	0.05	Annular	Annular	Correct
0.98	0.13	Annular	Annular	Correct
0.98	0.33	Annular	Annular	Correct
0.98	1.31	Annular	Annular	Correct
0.98	1.64	Annular	Annular	Correct
0.98	3.28	Annular	Annular	Correct
0.98	6.56	Annular	Annular	Correct
0.98	9.84	Annular	Annular	Correct
0.98	21.33	Annular	Annular	Correct
0.98	32.81	Annular	Annular	Correct
1.97	0.05	Slug	Slug	Correct
1.97	0.13	Slug	Slug	Correct
1.97	0.33	Slug	Slug	Correct
1.97	1.31	Slug	Slug	Correct
1.97	1.64	Slug	Slug	Correct
1.97	3.28	Slug	Slug	Correct
1.97	6.56	Slug	Slug	Correct
1.97	9.84	Slug	Slug	Correct
1.97	21.33	Annular	Annular	Correct
1.97	32.81	Annular	Annular	Correct
3.28	0.05	Slug	Slug	Correct
3.28	0.13	Slug	Slug	Correct
3.28	0.33	Slug	Slug	Correct
3.28	1.31	Slug	Slug	Correct
3.28	1.64	Slug	Slug	Correct

Properties are ρ_L = 62.12 lbm/ft3, μ_L =0.8 cP; ρ_G =0.00727 lbm/ft3, μ_G =0.0187 cP, σ = 0.005 lbf/ft (Raw data from Barnea, Shoham, Taitel, 1981)

5.1.4 Unit Pressure Drop result

Calculated unit pressure drop for two-phase flow from the program is compared with the pressure drop obtained from experiment as shown in this section. Unit pressure loss comparison is only made in cases where the experimental flow pattern and predicted flow pattern were the same. The cases tested were all for stratified flow and slug flow patterns as no data could be found for testing of the programs accuracy for other flow patterns, during the course of this study. Unit pressure drop results for stratified flow and slug flow in horizontal flow are compared with experimental data in this section.

For others flows patterns in the vertical direction no comparison has been indicated because experimental data for two phase flow in the vertical direction is not widely studies and this data was not available during the development and testing of the two-phase program in the limited period available.

Table 5.1.4-1 Pressure loss calculations for stratified flow compared with experimental data of air-water system data at room temperature, P= 1barA, ID= 29 mm, in horizontal flow direction

Superficial velocity		Flow pattern	Pressure loss (psi/100ft)	
ULS(ft/s)	UGS(ft/s)		Calculated	Experiment
0.11	8.08	Stratified	0.1775	0.0615
0.11	11.39	Stratified	0.2708	0.0841
0.11	13.88	Stratified	0.3460	0.1205
0.11	15.99	Stratified	0.4150	0.1635
0.11	17.85	Stratified	0.4959	0.2070
0.07	11.39	Stratified	0.2277	0.0785
0.07	15.99	Stratified	0.3760	0.1238
0.07	19.53	Stratified	0.4971	0.1725
0.07	22.52	Stratified	0.5948	0.2132
0.07	25.15	Stratified	0.7345	0.2713
0.07	27.52	Stratified	0.8023	0.3377
0.07	29.71	Stratified	0.9556	0.4174
0.07	31.72	Stratified	1.0111	0.4744
0.07	33.63	Stratified	1.1230	0.5463

Properties are ρ_L = 62.12 lbm/ft3, μ_L =0.8 cP; ρ_G =0.07 lbm/ft3, μ_G =0.02 cP , σ = 0.005 lbf/ft
(Raw data from Winai et. al, 1996)

Table 5.1.4-2 Pressure loss calculation for stratified flow compared with experimental data of air-water system data at room temperature, P= 1 BarA, ID=54 mm in horizontal flow direction

Superficial velocity		Flow pattern	Pressure loss (psi/100ft)	
ULS(ft/s)	UGS(ft/s)		Calculated	Experiment
0.24	4.73	Stratified	0.0843	0.0260
0.24	5.27	Stratified	0.0916	0.0285
0.24	5.73	Stratified	0.0974	0.0331
0.24	6.68	Stratified	0.1112	0.0441
0.24	7.06	Stratified	0.1164	0.0434
0.10	6.30	Stratified	0.0555	0.0198
0.10	7.06	Stratified	0.0637	0.0250
0.10	8.48	Stratified	0.0796	0.0320
0.10	11.17	Stratified	0.1113	0.0468
0.10	13.44	Stratified	0.1456	0.0542
0.10	15.76	Stratified	0.1772	0.0843
0.10	17.61	Stratified	0.2068	0.0885
0.10	20.63	Stratified	0.2597	0.1150

Properties are ρ_L = 62.12 lbm/ft3, μ_L =0.8 cP; ρ_G =0.07 lbm/ft3, μ_G =0.02 cP (Raw data from Winai et. al1996)

Table 5.1.4-3 Pressure loss calculation for stratified flow compared with experimental data of air-water system data at 20 oC, P= 5, 10.5 15 barG in ID=77.92mm in horizontal flow direction

Superficial velocity		Pressure	Pressure loss (psi/100ft)	
ULS(ft/s)	UGS(ft/s)	(BarG)	Calculated	Experiment
0.36	8.66	5	0.3138	0.2255
0.36	10.33	5	0.3917	0.2376
0.23	21.52	5	0.9363	0.4476
0.30	17.81	5	0.7540	0.3559
0.33	14.21	5	0.5777	0.2630
0.56	10.5	5	0.5360	0.3537
0.28	6.92	10.5	0.2925	0.1083
0.29	5.36	10.5	0.2179	0.0508
0.39	8.10	10.5	0.4320	0.1846
0.46	6.66	10.5	0.3821	0.1315
0.51	8.86	10.5	0.5723	0.2343
0.56	8.83	10.5	0.6055	0.2608
0.69	8.07	10.5	0.6460	0.2796

Properties are ρ_L = 62.12 lbm/ft3, μ_L =0.8 cP; ρ_G = 0.4589, 0.842, 1.2249 lbm/ft3 ,
σ = 0.005 lbf/ft (at 5,10.5,15 BarG respectively) (Raw data from Dr. Somprasong 1994)

Table 5.1.4-3 (Cont.) Pressure loss calculation for stratified flow compared with experimental data of air-water system data at 20 oC, P= 5, 10.5 15 barG in ID=77.92mm in horizontal flow direction

Superficial velocity		Pressure	Pressure loss (psi/100ft)	
ULS(ft/s)	UGS(ft/s)	(BarG)	Calculated	Experiment
0.21	8.91	15	0.4674	0.2420
0.31	8.32	15	0.5057	0.2796
0.45	6.00	15	0.4105	0.2597
0.58	5.74	15	0.4731	0.3227
0.24	10.06	15	0.5964	0.2708
0.29	11.4	15	0.7771	0.3404
0.41	9.53	15	0.6934	0.3260
0.65	6.45	15	0.5815	0.3890
0.72	5.67	15	0.5582	0.4752

Properties are ρ_L = 62.12 lbm/ft3, μ_L =0.8 cP; ρ_G = 0.4589, 0.842, 1.2249 lbm/ft3, σ = 0.005 lbf/ft (at 5, 10.5, 15 BarG respectively) (Raw data from Dr. Somprasong 1994)

Table 5.1.4-4 Pressure loss calculation for slug flow compared with experimental data of air-water data at 20 oC, P= 1, 3.5, 6 barG in ID=77.92mm in horizontal flow direction

Superficial velocity		Pressure	Pressure loss (psi/100ft)	
ULS(ft/s)	UGS(ft/s)	(BarG)	Calculated	Experiment
1.05	17.02	1.0	1.780	0.884
2.47	19.69	1.0	4.620	1.914
3.45	19.69	1.0	4.350	4.642
1.67	20.71	1.0	5.060	1.547
1.69	17.02	3.5	2.280	1.768
2.51	17.02	3.5	2.410	2.763
3.34	17.02	3.5	2.120	3.846
3.34	19.95	3.5	4.720	4.620
2.51	20.01	3.5	4.980	3.404
4.12	20.30	3.5	4.410	5.968

Properties are ρ_L = 62.12 lbm/ft3, μ_L =0.8 cP; ρ_G = 0.0743, 0.2601, 0.4459 lbm/ft3, σ = 0.005 lbf/ft (at 1, 3.5, 6 BarG respectively) (Raw data from Y. Manolis, 1994)

Table 5.1.4-4(cont.) Pressure loss calculation for slug flow compared with air-water data at 20 oC, P= 1, 3.5, 6 barG in ID=77.92mm in horizontal flow direction

Superficial velocity		Pressure	Pressure loss (psi/100ft)	
ULS(ft/s)	UGS(ft/s)	(BarG)	Calculated	Experiment
4.12	23.17	3.5	8.400	7.294
2.51	23.39	3.5	9.490	4.448
3.34	23.39	3.5	9.570	5.681
2.50	17.88	6.0	3.040	3.095
4.27	18.80	6.0	2.740	5.893
2.50	19.69	6.0	4.650	3.537
3.27	20.28	6.0	5.150	4.863
4.27	21.92	6.0	6.290	6.896
3.27	23.43	6.0	9.700	5.597
4.27	24.61	6.0	10.800	7.736

Properties are ρ_L = 62.12 lbm/ft3, μ_L =0.8 cP; ρ_G = 0.0743, 0.2601, 0.4459 lbm/ft3, σ = 0.005 lbf/ft (at 1, 3.5, 6 BarG respectively) (Raw data from Y. Manolis, 1994)

5.2 Program Discussion

5.2.1 Flow pattern

The two-phase program accuracy is tested by comparing the number of correctly predicted flow patterns with the visually observed pattern from experimental data in pipe diameters 0.75 to 3 inch at low pressure under atmospheric pressure to 15 barG in horizontal vertical upward and vertical downward flow direction.

In horizontal flow, the number of correctly predicting result per experimental result for stratified flow and annular flow are in a high ratio as shown in table-5.2.1-1 but for slug flow results are not consistent with the experiment.

In vertical upward direction in pipe sizes 0.75 inch to 2 inch, the number of correctly predicting result per experimental result for slug pattern and annular pattern are in high ratio. Bubble flow pattern predicted from the program is consistent with flow pattern observed in pipe size 1 inch to 2 inch but for a 0.75 inch pipe size, the program predicts slug flow pattern result which is differs from the bubble experimental data.

In vertical downward flow, experimental conditions for pipe sizes 25 mm and 50 mm is tested against the program prediction for bubble flow, annular flow and slug flow. The number of correctly predicting result per experimental result for slug and annular are good and moderate for bubble flow.

Table 5.2.1-1 Summary of correctly predicted flow patterns

Flow direction	Source of data	No. of data separated by flow pattern				Total No. of Data
		Stratified	Bubble	Slug	Annular	
Horizontal	Data from experiment lab	55	*	10	5	70
	No. of predict results which correspond to experimental result	49	*	0	5	54
	Ratio of correct flow pattern	0.89	-	0	1	0.77
Vertical upward	Data from experiment lab	-	50	109	8	167
	No. of predict results which correspond to experimental result	-	21	105	8	134
	Ratio of correct flow pattern	-	0.41	0.97	1	0.8
Vertical downward	Data from experiment lab	-	36	58	58	152
	No. of predict results which correspond to experimental result	-	17	44	57	118
	Ratio of correct flow pattern	-	0.47	0.76	0.98	0.78

* flow conditions for bubble pattern program verification are not available

Figure 5.2.1-1 Comparison of number of the correctly predicted flow patterns to experimental data in horizontal flow direction

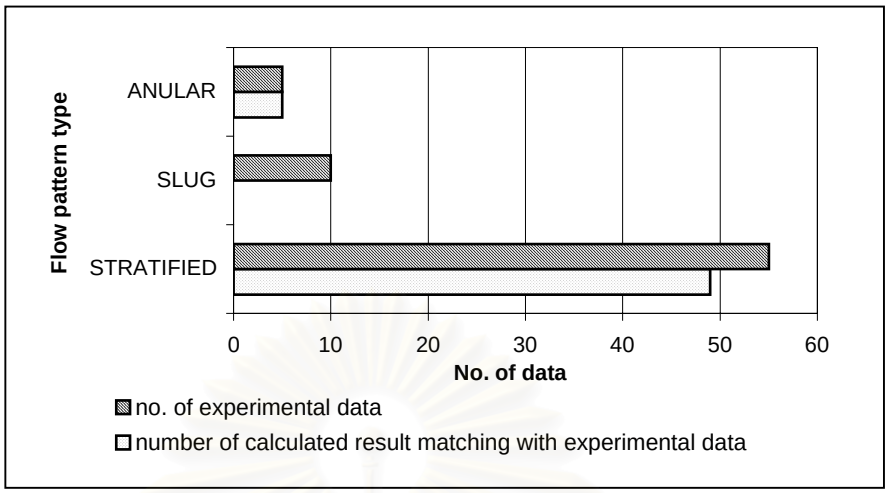

(Raw experimental data from Winai et.al 1996, Dr. Somprasong 1994)

In pipe diameters 1 to 2 inch at atmospheric pressure, the calculated flow pattern result and experimental data in the stratified region at atmospheric pressure are consistent. When air and water flow in the low velocity range, the flow is in stratified smooth flow, water flows in the lower section of the pipe and gas above because of the lower density of the gas. When the gas flow rate is increase, the influence of gas momentum causes disturbance on the liquid interface and some of the water is carried with the gas flow. This flow pattern called stratified wavy,

In 3 inch pipe at 5 barG, when water and air flow rate is increased, the calculated results are annular flow which differ from experimental data, of stratified flow as below figure.

Figure 5.2.1-2 Experimental data of two-phase of air and water, ID= 77.92 mm, horizontal direction, 5 BarG

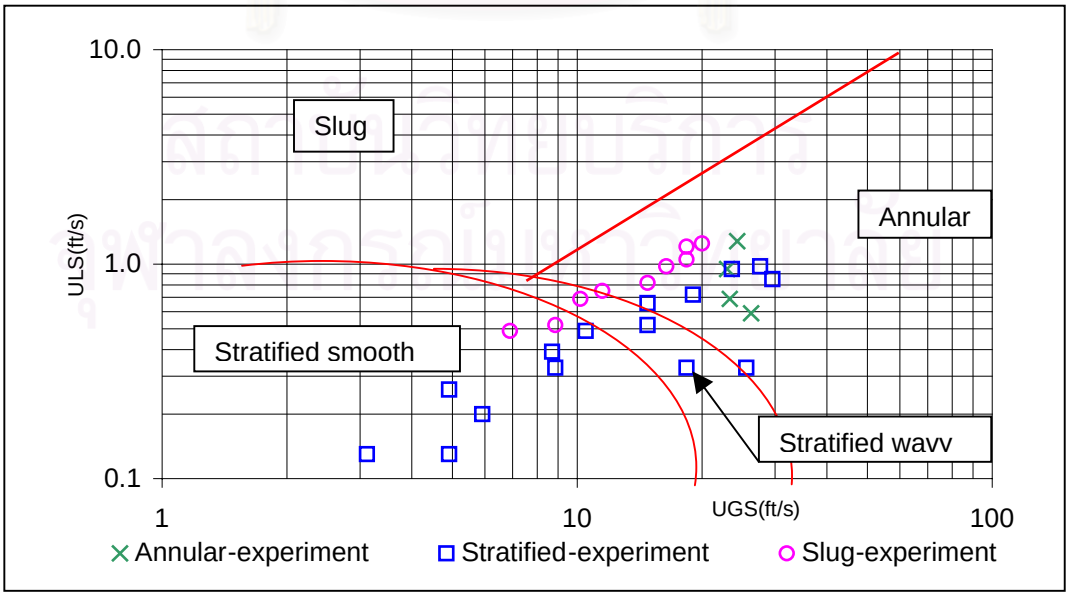

The transition lines denote the flow patterns from program calculation (Raw data from Dr. Somprasong, 1994)

The cause of the difference in the flow pattern prediction is caused by the effect of liquid surface tension and the liquid quantity in the pipe. In a small pipe, the gas momentum from the high gas rate will spread the water flow in an annular form around wall of the pipe and gas flows at high velocity in the core of pipe if liquid quantity is less than half of the pipe cross sectional area. In larger pipe sizes, the gas momentum will be much higher because of the higher water quantity in large pipe sizes. Because of the program which is based on small pipe diameters will predict the pattern to be annular flow which does not correspond to the experimental data. When the experimental flow exhibited slug flow patterns, the computer program predicted stratified flow and annular flow. It was found that these flow patterns are close to the flow pattern boundary between stratified and non stratified flow as shown in the Figure 5.2.1-2. The interpretation of the type of flow patterns in the transition band between each flow patterns by observation is difficult and may result in incorrect identification of the exact flow pattern type.

In vertical upward flow, the two-phase program is tested against the experimental data in 19 mm, 25 mm and 50 mm diameter pipe at low pressure conditions as shown below

Figure 5.2.1-3 Comparison of number of the correctly predicted flow patterns to experimental data in vertical upward flow direction

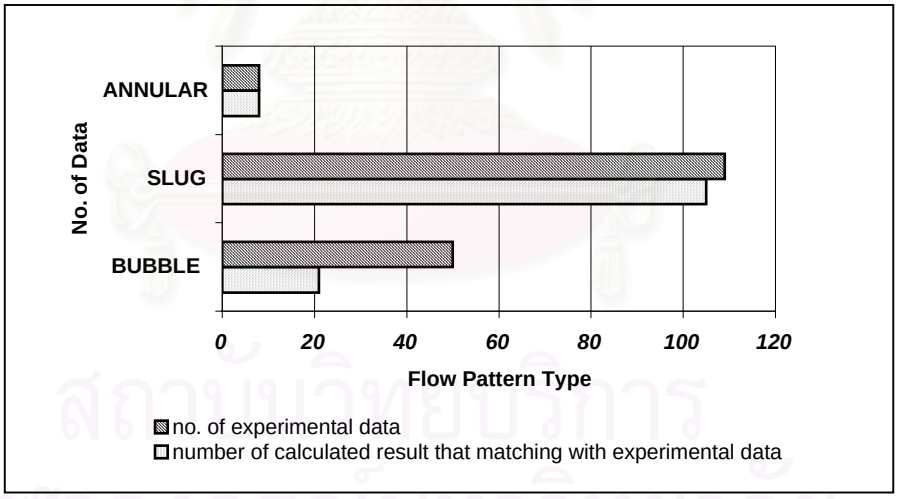

(Raw Data from experimental data from Fernandes et.al 1983, Marlasri 2001, Taitel et.al 1980)

In the small pipe (19 mm), at low superficial liquid velocities the calculated result indicates that slug flow should be present however experimental result of Malasri (2001) shows bubble flow pattern. The bubble flow pattern arises due to the effect of turbulent force in the liquid phase which forces dispersed gas bubble into the smaller bubbles and the liquid surface tension force which form the small rigid spherical bubble shape at low gas velocity. However from the condition of experimental data, turbulent force dominate the effect of the

combination of small bubble which tends to merging of bubbles to form slug flow if the void fraction is high enough. Slug flow pattern is occurred in this situation.

In the 25 mm diameter pipe, the calculated flow pattern result is consistent with the experimental result. Slug flow pattern and annular flow pattern are observed in the small pipe. At high gas superficial velocity the flow becomes annular. The liquid film flows upward adjacent to the wall. The upward flow of the liquid film against gravity results from the force exerted by the fast moving gas core. Liquid moves upwards due to the interfacial shear and form drag on the wave and drag on the liquid droplets.

Figure 5.2.1-4 Experimental data of two-phase of air and water flow in 50.74 mm, vertical upward direction, 1 barA

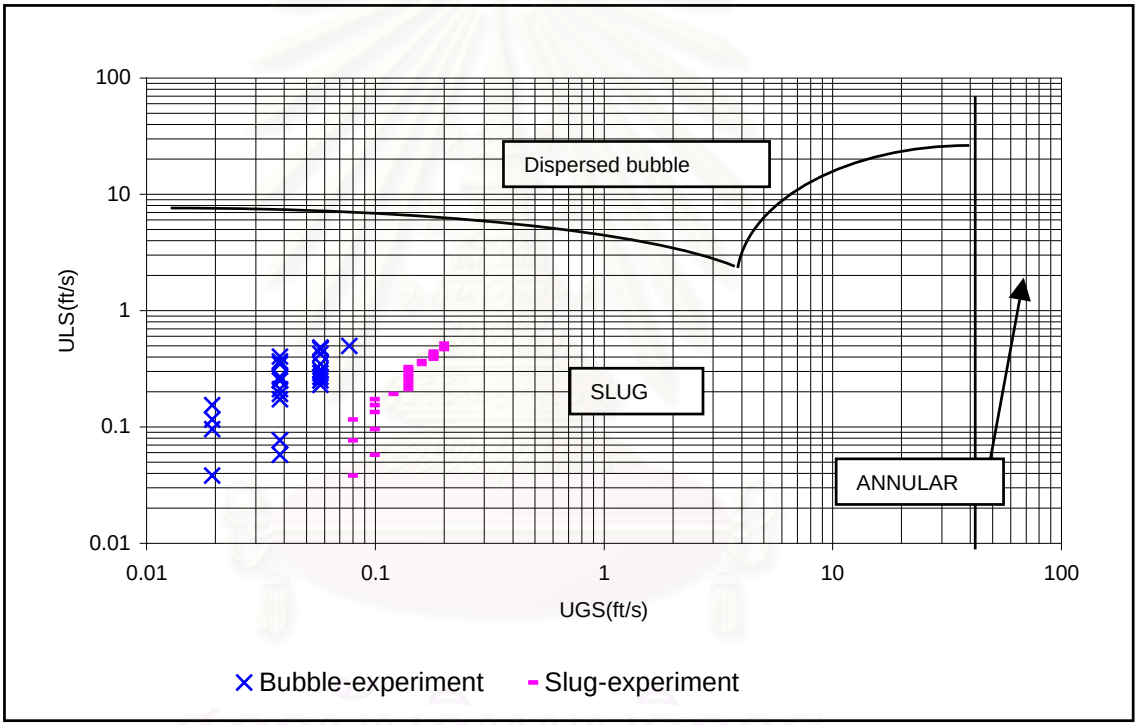

The transition lines denote the flow patterns from program calculation (Raw data from Malasri, 2001)

The difference in the flow pattern prediction against the experiment data in 50 mm pipe could be seen from below figure. Slug flow is observed in the high gas velocity which differ from program prediction of annular, This can be attributed to the fact that the test flow conditions are close to the flow pattern boundaries. In this region correct visual identification of the flow pattern is difficult because there is no clear transition line between flow pattern but rather than a transition region.

Figure 5.2.1-5 Experimental data of two-phase of air and water flow in 50.74 mm, vertical upward direction, 1 barA

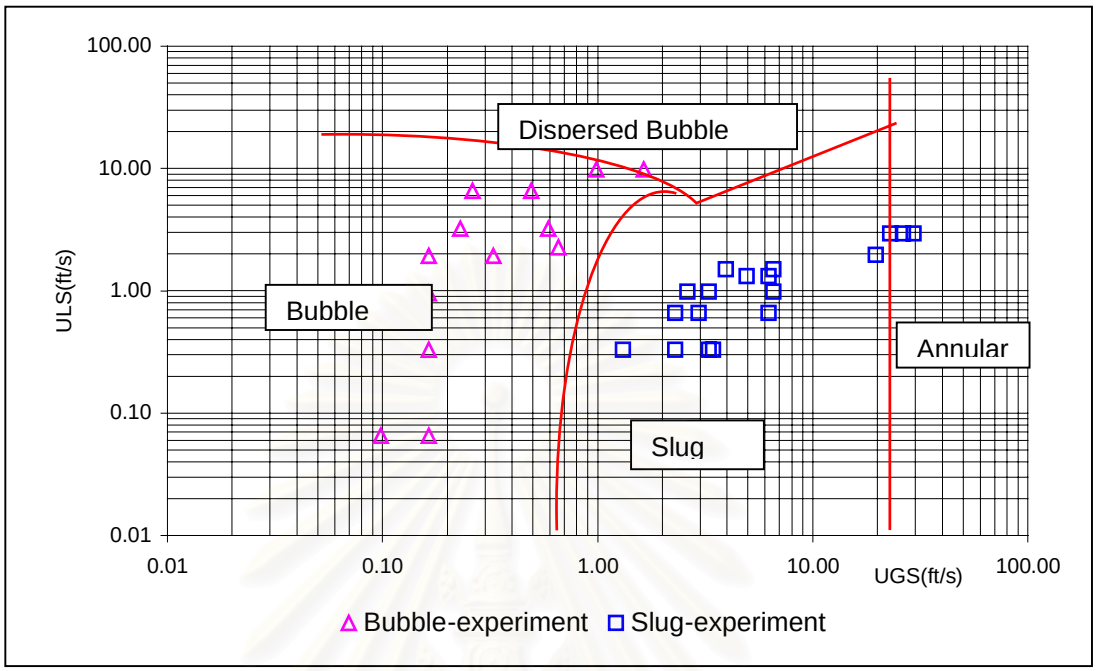

The transition lines denote the flow patterns from program calculation (Raw data from Fernandes et.al,1983)

In vertical downward flow, the two-phase program is tested against the experimental data in 51 mm, 25 mm diameter under low pressure condition as below.

Figure 5.2.1-6 Comparison of the number of correctly predict patterns and experimental data in vertical downward flow direction

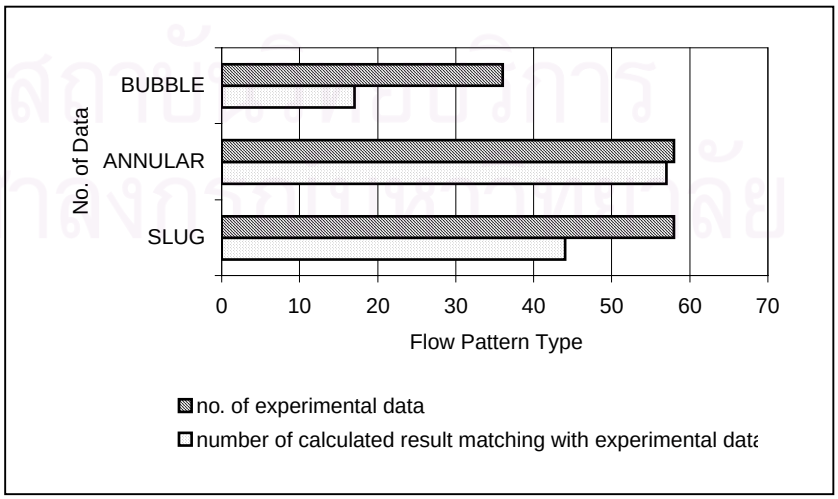

(Raw experimental data from Barnea et.al 1981)

The annular flow pattern from the calculated result is consistent with the experimental data at low liquid flow rate and when increase the liquid flow rate, slug pattern prediction result is consistent with the experimental data . At condition of low gas and liquid flow rates, liquid moves as a falling film and gas flows along the pipe core. Therefore the process of analyzing transition between flow regime starts from annular flow. Stable slugs will formed when the supplied of the liquid in the film is large and could have a liquid blockage in the two-phase flow then becomes slug flow. Based on the Taitel study (1980), the liquid hold up in the slug is assumed to be 0.7, this number is used to determine the flow pattern transition.

The transition from slug to dispersed bubble is the same manner as vertical upward flow. The transition will occur when the turbulent force overcome the interfacial tension force to dispersed gas into small bubbles. This bubble result occurs. The comparison of the calculated result and experimental data shows that the conditions closed to flow transition are accurately predicted compare to the experimental result. In 50 mm and incorrectly predict near the flow transition, the transition from annular to slug flow change at the lower liquid superficial velocity than the experimental data

Figure 5.2.1-7 Experimental data of two-phase of air and water flow,ID= 25 mm in vertical downward direction, P= 1 BarA

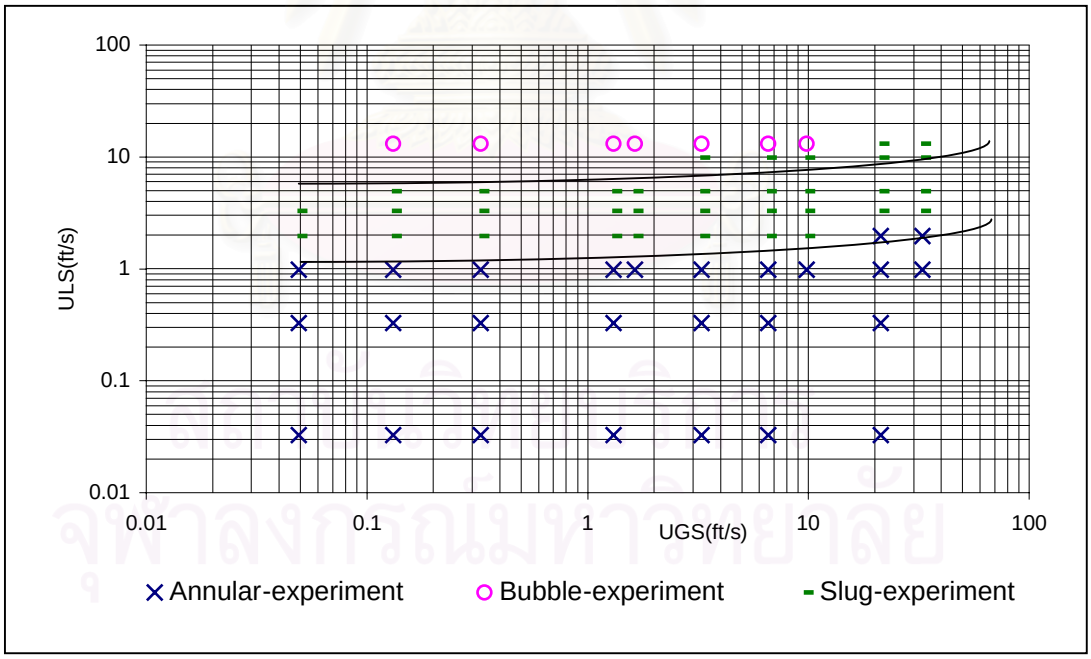

The lines denote the flow patterns from program calculation (Raw data from Barnea 1976)

5.2.2 Pressure loss

The raw data of two-phase flow is tested in the two phase program. Only data that corresponds with correctly predicted flow patterns was used. The analysis was performed by grouping of raw data into stratified flow and slugs flow region for horizontal flow direction.

In contrast to the horizontal flow direction, there are only few investigations of gas-liquid mixture in vertical flow direction. Information of pressure losses in vertical direction for testing the accuracy of the pressure loss in vertical direction could not be found during this study. The use of this program for pressure loss in vertical direction shall be verified when the data is available.

Figure 5.2.2-1 Comparison of the program calculated pressure loss and experimental data of air-water system data at room temperature, P= 1 Bar A in horizontal stratified flow

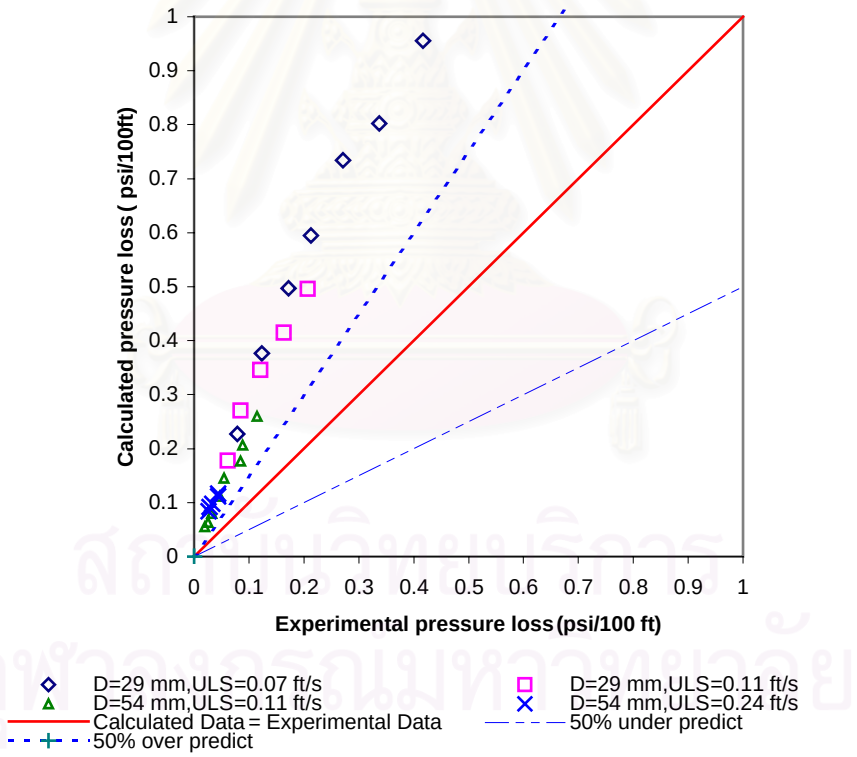

Raw data from Winai et. al(1996)

Figure 5.2.2-2 Comparison of the program calculated pressure loss and experimental data of air-water system data at 20°C, P =5, 10.5, 15 BarG, ID= 77.92 mm in horizontal stratified flow.

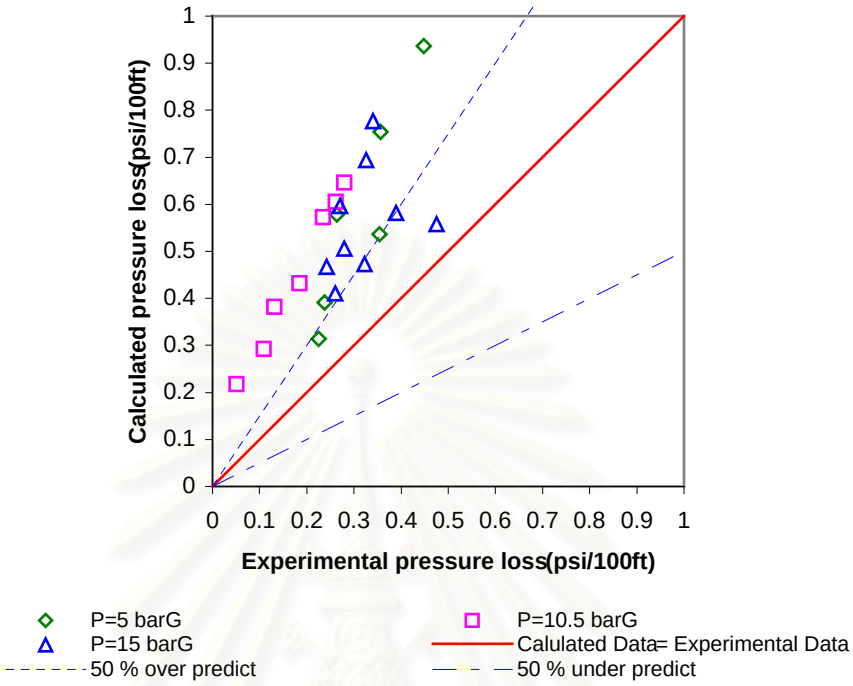

(Raw data from Dr. Somprosong ,1996)

Figure 5.2.2-2 Comparison of the program calculated pressure loss and experimental data of air-water system data at 20°C, P =1, 3.5, 6 BarA , ID= 77.92 mm in horizontal slug flow.

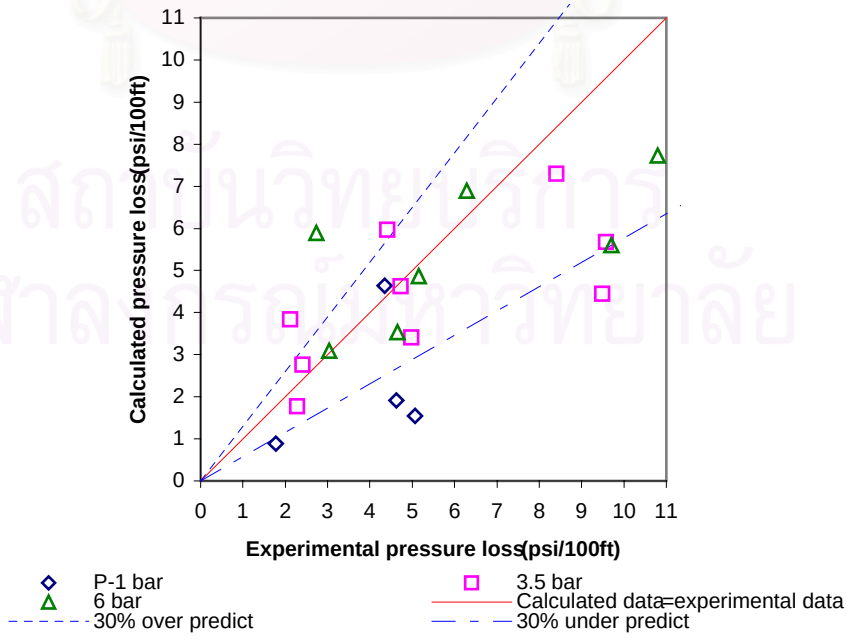

(Raw data from Y. Manolis ,1996)

The stratified model considers the effect of void fraction in two phase flow by using the relationship of gas and liquid flow rates as well as properties of fluid and pipe size, and transforms these to a dimensionless form related to the liquid hold up. Once the liquid hold up is evaluated the value of actual velocities, wetted surface area and hydraulic diameters for gas and liquid are determined. These parameters are then used to predict flow pattern by evaluating the physical mechanism and to evaluate the pressure loss in stratified flow.

Pressure losses calculated from the two-phase program are higher than the experimental data in pipes of internal diameter 29 mm and 54 mm under atmospheric pressure of Winai (1996). Pressure loss in two-phase stratified flow in the pipe comes from the effect of shear force between liquid phase to pipe wall, gas phase to pipe wall and shear between gas phase and liquid phase. Shear stresses are evaluated from the friction factor, actual velocities and fluid densities. The effect of actual velocity to the shear stress term is higher than that of other parameters due to the velocity 's square term relationship. This is also a dominant factor the higher pressure value over and above the effect of density.

A further assumption made is that the friction factor for the gas flow at the interface (f_i) is equal to the friction factor for the gas at the wall (f_G) in smooth stratified flow (Gazley 1949). Although many of the transitions considered are in the stratified wavy region, it is assumed that the relationship of gas phase interface friction factor to gas phase wall friction factor $f_i \approx f_G$ remains the same as in stratified smooth flow. This is based on the factor that gas phase velocity (u_G) is much higher than inter-phase velocity (u_i) thus inter face shear stress (τ_i) equals to gas shear stress (τ_G). This however leads to the result that the calculated pressure drop will be higher than that observed from experiment.

Pressure losses for horizontal slug flow were test against the experimental data in pipes of diameter 77.92 mm, at atmospheric pressure , 3 BarA and 6 BarA, superficial gas velocities in the range of 17 to 25 ft/s and liquid superficial velocities between 1 to 5 ft/s. Calculated pressure losses are within $\pm$30% of experimental data of Y. Monolis (1996).

The pressure losses in slug flow patterns come from the effect of the acceleration of the slow moving liquid film (u_t) to slug velocities (u_S). Because of the randomness of certain slug flow parameters such as slug frequency, slug holdup (R_S) and slug length (l_S), the pressure loss calculations are based on experimental data for these parameters within Reynolds number 30,000 to 400,000. The experimental data used for the pressure loss calculation may not applicable to other slug flow system which would result in some errors between experimental and calculated losses.

The calculated liquid film thickness in horizontal flow and vertical downward flow is within $\pm$0.01% of the result from force balance equation (3-47) and (3-137).

CHAPTER VI

CONCLUSIONS AND RECOMMENDATIONS

6.1 Conclusion

The two-phase program is a tool for prediction of the flow patterns as well as pressure loss calculations in gas liquid two-phase flow for horizontal and vertical orientation. The calculation time is faster than hand calculation method. The required inputs are the volumetric flow rate, density and viscosity of the gas phase and liquid phase as well as the surface tension of liquid phase. Once the input data is filled in and pipe orientation is selected, the flow pattern and unit pressure loss result will be shown in the out put section.

The program calculations to determine the type of flow are based on force balance performed on the liquid and gas phases under steady state conditions. Once the type of flow pattern has been determined, then program calculates the necessary parameters based on the type of flow pattern to determine the pressure drop.

For horizontal flow , the type of flow pattern is classified based on the studies of Taitel and Duckler (1976). Their studies classify flow patterns into one of the following: stratified smooth, stratified wavy, horizontal slug, bubble flow. For vertical upward flow, the classified flow pattern is based on the studies of Taitel, Barnea and Duckler (1980) and is categosized either or bubble flow, slug flow, Annular and dispersed bubble flow. For vertical downward flow, the classified flow pattern is classified according to the studies of Barnea, Shoham and Taitel (1981) and is categorized either as Annular, intermittent (slug) flow or dispersed bubble. The pressure loss calculation method depends on the flow model of each flow pattern, in general the pressure loss in two-phase system comprises of friction , hydrostatic , and acceleration from the momentum change in the flow pattern including minor losses from valves and fittings in the piping system. There are seven models provided in pressure loss calculation,

1) Stratified flow model for stratified smooth and stratified wavy pattern (Taitel and Duckler 1976)
2) Horizontal slug (Duckler and Hubbard,1975)
3) Similarity model (Duckler, Wicks and Cleveland, 1964) for Annular and dispersed bubble in horizontal flow and Annular for vertical upward flow
4) Vertical upward slug (Fernandes, Semiat and Duckler 1983)
5) Vertical upward bubble model (Duckler 1976)

6) Vertical downward Annular (Wallis 1969)

7) Vertical downward Slug (drift flux and similarity model)

8) Vertical downward bubble (drift flux and similarity model)

The developed program has been tested against the experimental data in 0.75 to 3 inch diameter pipe at low pressure for flow patterns in vertical upward and vertical downward flow direction additional horizontal prediction is tested with experimental data up to 5 barG. The results of the predicted flow patterns are acceptable for both the horizontal and vertical direction but in the region close to the transition boundary, the predicted result is not accurately represent as the experimental data. Calculated pressure losses in stratified flow for 29 mm, 54 mm are over predict more than 50% when compared to the experimental data of Winai et al (1996), outlet condition at atmospheric pressure, air superficial velocity between 8 to 33 ft/s, water superficial velocity between 0.07 to 0.24 ft/s.

Calculated pressure losses in stratified flow for 77.92 mm are over predict more than 50% when compared to the experimental data of Dr Somprasong (1994), under 5 barG, air superficial velocity between 0.28 to 0.56 ft/s, water superficial velocity between 5 to 22 ft/s

For slug flow pattern, the calculated pressure drop in the in range of $\pm 30\%$ when compared to the experimental data of Y, Manolis (1996) under pressure 1, 3.5, 6 bar A in 3 inch pipe, air superficial velocity between 17to 25 ft/s, water superficial velocity between1 to 5 ft/s.

6.2 Recommendation

6.2.1 The flow pattern prediction from the two-phase program has been tested against experimental data in stratified flow, bubble, slug and annular flow in the horizontal and vertical direction. Bubble flow in the horizontal direction was not tested as experimental data for bubble flow was not available for this study. It is recommended that the program be tested against experimental data for horizontal bubble flow to verify the accuracy of the predicted results. The result obtained from the program for horizontal bubble flow be used with caution until the accuracy of the results can be verified.

6.2.2 This program is developed from the force balance in the steady state flow which considers the effect of fluid properties in a pipe. The calculated flow pattern and pressure loss is tested against the experimental data for air and water in small pipes and low pressure conditions due to the set up of the laboratory equipment. It is recommended that the program results be compared to experimental data for systems other than air

water , as well as larger pipe sizes and higher pressure ranges in order to verify the accuracy of the predicted result when this data is available.

6.2.3 The effect of pressure loss in two phase flow results in a decrease in gas density but has little effect on the liquid density due to the incompressible nature of liquids. For greater accuracy when checking pressure loss in a pipe, the pipe line should be separated into small sections so that the effect of the changing in gas density can be assumed to be constant over the small section under consideration. Generally for pressure loss calculation in the gas flows the loss should not be greater than 10% of the upstream pressure. It the pressure exceeds this value, smaller sections should be used.

6.2.4 Friction pressure loss in the two-phase model is calculated from the single phase friction factor value. The friction correlation can be updated if two-phase friction factor is published and proved.

6.2.5 Pressure losses in Fittings and valves loss is based on the liquid single phase flow losses proposed by Courtesy ingersoll-rand company. The fitting loss for two phase flow would be higher. It is recommended that fittings and valves losses are used with a safety factor and the results should be compared with other experimental data.

6.2.6 To add fluid physical properties such as density, viscosity, etc. for water in the program database for calculation.

6.2.7 To add a graphic display of the pipeline layout, fittings and valves into the input and output section.

6.2.8 To show the calculated flow pattern map to indicate the predicted flow pattern compared with the other flow pattern regions for the input flow rate range.

REFERENCES

Abbraham, E Duckler and Martin, G. Hubbard. A Model for Gas-Liquid Slug in Horizontal and Near Horizontal Tubes. Ind. Eng. Chem.,Fundamental Vol 14, No. 4. (1975) : 337-347.

A.E., Dukler, Moye, Wicks,iii,and R.G., Cleveland. Frictional Pressure Drop in Two-Phase Flow: A. A Comparison of Existing Correlations for Pressure Loss and Hold up. AIChE Journal. Vol 10, No. 1. (January 1964) : 38-43.

A.E., Dukler, Moye , Wicks, iii, and R.G., Cleveland. Frictional Pressure Drop in Two-Phase Flow: B. An Approach Trough Similarity Annalysis. AIChE Journal. Vol 10, No. 1. (January 1964) : 44-51.

David, T. Clindric, Satish L., Gandhi and Ray, A.Williams. Designing Piping Systems for Two-Phase Flow. Chemical Engineering Progress. (March 1987) : 51-55

Dvora, Barnea., Ovadia, Shoham and Yehuda, Taitel. Flow Pattern Transition for Vertical Downward Two Phase Flow. Chemical Engineering Science Vol 37, No.5. (1982) : 741-744.

J.F., Douglas,J.M., Gasiorek,J.A.,Swaffield. Fluid Mechanics, 3rd Edition, Singapore. Longman Scientific& Technical. (1995)

J.M., Coulson., J.F. Richardson, J.R. Backhurst and J.H. Harker Chemical Engineering 5thEdition , Singapore. Butterworth Heinemann .Vol 1

Malasri J. Two-Phase flow in vertical tubes ,Master Degree dissertation The Petroleum and Petrochemical College, Chulalongkorn University, 2001.

Manolis Y. High Pressure Slug Two-Phase Flow PhD. dissertation , Imperial College of Science, Technology and Medicine ,1994.

Robert, Kern. How to size Process Piping For Two Phase Flow. Hydrocarbon Processing. (October 1969). 105-116.

Robert, W. Fox and Alan, T. McDonald. Introduction to Fluid Mechanics. Republic of Singapore: John Wiley &Son. 1985.

R.C., Fernandes, R., Semiat and A.E., Duckler. Hydrodynamic Model for Gas-Liquid Slug Flow in Vertical Tubes. AIChE Journal. Vol 29, No. 6. (November 1983) : 981-989

Winai W and Wattanapong K. Prediction of hold up and Pressure loss for the two phase flow in horizontal pipe. Bachelor dissertation , King Monkut 's Institute of Technology Thonburi ,1996.

Somprasong S. High Pressure Separated Two-Phase Flow PhD. dissertation , Imperial Cooollege of Science, Technology and Medicine ,1994.

REFERENCES(CONTINUE)

Steven, C.Chapra, Raymond, P. Canale. Numerical Methods for Engineers. Singapore: Mc Graw-Hill. 1998

Sutra S. N Visual Basic 6.0 Professional Step by Step. Thailand. Se-education PCL. 1999

The Cran Co. Flow of Fluids through Valves, Fittings and Pipe: Technical Paper No. 410 24th Edition, U.S.A., 1988.

Yehuda, Taitel and Dvora, Bornea. Modelling Flow Pattern Transitions for Steady Upward Gas-Liquid Flow in Vertical Tubes. AIChE Journal. Vol 26, No. 3. (May 1980) : 345-354.

Yemada, Taitel and A.E., Dukler. A Model for Predicting Flow Regime Transitions in Horizontal and near Horizontal Gas-Liquid Flow. AIChE Journal. Vol 22, No.1. (January 1976) : 47-54.

APPENDICES

Appendix A

PIPE DATA

Table A1 Pipe Property(Data from The Crane, technical paper no.410,1988)

Nominal Pipe Size, Inches	Outside Diam., Inches	Identification: Steel, Iron Pipe Size	Identification: Steel, Sched. No.	Identification: Stainless Steel Sched. No.	Wall Thickness (t), Inches	Inside Diameter (d), Inches	Area of Metal, Square Inches	Transverse Internal Area: (a) Square Inches	Transverse Internal Area: (A) Square Feet	Moment of Inertia (I), Inches⁴	Weight Pipe, Pounds per foot	Weight Water, Pounds per foot of pipe	External Surface, Sq. Ft. per foot of pipe	Section Modulus $\left(2\frac{I}{O.D.}\right)$
1/8	0.405	...	...	10S	.049	.307	.0548	.0740	.00051	.00088	.19	.032	.106	.00437
		STD	40	40S	.068	.269	.0720	.0568	.00040	.00106	.24	.025	.106	.00523
		XS	80	80S	.095	.215	.0925	.0364	.00025	.00122	.31	.016	.106	.00602
1/4	0.540	...	...	10S	.065	.410	.0970	.1320	.00091	.00279	.33	.057	.141	.01032
		STD	40	40S	.088	.364	.1250	.1041	.00072	.00331	.42	.045	.141	.01227
		XS	80	80S	.119	.302	.1574	.0716	.00050	.00377	.54	.031	.141	.01395
3/8	0.675	...	...	10S	.065	.545	.1246	.2333	.00162	.00586	.42	.101	.178	.01736
		STD	40	40S	.091	.493	.1670	.1910	.00133	.00729	.57	.083	.178	.02160
		XS	80	80S	.126	.423	.2173	.1405	.00098	.00862	.74	.061	.178	.02554
1/2	0.840	...	...	5S	.065	.710	.1583	.3959	.00275	.01197	.54	.172	.220	.02849
		...	...	10S	.083	.674	.1974	.3568	.00248	.01431	.67	.155	.220	.03407
		STD	40	40S	.109	.622	.2503	.3040	.00211	.01709	.85	.132	.220	.04069
		XS	80	80S	.147	.546	.3200	.2340	.00163	.02008	1.09	.102	.220	.04780
		...	160	...	.187	.466	.3836	.1706	.00118	.02212	1.31	.074	.220	.05267
		XXS	...	...	.294	.252	.5043	.050	.00035	.02424	1.71	.022	.220	.05772
3/4	1.050	...	...	5S	.065	.920	.2011	.6648	.00462	.02450	.69	.288	.275	.04667
		...	...	10S	.083	.884	.2521	.6138	.00426	.02969	.86	.266	.275	.05655
		STD	40	40S	.113	.824	.3326	.5330	.00371	.03704	1.13	.231	.275	.07055
		XS	80	80S	.154	.742	.4335	.4330	.00300	.04479	1.47	.188	.275	.08531
		...	160	...	.219	.612	.5698	.2961	.00206	.05269	1.94	.128	.275	.10036
		XXS	...	...	.308	.434	.7180	.148	.00103	.05792	2.44	.064	.275	.11032
1	1.315	...	...	5S	.065	1.185	.2553	1.1029	.00766	.04999	.87	.478	.344	.07603
		...	...	10S	.109	1.097	.4130	.9452	.00656	.07569	1.40	.409	.344	.11512
		STD	40	40S	.133	1.049	.4939	.8640	.00600	.08734	1.68	.375	.344	.1328
		XS	80	80S	.179	.957	.6388	.7190	.00499	.1056	2.17	.312	.344	.1606
		...	160	...	.250	.815	.8365	.5217	.00362	.1251	2.84	.230	.344	.1903
		XXS	...	...	.358	.599	1.0760	.282	.00196	.1405	3.66	.122	.344	.2136
1 1/4	1.660	...	...	5S	.065	1.530	.3257	1.839	.01277	.1038	1.11	.797	.435	.1250
		...	...	10S	.109	1.442	.4717	1.633	.01134	.1605	1.81	.708	.435	.1934
		STD	40	40S	.140	1.380	.6685	1.495	.01040	.1947	2.27	.649	.435	.2346
		XS	80	80S	.191	1.278	.8815	1.283	.00891	.2418	3.00	.555	.435	.2913
		...	160	...	.250	1.160	1.1070	1.057	.00734	.2839	3.76	.458	.435	.3421
		XXS	...	...	.382	.896	1.534	.630	.00438	.3411	5.21	.273	.435	.4110
1 1/2	1.900	...	...	5S	.065	1.770	.3747	2.461	.01709	.1579	1.28	1.066	.497	.1662
		...	...	10S	.109	1.682	.6133	2.222	.01543	.2468	2.09	.963	.497	.2598
		STD	40	40S	.145	1.610	.7995	2.036	.01414	.3099	2.72	.882	.497	.3262
		XS	80	80S	.200	1.500	1.068	1.767	.01225	.3912	3.63	.765	.497	.4118
		...	160	...	.281	1.338	1.429	1.406	.00976	.4824	4.86	.608	.497	.5078
		XXS	...	...	.400	1.100	1.885	.950	.00660	.5678	6.41	.42	.497	.5977
2	2.375	...	...	5S	.065	2.245	.4717	3.958	.02749	.3149	1.61	1.72	.622	.2652
		...	...	10S	.109	2.157	.7760	3.654	.02538	.4992	2.64	1.58	.622	.4204
		STD	40	40S	.154	2.067	1.075	3.355	.02330	.6657	3.65	1.45	.622	.5606
		XS	80	80S	.218	1.939	1.477	2.953	.02050	.8679	5.02	1.28	.622	.7309
		...	160	...	.344	1.687	2.190	2.241	.01556	1.162	7.46	.97	.622	.979
		XXS	...	...	.436	1.503	2.656	1.774	.01232	1.311	9.03	.77	.622	1.104
2 1/2	2.875	...	...	5S	.083	2.709	.7280	5.764	.04002	.7100	2.48	2.50	.753	.4939
		...	...	10S	.120	2.635	1.039	5.453	.03787	.9873	3.53	2.36	.753	.6868
		STD	40	40S	.203	2.469	1.704	4.788	.03322	1.530	5.79	2.07	.753	1.064
		XS	80	80S	.276	2.323	2.254	4.238	.02942	1.924	7.66	1.87	.753	1.339
		...	160	...	.375	2.125	2.945	3.546	.02463	2.353	10.01	1.54	.753	1.638
		XXS	...	...	.552	1.771	4.028	2.464	.01710	2.871	13.69	1.07	.753	1.997
3	3.500	...	...	5S	.083	3.334	.8910	8.730	.06063	1.301	3.03	3.78	.916	.7435
		...	...	10S	.120	3.260	1.274	8.347	.05796	1.822	4.33	3.62	.916	1.041
		STD	40	40S	.216	3.068	2.228	7.393	.05130	3.017	7.58	3.20	.916	1.724
		XS	80	80S	.300	2.900	3.016	6.605	.04587	3.894	10.25	2.86	.916	2.225
		...	160	...	.438	2.624	4.205	5.408	.03755	5.032	14.32	2.35	.916	2.876
		XXS	...	...	.600	2.300	5.466	4.155	.02885	5.993	18.58	1.80	.916	3.424

Table A1 Pipe Property (Cont.) (Data from The Crane, technical paper no.410,1988)

Nominal Pipe Size	Outside Diam.	Identification			Wall Thickness (t)	Inside Diameter (d)	Area of Metal	Transverse Internal Area		Moment of Inertia (I)	Weight Pipe	Weight Water	External Surface	Section Modulus
		Steel		Stainless Steel				(a)	(d)					
		Iron Pipe Size	Sched. No.	Sched. No.							Pounds per foot	Pounds per foot of pipe	Sq. Ft. per foot of pipe	$\left(2\frac{I}{O.D.}\right)$
Inches	Inches				Inches	Inches	Square Inches	Square Inches	Square Feet	Inches^4				
		...	...	5S	.083	3.834	1.021	11.545	.08017	1.960	3.48	5.00	1.047	.9799
		...	...	10S	.120	3.760	1.463	11.104	.07711	2.755	4.97	4.81	1.047	1.378
3½	4.000	STD	40	40S	.226	3.548	2.680	9.886	.06870	4.788	9.11	4.29	1.047	2.394
		XS	80	80S	.318	3.364	3.678	8.888	.06170	6.280	12.50	3.84	1.047	3.140
		...	...	5S	.083	4.334	1.152	14.75	.10245	2.810	3.92	6.39	1.178	1.249
		...	...	10S	.120	4.260	1.651	14.25	.09898	3.963	5.61	6.18	1.178	1.761
		STD	40	40S	.237	4.026	3.174	12.73	.08840	7.233	10.79	5.50	1.178	3.214
4	4.500	XS	80	80S	.337	3.826	4.407	11.50	.07986	9.610	14.98	4.98	1.178	4.271
		...	120	...	.438	3.624	5.595	10.31	.0716	11.65	19.00	4.47	1.178	5.178
		...	160	...	.531	3.438	6.621	9.28	.0645	13.27	22.51	4.02	1.178	5.898
		XXS	...	...	.674	3.152	8.101	7.80	.0542	15.28	27.54	3.38	1.178	6.791
		...	...	5S	.109	5.345	1.868	22.44	.1558	6.947	6.36	9.72	1.456	2.498
		...	...	10S	.134	5.295	2.285	22.02	.1529	8.425	7.77	9.54	1.456	3.029
		STD	40	40S	.258	5.047	4.300	20.01	.1390	15.16	14.62	8.67	1.456	5.451
5	5.563	XS	80	80S	.375	4.813	6.112	18.19	.1263	20.67	20.78	7.88	1.456	7.431
		...	120	...	.500	4.563	7.953	16.35	.1136	25.73	27.04	7.09	1.456	9.250
		...	160	...	.625	4.313	9.696	14.61	.1015	30.03	32.96	6.33	1.456	10.796
		XXS	...	...	.750	4.063	11.340	12.97	.0901	33.63	38.55	5.61	1.456	12.090
		...	...	5S	.109	6.407	2.231	32.24	.2239	11.85	7.60	13.97	1.734	3.576
		...	...	10S	.134	6.357	2.733	31.74	.2204	14.40	9.29	13.75	1.734	4.346
		STD	40	40S	.280	6.065	5.581	28.89	.2006	28.14	18.97	12.51	1.734	8.496
6	6.625	XS	80	80S	.432	5.761	8.405	26.07	.1810	40.49	28.57	11.29	1.734	12.22
		...	120	...	.562	5.501	10.70	23.77	.1650	49.61	36.39	10.30	1.734	14.98
		...	160	...	.719	5.187	13.32	21.15	.1469	58.97	45.35	9.16	1.734	17.81
		XXS	...	...	.864	4.897	15.64	18.84	.1308	66.33	53.16	8.16	1.734	20.02
		...	...	5S	.109	8.407	2.916	55.51	.3855	26.44	9.93	24.06	2.258	6.131
		...	...	10S	.148	8.329	3.941	54.48	.3784	35.41	13.40	23.61	2.258	8.212
		...	20	...	.250	8.125	6.57	51.85	.3601	57.72	22.36	22.47	2.258	13.39
		...	30	...	.277	8.071	7.26	51.16	.3553	63.35	24.70	22.17	2.258	14.69
		STD	40	40S	.322	7.981	8.40	50.03	.3474	72.49	28.55	21.70	2.258	16.81
8	8.625	...	60	...	.406	7.813	10.48	47.94	.3329	88.73	35.64	20.77	2.258	20.58
		XS	80	80S	.500	7.625	12.76	45.66	.3171	105.7	43.39	19.78	2.258	24.51
		...	100	...	.594	7.437	14.96	43.46	.3018	121.3	50.95	18.83	2.258	28.14
		...	120	...	.719	7.187	17.84	40.59	.2819	140.5	60.71	17.59	2.258	32.58
		...	140	...	.812	7.001	19.93	38.50	.2673	153.7	67.76	16.68	2.258	35.65
		XXS	...	...	.875	6.875	21.30	37.12	.2578	162.0	72.42	16.10	2.258	37.56
		...	160	...	.906	6.813	21.97	36.46	.2532	165.9	74.69	15.80	2.258	38.48
		...	...	5S	.134	10.482	4.36	86.29	.5992	63.0	15.19	37.39	2.814	11.71
		...	...	10S	.165	10.420	5.49	85.28	.5922	76.9	18.65	36.95	2.814	14.30
		...	20	...	.250	10.250	8.24	82.52	.5731	113.7	28.04	35.76	2.814	21.15
		...	30	...	.307	10.136	10.07	80.69	.5603	137.4	34.24	34.96	2.814	25.57
		STD	40	40S	.365	10.020	11.90	78.86	.5475	160.7	40.48	34.20	2.814	29.90
10	10.750	XS	60	80S	.500	9.750	16.10	74.66	.5185	212.0	54.74	32.35	2.814	39.43
		...	80	...	.594	9.562	18.92	71.84	.4989	244.8	64.43	31.13	2.814	45.54
		...	100	...	.719	9.312	22.63	68.13	.4732	286.1	77.03	29.53	2.814	53.22
		...	120	...	.844	9.062	26.24	64.53	.4481	324.2	89.29	27.96	2.814	60.32
		XXS	140	...	1.000	8.750	30.63	60.13	.4176	367.8	104.13	26.06	2.814	68.43
		...	160	...	1.125	8.500	34.02	56.75	.3941	399.3	115.64	24.59	2.814	74.29
		...	...	5S	.156	12.438	6.17	121.50	.8438	122.4	20.98	52.65	3.338	19.2
		...	...	10S	.180	12.390	7.11	120.57	.8373	140.4	24.17	52.25	3.338	22.0
		...	20	...	.250	12.250	9.82	117.86	.8185	191.8	33.38	51.07	3.338	30.2
		...	30	...	.330	12.090	12.87	114.80	.7972	248.4	43.77	49.74	3.338	39.0
		STD	...	40S	.375	12.000	14.58	113.10	.7854	279.3	49.56	49.00	3.338	43.8
		...	40	...	.406	11.938	15.77	111.93	.7773	300.3	53.52	48.50	3.338	47.1
		XS	...	80S	.500	11.750	19.24	108.43	.7528	361.5	65.42	46.92	3.338	56.7
12	12.75	...	60	...	.562	11.626	21.52	106.16	.7372	400.4	73.15	46.00	3.338	62.8
		...	80	...	.688	11.374	26.03	101.64	.7058	475.1	88.63	44.04	3.338	74.6
		...	100	...	.844	11.062	31.53	96.14	.6677	561.6	107.32	41.66	3.338	88.1
		XXS	120	...	1.000	10.750	36.91	90.76	.6303	641.6	125.49	39.33	3.338	100.7
		...	140	...	1.125	10.500	41.08	86.59	.6013	700.5	139.67	37.52	3.338	109.9
		...	160	...	1.312	10.126	47.14	80.53	.5592	781.1	160.27	34.89	3.338	122.6

Table A1 Pipe Property (Cont.) (Data from The Crane, technical paper no.410,1988)

Nominal Pipe Size	Outside Diam.	Identification: Steel: Iron Pipe Size	Identification: Steel: Sched. No.	Identification: Stainless Steel Sched. No.	Wall Thickness (t)	Inside Diameter (d)	Area of Metal	Transverse Internal Area: (a)	Transverse Internal Area: (A)	Moment of Inertia (I)	Weight Pipe	Weight Water	External Surface	Section Modulus
Inches	Inches				Inches	Inches	Square Inches	Square Inches	Square Feet	Inches^4	Pounds per foot	Pounds per foot of pipe	Sq. Ft. per foot of pipe	$\left(2\frac{I}{O.D.}\right)$
		...	...	5S	.156	13.688	6.78	147.15	1.0219	162.6	23.07	63.77	3.665	23.2
		...	...	10S	.188	13.624	8.16	145.78	1.0124	194.6	27.73	63.17	3.665	27.8
		...	10	...	.250	13.500	10.80	143.14	.9940	255.3	36.71	62.03	3.665	36.6
		...	20	...	.312	13.376	13.42	140.52	.9758	314.4	45.61	60.89	3.665	45.0
		STD	30	...	.375	13.250	16.05	137.88	.9575	372.8	54.57	59.75	3.665	53.2
		...	40	...	.438	13.124	18.66	135.28	.9394	429.1	63.44	58.64	3.665	61.3
14	14.00	XS	...	...	.500	13.000	21.21	132.73	.9217	483.8	72.09	57.46	3.665	69.1
		...	60	...	.594	12.812	24.98	128.96	.8956	562.3	85.05	55.86	3.665	80.3
		...	80	...	.750	12.500	31.22	122.72	.8522	678.3	106.13	53.18	3.665	98.2
		...	100	...	.938	12.124	38.45	115.49	.8020	824.4	130.85	50.04	3.665	117.8
		....	120	...	1.094	11.812	44.32	109.62	.7612	929.6	150.79	47.45	3.665	132.8
		...	140	...	1.250	11.500	50.07	103.87	.7213	1027.0	170.28	45.01	3.665	146.8
		...	160	...	1.406	11.188	55.63	98.31	.6827	1117.0	189.11	42.60	3.665	159.6
		...	...	5S	.165	15.670	8.21	192.85	1.3393	257.3	27.90	83.57	4.189	32.2
		...	...	10S	.188	15.624	9.34	191.72	1.3314	291.9	31.75	83.08	4.189	36.5
		...	10	...	.250	15.500	12.37	188.69	1.3103	383.7	42.05	81.74	4.189	48.0
		...	20	...	.312	15.376	15.38	185.69	1.2895	473.2	52.27	80.50	4.189	59.2
		STD	30	...	.375	15.250	18.41	182.65	1.2684	562.1	62.58	79.12	4.189	70.3
16	16.00	XS	40	...	.500	15.000	24.35	176.72	1.2272	731.9	82.77	76.58	4.189	91.5
		...	60	...	.656	14.688	31.62	169.44	1.1766	932.4	107.50	73.42	4.189	116.6
		...	80	...	.844	14.312	40.14	160.92	1.1175	1155.8	136.61	69.73	4.189	144.5
		...	100	...	1.031	13.938	48.48	152.58	1.0596	1364.5	164.82	66.12	4.189	170.5
		...	120	...	1.219	13.562	56.56	144.50	1.0035	1555.8	192.43	62.62	4.189	194.5
		...	140	...	1.438	13.124	65.78	135.28	.9394	1760.3	223.64	58.64	4.189	220.0
		...	160	...	1.594	12.812	72.10	128.96	.8956	1893.5	245.25	55.83	4.189	236.7
		...	...	5S	.165	17.670	9.25	245.22	1.7029	367.6	31.43	106.26	4.712	40.8
		...	...	10S	.188	17.624	10.52	243.95	1.6941	417.3	35.76	105.71	4.712	46.4
		...	10	...	.250	17.500	13.94	240.53	1.6703	549.1	47.39	104.21	4.712	61.1
		...	20	...	.312	17.376	17.34	237.13	1.6467	678.2	58.94	102.77	4.712	75.5
		STD	...	...	.375	17.250	20.76	233.71	1.6230	806.7	70.59	101.18	4.712	89.6
		...	30	...	.438	17.124	24.17	230.30	1.5990	930.3	82.15	99.84	4.712	103.4
18	18.00	XS	...	...	.500	17.000	27.49	226.98	1.5763	1053.2	93.45	98.27	4.712	117.0
		...	40	...	.562	16.876	30.79	223.68	1.5533	1171.5	104.67	96.93	4.712	130.1
		...	60	...	.750	16.500	40.64	213.83	1.4849	1514.7	138.17	92.57	4.712	168.3
		...	80	...	.938	16.124	50.23	204.24	1.4183	1833.0	170.92	88.50	4.712	203.8
		...	100	...	1.156	15.688	61.17	193.30	1.3423	2180.0	207.96	83.76	4.712	242.3
		...	120	...	1.375	15.250	71.81	182.66	1.2684	2498.1	244.14	79.07	4.712	277.6
		...	140	...	1.562	14.876	80.66	173.80	1.2070	2749.0	274.22	75.32	4.712	305.5
		...	160	...	1.781	14.438	90.75	163.72	1.1369	3020.0	308.50	70.88	4.712	335.6
		...	...	5S	.188	19.624	11.70	302.46	2.1004	574.2	39.78	131.06	5.236	57.4
		...	...	10S	.218	19.564	13.55	300.61	2.0876	662.8	46.06	130.27	5.236	66.3
		...	10	...	.250	19.500	15.51	298.65	2.0740	765.4	52.73	129.42	5.236	75.6
		STD	20	...	.375	19.250	23.12	290.04	2.0142	1113.0	78.60	125.67	5.236	111.3
		XS	30	...	.500	19.000	30.63	283.53	1.9690	1457.0	104.13	122.87	5.236	145.7
		...	40	...	.594	18.812	36.15	278.00	1.9305	1703.0	123.11	120.46	5.236	170.4
20	20.00	...	60	...	.812	18.376	48.95	265.21	1.8417	2257.0	166.40	114.92	5.236	225.7
		...	80	...	1.031	17.938	61.44	252.72	1.7550	2772.0	208.87	109.51	5.236	277.1
		...	100	...	1.281	17.438	75.33	238.83	1.6585	3315.2	256.10	103.39	5.236	331.5
		...	120	...	1.500	17.000	87.18	226.98	1.5762	3754.0	296.37	98.35	5.236	375.5
		...	140	...	1.750	16.500	100.33	213.82	1.4849	4216.0	341.09	92.66	5.236	421.7
		...	160	...	1.969	16.062	111.49	202.67	1.4074	4585.5	379.17	87.74	5.236	458.5
		...	...	5S	.188	21.624	12.88	367.25	2.5503	766.2	43.80	159.14	5.760	69.7
		...	...	10S	.218	21.564	14.92	365.21	2.5362	884.8	50.71	158.26	5.760	80.4
		...	10	...	.250	21.500	17.08	363.05	2.5212	1010.3	58.07	157.32	5.760	91.8
		STD	20	...	.375	21.250	25.48	354.66	2.4629	1489.7	86.61	153.68	5.760	135.4
		XS	30	...	.500	21.000	33.77	346.36	2.4053	1952.5	114.81	150.09	5.760	117.5
22	22.00	...	60	...	.875	20.250	58.07	322.06	2.2365	3244.9	197.41	139.56	5.760	295.0
		...	80	...	1.125	19.75	73.78	306.35	2.1275	4030.4	250.81	132.76	5.760	366.4
		...	100	...	1.375	19.25	89.09	291.04	2.0211	4758.5	302.88	126.12	5.760	432.6
		...	120	...	1.625	18.75	104.02	276.12	1.9175	5432.0	353.61	119.65	5.760	493.8
		...	140	...	1.875	18.25	118.55	261.59	1.8166	6053.7	403.00	113.36	5.760	550.3
		...	160	...	2.125	17.75	132.68	247.45	1.7184	6626.4	451.06	107.23	5.760	602.4

Figure A2 Relative roughness values for pipe of common engineering material (Data from The Crane, Technical Paper No.410,1988)

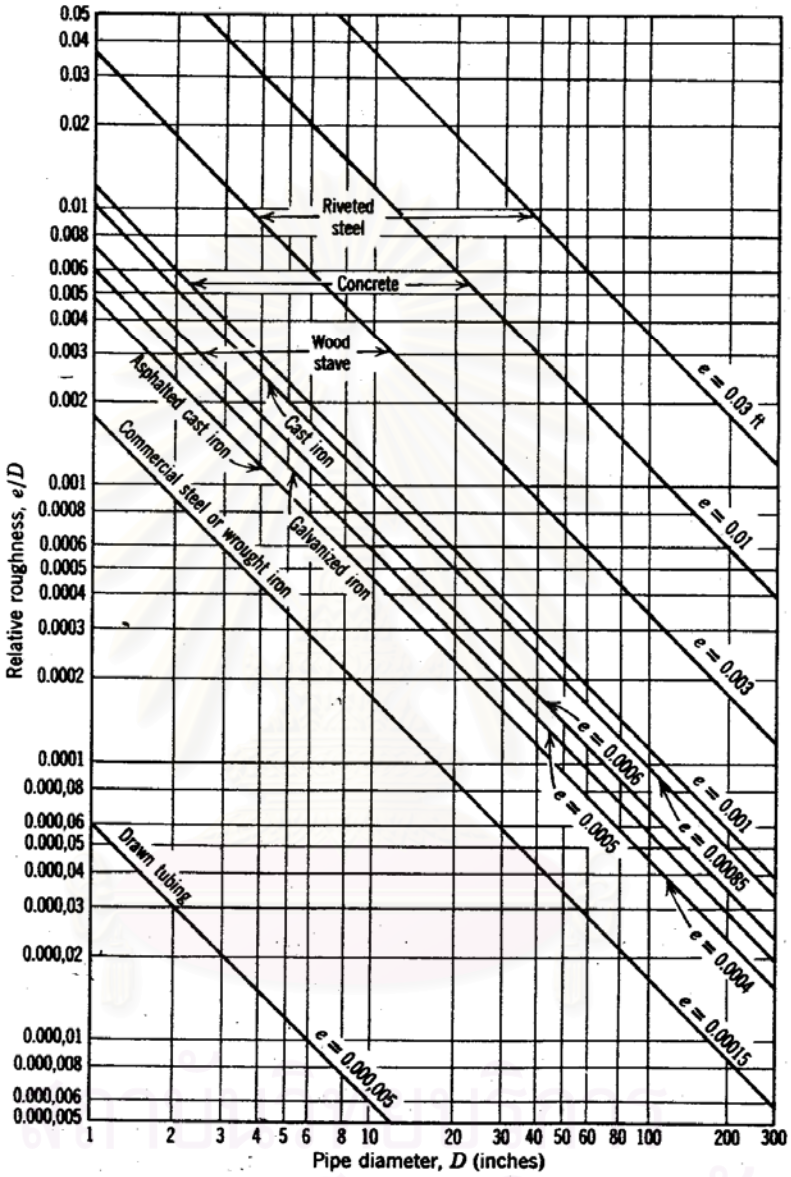

Figure A2 Relative roughness values for pipe of common engineering material (Data from The Crane, Technical Paper No.410, 1988)

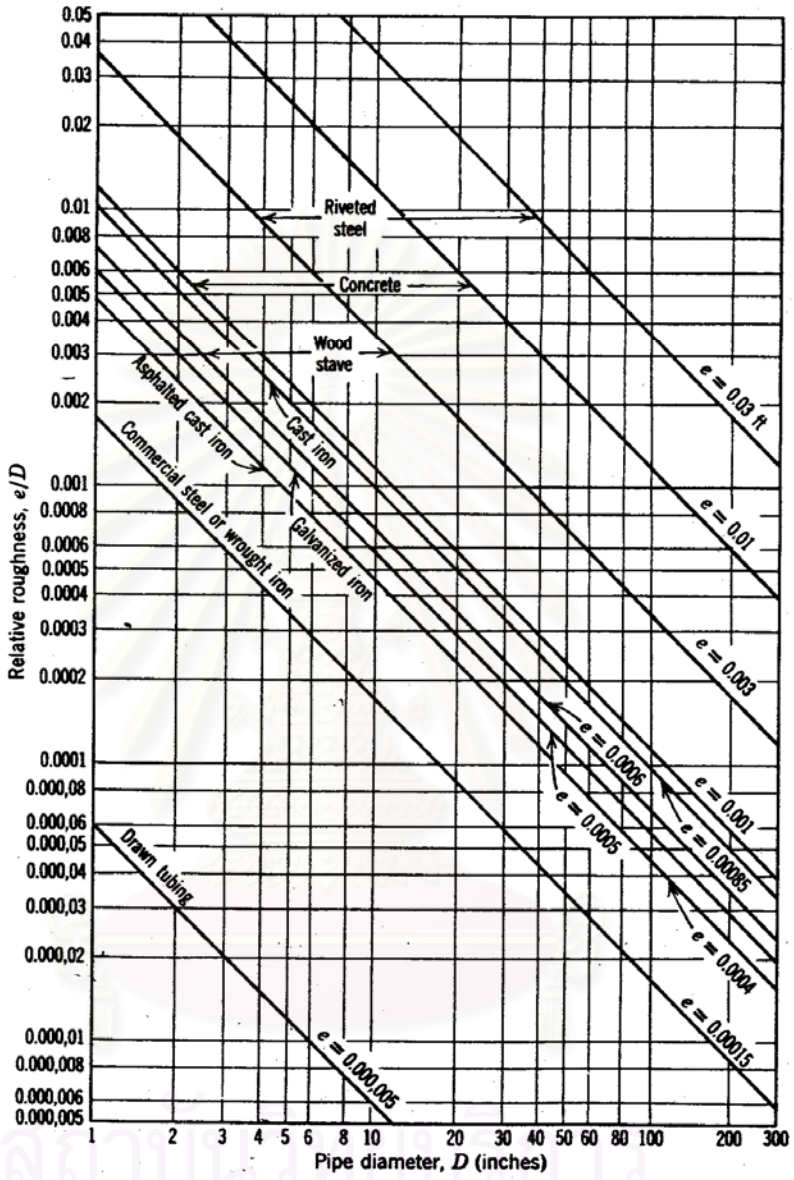

Figure A-3 Friction factor (Data from The Crane, Technical paper no.410,1988)

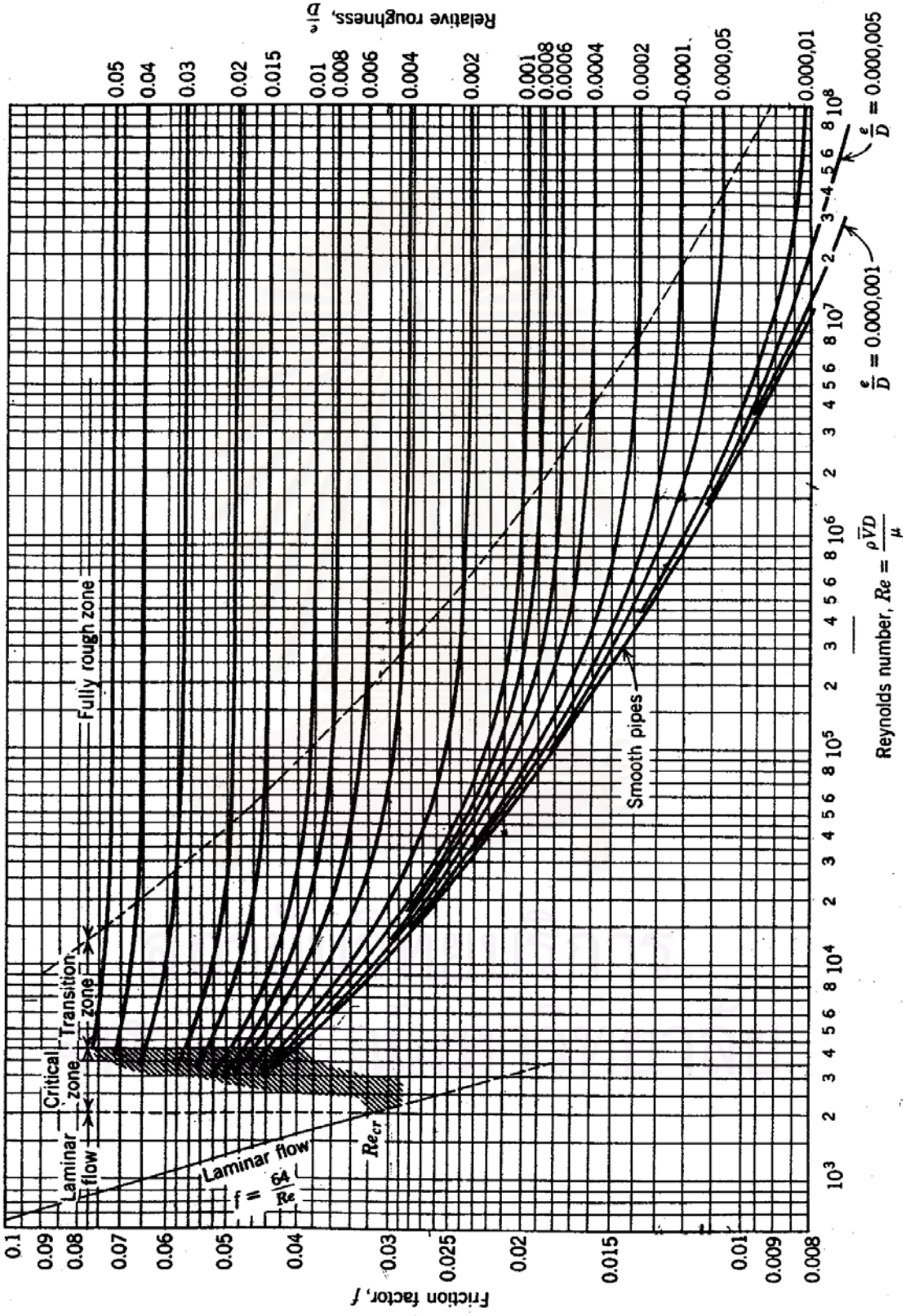

Appendix B

FLUID PHYSICAL PROPERTIES

Table B1 Viscosity of water and liquid Petroleum Product Data (Data from The Crane, Technical paper no.410,1988)

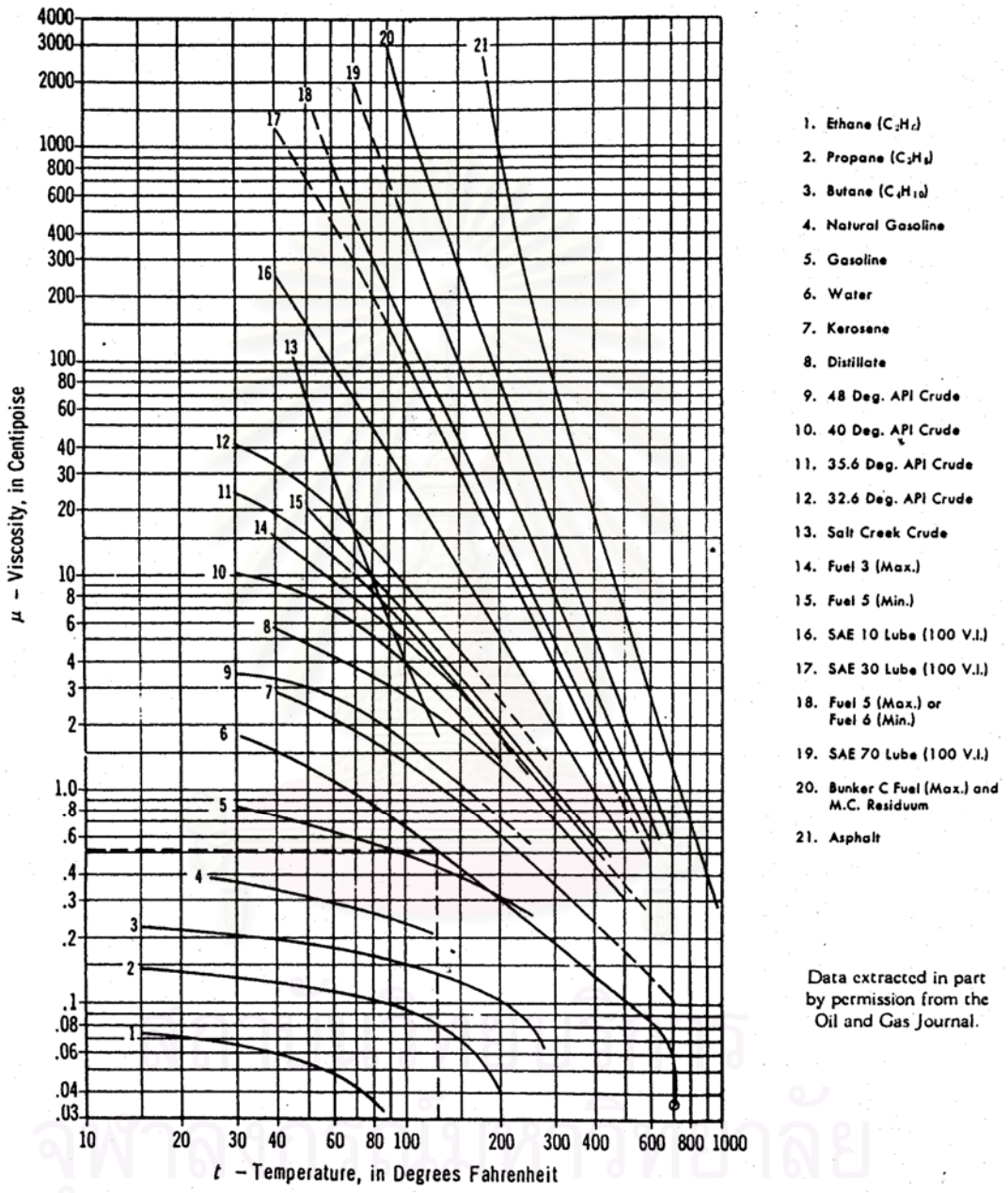

Table B2 Weight Density and Specific Gravity of various Liquids (Data from The Crane Technical paper no. 410,1988)

Name of Gas	Chemical Formula or Symbol	Approx. Molecular Weight M	Weight Density, Pounds per Cubic Foot ρ	Specific Gravity Relative to Air S_g	Individual Gas Constant R	Specific Heat at Room Temperature Btu/Lb °F c_p	c_v	Heat Capacity per Cubic Foot c_p	c_v	k equal to c_p/c_v
Acetylene (ethyne)	C_2H_2	26.0	.0682	0.907	59.4	0.350	0.269	.0239	.0184	1.30
Air	—	29.0	.0752	1.000	53.3	0.241	0.172	.0181	.0129	1.40
Ammonia	NH_3	17.0	.0448	0.596	91.0	0.523	0.396	.0234	.0178	1.32
Argon	A	39.9	.1037	1.379	38.7	0.124	0.074	.0129	.0077	1.67
Butane	C_4H_{10}	58.1	.1554	2.067	26.5	0.395	0.356	.0614	.0553	1.11
Carbon dioxide	CO_2	44.0	.1150	1.529	35.1	0.205	0.158	.0236	.0181	1.30
Carbon monoxide	CO	28.0	.0727	0.967	55.2	0.243	0.173	.0177	.0126	1.40
Chlorine	Cl_2	70.9	.1869	2.486	21.8	0.115	0.086	.0215	.0162	1.33
Ethane	C_2H_6	30.0	.0789	1.049	51.5	0.386	0.316	.0305	.0250	1.22
Ethylene	C_2H_4	28.0	.0733	0.975	55.1	0.400	0.329	.0293	.0240	1.22
Helium	He	4.0	.01039	0.1381	386.3	1.250	0.754	.0130	.0078	1.66
Hydrogen chloride	HCl	36.5	.0954	1.268	42.4	0.191	0.135	.0182	.0129	1.41
Hydrogen	H_2	2.0	.00523	0.0695	766.8	3.420	2.426	.0179	.0127	1.41
Hydrogen sulphide	H_2S	34.1	.0895	1.190	45.2	0.243	0.187	.0217	.0167	1.30
Methane	CH_4	16.0	.0417	0.554	96.4	0.593	0.449	.0247	.0187	1.32
Methyl chloride	CH_3Cl	50.5	.1342	1.785	30.6	0.240	0.200	.0322	.0268	1.20
Natural gas	—	19.5	.0502	0.667	79.1	0.560	0.441	.0281	.0221	1.27
Nitric oxide	NO	30.0	.0780	1.037	51.5	0.231	0.165	.0180	.0129	1.40
Nitrogen	N_2	28.0	.0727	0.967	55.2	0.247	0.176	.0180	.0127	1.41
Nitrous oxide	N_2O	44.0	.1151	1.530	35.1	0.221	0.169	.0254	.0194	1.31
Oxygen	O_2	32.0	.0831	1.105	48.3	0.217	0.155	.0180	.0129	1.40
Propane	C_3H_8	44.1	.1175	1.562	35.0	0.393	0.342	.0462	.0402	1.15
Propene (propylene)	C_3H_6	42.1	.1091	1.451	36.8	0.358	0.314	.0391	.0343	1.14
Sulphur dioxide	SO_2	64.1	.1703	2.264	24.0	0.154	0.122	.0262	.0208	1.26

VITA

Mrs. Varisara Padiporn was born on October 23, 1971 in Bangkok, Thailand. She received her Bachelor Degree of Engineering from Department of Chemical Engineering, Faulty of Engineering, King Monkut's Institute of Technology Thonburi in 1994. Currently, she is a Project Engineer at Foster Wheeler International Corporation (Thailand Operations).